ANALYSIS OF BORDER STRIP IRRIGATION AND ESTIMATION OF INFILTRATION PARAMETERS

A THESIS

Submitted in partial fulfilment of the requirements for the award of the degree of

DOCTOR OF PHILOSOPHY

in

CIVIL ENGINEERING

by

SHOBHA RAM

DEPARTMENT OF CIVIL ENGINEERING
INDIAN INSTITUTE OF TECHNOLOGY ROORKEE
ROORKEE - 247 667 (INDIA)

JANUARY, 2010

INDIAN INSTITUTE OF TECHNOLOGY ROORKEE
ROORKEE

CANDIDATE'S DECLARATION

I hereby certify that the work which is being presented in the thesis entitled **ANALYSIS OF BORDER STRIP IRRIGATION AND ESTIMATION OF INFILTRATION PARAMETERS** in partial fulfilment of the requirements for the award of the Degree of Doctor of Philosophy and submitted in the Department of Civil Engineering of the Indian Institute of Technology Roorkee, Roorkee is an authentic record of my own work carried out during a period from July 2003 to January 2010 under the supervision of Dr. K. S. Hari Prasad, Dr. Ajay Gairola, Associate Professors, Department of Civil Engineering, Indian Institute of Technology Roorkee and Dr. M. K. Jose, Scientist, National Institute of Hydrology, Regional Centre Belgaum. The matter presented in this thesis has not been submitted by me for the award of any other degree of this or any other Institute.

(SHOBHA RAM)

This is to certify that the above statement made by the candidate is correct to the best of our knowledge.

(M. K. JOSE)	(AJAY GAIROLA)	(K. S. HARI PRASAD)
Supervisor	Supervisor	Supervisor

Date:

The Ph.D. Viva-Voce Examination of **Mr. Shobha Ram**, Research Scholar has been held on 5/7/2010

Signature of Supervisors	Signature of External Examiner
5/7/2010 05.07.10	5/7/2010

ABSTRACT

Modelling border strip irrigation system is a complex process since it involves both the overland and subsurface flow. The numerical solution of border strip irrigation involves the solution of both surface and subsurface flows. The present study is concerned with developing a hydrodynamic numerical model for the simulation of overland and subsurface flow for border strip irrigation and estimation of field infiltration parameters. A numerical model is developed by solving the differential equations governing overland flow (Saint Venants equations) and subsurface flow (Richards equation). Explicit MacCormack scheme is used to solve the Saint Venants equations while the Richards equation is solved using a mass conservative fully implicit finite difference method. The model performance is assessed by comparing model predictions by numerically as well as experimentally observed irrigation events such as irrigation advance and recession data reported in literature. The model is validated with the data of surface irrigation experiments on three different soils reported in literature.

A detailed surface irrigation field experiments has been conducted involving both overland and subsurface measurements to asses the performance and applicability of the numerical model developed in predicting both overland and subsurface flow variables. In addition to the surface measurements such as advance, recession and flow depths, subsurface measurements such as pressure heads and moisture contents are also measured. The pressure heads are measured using tensiometers and the moisture contents are measured using Time Domain reflectometer (TDR). The model is validated by comparing model predicted irrigation advance, recession and subsurface moisture profiles with experimental data.

The accurate prediction of border strip irrigation events such as such as irrigation advance, recession and subsurface wetting front movement mainly depends on the system

parameters, like Manning's roughness coefficient n and infiltration parameters: saturated hydraulic conductivity K_{sat}, Van Genuchten water retention parameters (Van Genuchten, 1990), α_v, n_v, θ_s and θ_r. Among these, the estimation of infiltration parameters at field level is one of the difficult tasks (Walker and Skogerboe, 1987). For a relatively big field, estimation of infiltration parameters using infiltrometers requires that the test be conducted at many places. Further, these parameters may not represent the infiltration phenomenon at field scale. An alternative to these direct measurement techniques is to employ inverse techniques for parameter estimation. In such an approach, the infiltration parameters are estimated by minimizing the deviations between the model predicted and field observed flow attributes such as irrigation advance, recession, flow depth and wetting front movement. In this study, a parameter estimation model is developed by coupling the numerical model with a Sequential unconstrained minimization technique (SUMT). The issues of identifiability and uniqueness are discussed by estimating the parameters from hypothetical data. The robustness of the model is assessed by varying the number of estimated parameters from 1 to 3. In this study, saturated hydraulic conductivity K_{sat}, water retention parameters α_v, and n_v, are identified. The irrigation advance and summation of flow depths are used to identify single parameter. It is observed that the parameter estimates using summation of flow depths are in good agreement with their true values. Further, the summation of flow depths is used to identify two and three parameters. The results of simultaneous estimates of two parameters show that the optimization technique converges to the true values. However, simultaneous estimation of all the three infiltration parameters is not possible with flow depth data. Inclusion of moisture content in the objective function does not guarantee unique solutions.

ACKNOWLEDGEMENTS

I feel great pleasure in expressing my profound gratitude and indebtedness to my supervisors Dr. K. S. Hari Prasad, Dr. Ajay Gairola Associate Professors of Civil Engineering and Dr. M. K. Jose Scientist of National Institute of Hydrology, who gave valuable and inspiring guidance during the course of the work. I am really thankful to them for their keen interest, constant encouragement and untiring efforts during the discussions of the work. I feel very fortunate to be a student of them and I have no words to explain their generosity and simplicity.

I take this opportunity to thank the faculty members of Civil Engineering Department, Indian Institute of Technology Roorkee, Roorkee and staff of CAD and hydraulic lab for their constant helping hands at all time of my work.

I am grateful to my institute, National Institute of Hydrology Roorkee, Roorkee for providing me the opportunity of doing the Ph. D. I am also thankful to Dr. N. C. Ghosh and other scientists of the division and the institute for their help and support.

I thank all my family members for their immense patience, personal sacrifices and constant encouragement, which helped me in the completion of this work.

Lastly, I thank all my friends who extended their big hand to me during completion of this work

(SHOBHA RAM)

LIST OF CONTENTS

LIST OF FIGURES

LIST OF TABLES

LIST OF PLATES

LIST OF NOTATIONS

Symbol	Description	Dimension
h	Surface water depth	[L]
q	Discharge per unit width	$[L^2T^{-1}]$
q_s	Volumetric Rate of Infiltration per unit area	$[LT^{-1}]$
g	Acceleration due to Gravity	$[LT^{-2}]$
S_0	Longitudinal slope of the Border	$[LL^{-1}]$
x	Distance Along the Border	[L]
t	Time coordinate	[T]
z	Vertical Coordinate taken positive upwards	[L]
L	Length of the Border	[L]
h_{ini}	Initial Flow Depth	[L]
q_{ini}	Initial Discharge	$[L^3T^{-1}L^{-1}]$
q_{us}	Inlet Discharge	$[L^3T^{-1}L^{-1}]$
t_{ds}	Time of the Advance front to reach the Downstream end	[T]
t_c	Time of cutoff of water supply	[T]
K	Hydraulic Conductivity	$[LT^{-1}]$
ψ	Pressure head	[L]
θ	Volumetric Moisture Content	$[L^3L^{-3}]$
θ	Moisture content	$[L^3L^{-3}]$
θ_s	Saturated moisture content	$[L^3L^{-3}]$
θ_r	Residual moisture content	$[L^3L^{-3}]$
α_v	Unsaturated soil parameters	$[L^{-1}]$
n_v	Unsaturated soil parameters	[*]

m_v	Unsaturated soil parameters	[*]
S_e	Effective saturation	[*]
K_s	Saturated hydraulic conductivity	$[LT^{-1}]$
D_s	Vertical depth of the subsurface considered	[L]
ψ_{ini}	Initial pressure head	[L]
$t_{adv,p}$	Times at which the irrigation advance front arrives to a point 'p'	[T]
$t_{rec,p}$	Times at which the irrigation recession front arrives to a point 'p'	[T]
i	Refers to a typical surface node in the x-direction	-
j	Refers to a typical node in the z-direction	-
k	Refers to the discrete time at which solution is known	-
k+1	Refers to the discrete time at which solution is sought	-
Δt	The time increment between time levels k and k+1	[T]
Δx	The nodal spacing (grid distance) in x-direction	[L]
Δz	The nodal spacing (grid distance) in z-direction	[L]
T	Tridiagonal coefficient matrix	-
$\boldsymbol{b}$	Vector of model parameters	-
b	Constant in Campbell's equation	-
C	Soil moisture capacity	$[L^{-1}]$
D	Soil moisture diffusivity	$[L^2T^{-1}]$
H_b	Scaling parameter in Campbell equation	[L]
n	Manning's roughness coefficient	$[L^{-1/3}T]$
p	Picard iteration level	-
$\phi(\boldsymbol{b})$	Objective function	-

$\boldsymbol{L^*}$	Observation vector	-
$\boldsymbol{L(b)}$	Predicted response	-
$\boldsymbol{R}$	Response	
SMC	Soil moisture characteristics	-
TDR	Time domain reflectometer	-
VMC	Volumetric moisture content	$[L^3L^{-3}]$
$\boldsymbol{W}$	Symmetric weighting matrix	-
λ	Pore size index in Brooks and Corey parameter	[*]
ψ_b	Bubbling pressure head	[L]

Note: [*] denotes dimensionless

CHAPTER 1

INTRODUCTION

1.1 GENERAL

Water is the most precious commodity available on the earth. It is an essential ingredient for the survival of various kinds of living species (human, animals and plants). Although more than two-third of the earth's surface is covered with water, only a minute fraction is available as fresh water for utilization by humans and plants. The agriculture sector alone demands a largest amount, nearly 70 percent of all water withdrawals worldwide. In addition, more land is being added under irrigated area continuously to increase the food production to meet the increasing population thrust.

The term "surface irrigation" refers to a broad class of irrigation methods in which water is distributed over the field by gravity. Surface irrigation is the oldest and most extensively used irrigation method. In surface irrigation, flow is introduced at a high point or along a high edge of the field and allowed to cover the field by overland flow. The rate of flow is dependent almost entirely on the quantitative difference between inlet discharge and the accumulating infiltration; the other factors include field slope and surface roughness (Walker and Skogerboe 1987).

Surface irrigation has few advantages such as minimum capital investment, low maintenance cost and low energy requirement. However, the efficiency of surface irrigation system is typically low. Strelkoff and Katopodes, (1977) estimated that only about one half of the water applied to the field in surface irrigation systems is used by the plants. The remainder evaporates, drains off at the end of the field as surface runoff or percolates through the soil eventually to join the groundwater reservoir. This poor

performance is attributed to some extent, to imperfect design, unsuitable operation and other factors. One of the first priorities in agriculture today is the development of irrigation designs that are more efficient in the use of water and energy resources for a variety of crops and farming practices.

Efficient use of irrigation water necessitates proper evaluation of available resources and management of these resources in sustainable manner. Therefore, efforts should be made to increase the efficiency of water-use rather than to increase the supply of water, which requires the optimal use of water for irrigation. Optimal use of irrigation becomes more important, in case, if only groundwater is used for irrigation purpose, since in addition to the other effects of excess irrigation, deterioration of soil occurs due to continuous salinisation, if groundwater is saline in nature. Thus, an irrigation system is needed to be evaluated to identify an economical, effective and feasible alternative, which can improve the performance of an irrigation system.

Surface irrigation systems include basin irrigation, border irrigation, furrow irrigation and wild flooding. Border irrigation system, including level basins represent an important class of surface irrigation systems widely used in agriculture since ancient times, in which water flows on a sloping rectangular field bounded by low soil dykes along both the edges of the field. These systems are flexible and their simulation has been the objective of an extensive modeling effort in recent years. Hydraulic analysis of all the phases of irrigation from advance to recession is important for the successful design and operation of a border irrigation system.

Water flow in border irrigation is considered as an unsteady, nonuniform, gradually varied free surface open channel flow over a porous bed (sub surface) with a time dependent infiltration rate (Sherman and Singh 1978). Mathematical analysis of such a flow system involves the coupling of differential equations governing overland

and subsurface flows. In addition, proper estimation of infiltration parameters is important for accurate prediction of border advance. Direct estimation of these parameters at field level is difficult due to the requirement to meet the prescribed initial and boundary conditions needed for direct inversion. One has to resort to indirect methods for parameter estimation.

1.2 PROBLEM IDENTIFICATION

Knowledge of different phases of surface irrigation like advance, recession and infiltration of water into the root zone is essential for proper design of surface irrigation system. Analysis of surface irrigation system is usually carried out by solving the differential equations governing overland and subsurface flows. A number of analytical and numerical models for simulation of surface and subsurface flow have been developed. Analytical solutions are of limited value to simulate surface irrigation, especially when, infiltration and inflow are time dependent, therefore, a number of numerical models for surface irrigation have been developed. Most of the numerical models of surface irrigation can be classified in order of increasing complexity as (1) storage models, (2) kinematic wave models, and (3) hydrodynamic models (Singh and Bhallamudi, 1996, Wohling and Schmitz, 2007).

Storage models are based on the equation of mass continuity with some assumptions (Hart et al., 1968; and Cunge and Woolhiser, 1975). In such an approach, the rate of advance of surface irrigation is related to variables of soil, crop and topography through storage shape factors. It is observed that, even though such models have been somewhat successfully applied in the design of irrigation systems, they contribute little to the understanding of irrigation phenomena (Sherman and Singh, 1978)

Kinematic models utilize Kinematic wave theory to describe surface irrigation (Hart et al., 1968; Smith, 1972; Walker and Humpherys, 1983 and Singh and Ram 1983). Woolhiser (1970) has demonstrated that, even though Kinematic models yield good results in predicting the length of irrigation advance, the models fail to track the advancing front since the Kinematic assumption is not valid in the immediate region of the front. Singh and Ram (1983) verified the Kinematic model predictions with experimental data. They concluded that the predicted surface profile match well with the experimental data. However, the model is not capable of accommodating the vertical recession.

Hydrodynamic models utilize one-dimensional form of the St. Venant equations or their approximations in hydraulic modeling of surface irrigation. (Katopodes and Strelkoff, 1977; Bautista and Wallender, 1992; Singh and Bhallamudi 1996 and Wohling and Schmitz 2007). Bautista and Wallender (1992) developed a complete hydrodynamic irrigation model with specified space steps that solves for time of advance as a function of distance using shooting method to simulate storage, depletion, and recession phases of irrigation. The model uses a modified version of the extended Kostiakov equation to compute infiltration. Singh and Bhallamudi (1996) presented a hydrodynamic model for simulating all phases of border-strip irrigation using explicit, second-order accurate MacCormack scheme for solving the governing equation of surface irrigation. They used the empirical Kostiakov equation and the Parlange's analytical solution for computing infiltration. Singh and Bhallamudi (1998) developed a conjunctive surface-subsurface numerical model for the simulation of overland flow using the complete Saint-Venant equations and two-dimensional Richards equation in the mixed form to estimate the subsurface flow component.

From literature, it is observed that most of the hydrodynamic models gave more emphasis on accurately simulating the irrigation advance on the land and lesser emphasis on modelling infiltration process. Infiltration plays a significant role in the accurate prediction of irrigation advance and recession. Further, proper estimation of infiltration parameters is necessary for accurate analysis of surface irrigation events. Determination of infiltration parameters using infiltrometers may not adequately represent the infiltration phenomena at the field scale. One has to resort to indirect methods for the estimation of infiltration parameters at the field scale by minimizing the deviations between the model predicted and field observed irrigation advance and recession data. The problem of parameter estimation using indirect methods is often illposed. The illposedness may be due to unidentifiability, errors in the data or due to non unique solutions.

1.3 OBJECTIVES OF THE PRESENT STUDY

The present study is concerned with the numerical modeling of surface and subsurface flow and estimation of infiltration parameters. Keeping this in view, the following objectives are considered.

1. To develop a numerical model for the analysis of different phases of border strip irrigation system by solving coupled differential equations governing both overland (Saint-Venant equations) and subsurface (Richrads equation) flows.
2. To validate the numerical model by comparing the model results with experimentally observed advance and recession phases of irrigation events reported in literature.
3. To conduct field experiments to study the performance of the numerical model in predicting the advance and recession phases of border strip irrigation and soil moisture movement in subsurface.

4. To develop a parameter estimation model for the estimation of infiltration parameters from the measured irrigation advance, flow depth and moisture content data.
5. To address the issue of identifiability of model parameters from the irrigation advance, flow depth and moisture content data.

1.4 ORGANISATION OF THESIS

A brief description of the layout of the thesis is presented in the following paragraphs.

A comprehensive literature review on modeling of unsaturated zone, solution techniques and estimation of infiltration parameters by direct and indirect methods is presented in Chapter 2

Chapter 3 deals with the development of a hydrodynamic numerical model for the simulation of overland and subsurface flow for border strip irrigation. A numerical model is developed for solving the differential equations governing overland flow (Saint Venant equations) and subsurface flow (Richards equation). The MacCormack scheme is used to solve the Saint Venants equations. The Richards equation is solved with a mass conservative fully implicit finite difference method using Van Genuchten constitutive relationships for hydraulic conductivity-pressure head-moisture content relationships. The model is validated by comparing model predicted irrigation advance and recession with the data reported in literature.

Chapter 4 discusses in detail the laboratory and field experimental programme. The laboratory experiments involve the determination of textural properties, bulk density, particle density, porosity saturated hydraulic conductivity and soil moisture characteristic using Pressure Plate Extractor test. Detailed field irrigation experiments

the numerical model developed in Chapter 3 in predicting both overland and subsurface flow variables.

In Chapter 5, a parameter estimation model is developed by coupling the numerical model developed in Chapter 3 with a Sequential unconstrained minimization technique (SUMT). The issues of identifiability and uniqueness are discussed by estimating the parameters from hypothetical data. This Chapter involves the estimation of infiltration parameters such as K_{sat}, α_v, and n_v from irrigation event data of border strip irrigation using inverse technique. In such an approach, the infiltration parameters are estimated by minimizing the deviations between the model predicted and field observed flow attributes such as irrigation advance, recession, flow depth and moisture content data. This Chapter also presents the application of the parameter estimation model to estimate the infiltration parameters from border strip experimental data.

Chapter 6 presents the main findings of the study and the scope for future investigations.

CHAPTER 2
LITERATURE REVIEW

2.1 INTRODUCTION

Mathematical models of surface irrigation are generally classified as volume balance, zero inertia, kinematic wave and hydrodynamic models. Numerical modeling of border strip irrigation systems have been increasingly used nowadays to understand the effectiveness of various irrigation efficiency improvement measures. Modelling border strip irrigation is a complex process since it involves both the overland and subsurface flow. In the following sections a comprehensive review of mathematical/numerical and experimental investigations carried out for the understanding of surface irrigation process is presented.

2.2 EXPERIMENTAL STUDIES

A few field and laboratory experimental studies have been conducted to validate results obtained by the various numerical studies. Langford and Turner (1973) conducted an experimental study to evaluate the accuracy of the Kinematic wave theory to predict overland flow over a rough, uneven surface. They established rainfall simulator and runoff measurement system to simulate the rain and experiments were carried out on a plot of 75ft × 15ft. They conducted separate tests to measure the depression storage and the hydraulic roughness for flows without rain and under rain to predict the behaviour of overland flow and provided a series of recession curves using Kinematic wave theory. Vogel and Hopmans (1992) presented a two-dimensional analysis of furrow infiltration using 2-d finite element transient water flow model developed earlier. They monitored furrow irrigation during the growing season of calendar year 1989 in a 24 ha Cotton field in California. They measured infiltration and

ground water levels during each of the four irrigation events and measured infiltration at 20-25 locations during each irrigation using a flow through infiltrometer. Field soil measurements were used to compare field-measured and simulated infiltrated water for two-layered soil system. Wohling, et al. (2004) analyzed a surface-subsurface flow during furrow irrigation employing both a laboratory experiment and a surface-subsurface flow model. The model consists of an analytical zero-inertia surface irrigation model for the advance phase and a physically based two-dimensional (Hydrus-2D) infiltration model, which are coupled by an iterative procedure. To validate the coupled surface-subsurface model, furrow irrigation experiments were conducted in 26.4 m long, 0.88 m wide, and 1.0 m deep experimental tank filled with 50 tons of sandy loam soil. The experimental set up equipped with surface and subsurface measuring devices was built in the laboratory of the Institute of Hydraulic Engineering and applied Hydromechanics, Germany.

2.3 NUMERICAL STUDIES

The numerical solution of border strip irrigation involves the solution of both surface and subsurface flows. Most of the numerical models give greater importance to solve the surface flow more accurately and the subsurface flow is commonly taken in to account by using analytical solutions such as Kostiakov, Kostiakov-Lewis and Parlange equations. In the present study, the subsurface flow is solved using Richards equation. Hence, a comprehensive literature review is presented for both surface and subsurface flows.

2.3.1 Surface flow models

Strelkoff and. Katopodes (1977) developed a Zero-Inertia model for the analysis of border irrigation by neglecting the inertial terms in Saint Venant's equations governing overland flow. They employed Kostiakov infiltration equation for the

subsurface flow. They found that model computed irrigation advance match with the experimental data satisfactorily. Jaynes (1986) described a zero inertia model for complete irrigation cycles of sloping and level borders with different boundary conditions. The model solves the combined equations for the conservation of mass and momentum (Acceleration terms neglected) for surface flow simulation and for subsurface flow modeling, modified Kostiakov equation is used. Schwankl et al. (2000) used a zero inertia furrow irrigation model with specified space solution to investigate the effects of variability in inflow rate and spatial variability in infiltration, geometry and roughness on end of furrow advance and average infiltrated depth. They observed that the irrigation performance gets affected by inflow rate, infiltration, geometry and roughness in decreasing order. Wohling et al., (2006) developed a Furrow Advance Phase Model (FAP) by coupling Zero-Inertia surface flow model with the surface moisture transport model HYDRUS-2. FAPS exhibited better convergence numerical stability and required less computational time than the fixed time interval solution. Wohling and Schmitz (2007) extended FAPS by including storage, depletion, recession and plant water uptake which can be used for the entire crop growth period. Wohling and Mailhol (2007) applied the seasonal furrow irrigation model developed by Wohling and Schmitz (2007) to predict irrigation event data from real scale laboratory experiments conducted at Hubert-englis laboratory, Germany (Wohling etal., 2004 and 2006), field experimental data from Kharagpur, India (Schmitz et al., 2005 and Wohling et al., 2006). Their analysis revealed that calculated runoff is four to five times more sensitive to the inlet flow rate than to infiltration parameters. Furrow geometry parameters are most sensitive to calculated advance times in the short furrow with low opportunity time, whereas the inflow rate and infiltration parameters are more sensitive to calculated advance times in the long furrow with larger infiltration opportunity time.

Sherman and Singh (1978) discussed the analysis of surface irrigation process with kinematic wave theory. Depending on the variability of infiltration and kinematic wave friction parameter, three cases were distinguished (i) when infiltration is zero, (ii) when infiltration is constant and (iii) when infiltration is variable. They provided explicit analytical solutions for the case when infiltration is constant. However, explicit analytical solutions were not possible and a numerical approach based on specification of water depth using iterative scheme is suggested for variable infiltration. Sherman and Singh (1982) extended the kinematic model for surface irrigation reported previously by Sherman and Singh (1978). Depending upon the duration of irrigation and time variability of infiltration, they obtained explicit solutions for the case when infiltration is constant, and a stable and convergent numerical procedure is developed for the case when infiltration is varying in time. Singh and Ram (1983) discussed the applicability of a kinematic model for entire surface irrigation cycle by comparing model predictions with experimental data for 31 borders of varied characteristics with different end conditions. They used the method of characteristics to solve the governing equations and Kostiakov equation to determine the infiltration rate. Weir (1983) developed a kinematic model to study the surface irrigation process when the infiltration function consists of a long-time gravity term plus a short-time capilliary. He solved the model equations either exactly or numerically and presented several graphical solutions. Walker and Humpherys (1983) developed and verified a kinematic-wave model of furrow irrigation under both continuous and surged flow conditions. Numerical solution of the continuity equation is accomplished with first-order Eulerian integration coupled with the assumption that flow rate and flow area are uniquely related by the Manning's equation. They used Kostiakov-Lewis equation to estimate the infiltration.

Katopodes and Strelkoff (1977) presented a complete hydrodynamic model for border irrigation with the method of characteristics using Kostiakov equation for infiltration. They used second order accurate numerical scheme for the solution. Singh and Bhallamudi (1996) presented a hydrodynamic model for simulating all phases of border-strip irrigation using explicit, second-order accurate MacCormack scheme for the solution of the governing equations (Saint-Venant equations) for surface irrigation. In their study, Kostiakov and Parlange equations are used to compute infiltration. They proposed a simple subgrid technique to obtain a high grid resolution near the advancing front to minimize computational cost. Later, Singh and Bhallamudi (1998) developed a conjunctive surface-subsurface numerical model for the simulation of overland flow using the complete Saint-Venant equations and two-dimensional Richards equation in the mixed form for the subsurface flow. They found from the numerical simulation studies that, in many cases where the ground water table is deep, the unsaturated flow in the ground may be considered one dimensional. Such an assumption may be valid if the spatial variation in the subsoil characteristics is only in the vertical direction. However, two-dimensional effect does become significant if the spatial variation of the soil characteristics is complex. Wallender and Rayej (1990) presented a shooting method for Saint Venant equations of furrow irrigation. Unlike the two-point boundary-value solution of the full hydrodynamic model where the process started at the upstream end and swept downstream and then upstream during each iteration, the shooting or initial-value method started from the downstream end and proceeded upstream against the flow. They calculated flow area and discharge simultaneously for all nodes and advance distance was calculated for the given time step. Bautista and Wallender (1992) developed a complete hydrodynamic furrow irrigation model with specified space steps that solves for time of advance as a function of distance. The

model uses fixed time increments to compute storage and recession phases. They solved the system of finite difference equations with a shooting algorithm and used a modified version of the extended Kostiakov equation to compute infiltration that allows intake to vary with opportunity time and flow depth.

2.3.2 Subsurface flow models

The voids present in the unsaturated soil, is partly filled with water partly with air. Water is held in the voids due to surface tension forces. The pressure in the unsaturated zone is always less than the atmospheric pressure. The flow and storage characteristics are function of the pressure head. The subsurface can be accurately modelled by solving Richards equation (Richards, 1931) governing water flow through unsaturated zone.

Richards equation can be expressed in several forms with either pressure head (ψ) or moisture content (θ) as the dependent variable (Celia et al., 1990). The constitutive relationships between the moisture content and the pressure head allow conservation of one form of the equation to another. Three standard forms of the Richards equation may be identified as: the ψ-based form, the θ-based form and the mixed form.

***Pressure head based* (ψ-based)**

$$C(\psi)\frac{\partial \psi}{\partial t} = \frac{\partial}{\partial z}\left\{K(\theta)\left(\frac{\partial \psi}{\partial z} + 1\right)\right\} \tag{2.1}$$

***Moisture content based* (θ-based)**

$$\frac{\partial \theta}{\partial t} = \frac{\partial}{\partial z}\left(D(\theta)\frac{\partial \theta}{\partial z}\right) + \frac{\partial K(\theta)}{\partial z} \tag{2.2}$$

Mixed form

$$\frac{\partial \theta}{\partial t} = \frac{\partial}{\partial z}\left\{K(\psi)\left(\frac{\partial \psi}{\partial z} + 1\right)\right\} \tag{2.3}$$

In equations (2.1)-(2.3), ψ is the pressure head, θ is the moisture content, z is the vertical coordinate taken positive upwards, t is the time coordinate, $C = \frac{d\theta}{d\psi}$ is the specific moisture capacity of the soil, K is the unsaturated hydraulic conductivity of the soil and $D = K/C$ is the soil moisture diffusivity.

Relative merits of different forms

The θ-based formulation results in significantly improved performance (Hills et al., 1989) as compared to ψ-based formulation when modeling infiltrations into very dry soils. But θ-based algorithms can not be used for problems containing saturated regions, since the soil moisture diffusivity becomes infinity in the saturated regions. In contrast, the ψ-based formulation can be used for both saturated and unsaturated soils. However, while simulating problems involving steep wetting fronts moving into a very dry soil, ψ-based formulation requires very small time steps in order to maintain stability and minimize truncation errors. Celia et al., (1990) concluded that the solution of the ψ-based form is generally inaccurate and conserve mass poorly. El Kadi and Ge Ling (1993) proposed the Courant and Peclet number criteria for solving the ψ-based Richards equation with good accuracy. A mixed form of the Richards equation that includes both moisture content and pressure head as unknowns has the advantage over the ψ-based Richards equation because the former is more mass conservative than the latter (Celia et al., 1990; Clement et al., 1994). The mixed form can be solved in a computationally efficient manner and is capable of modeling a wide variety of problems including infiltration into very dry soils.

Richards equation is nonlinear in nature, since the flow and storage properties (K, C, D) are functions of the dependent variable ψ. The functional relationships between soil hydraulic properties (K, θ, ψ) are needed for analyzing unsaturated water flow in soils (Govindraju et al., 1992). In order to solve Richards equation, constitutive relationships between ψ and the nonlinear terms (θ, C and K) have to be specified. It is common practice to use a K- ψ relationship which is derived from θ- ψ relationship, using some physically based approach such as the distribution of pore sizes (Mualem, 1976).

θ- ψ relationship

The water retention characteristic (θ- ψ relationship) of the soil describes the soil's ability to store and release water. The θ- ψ relationship is called soil moisture retention curve or soil moisture characteristics (SMC). The shape of the SMC depends upon the pore size distribution of the soil. Many empirical functional forms exist in the literature for the SMC, the most popular being Brooks and Corey (1964), Campbell (1974) and Van Genuchten (1980) relationships. The parameters involved in these empirical relationships can be obtained from the pressure head moisture content data or by the mechanical properties such as particle size distribution, organic content, bulk density etc. Gupta and Larsen (1979) presented regression models for determining characteristics of soil from particle size distribution, percent organic matter and bulk density. Ghosh (1980) proposed methods for estimating soil moisture characteristics from mechanical properties. Saltar and Williams (1965) discussed the influence of texture on the θ- ψ characteristics.

The SMC should be such that the continuity should be present in the slope of the soil moisture retention curve and it should be amenable to yield closed form equations for the hydraulic conductivity. The relationship proposed by Van Genuchten

(1980) permits a representation of the total soil moisture characteristic (SMC). Campbell (1974) and Brooks and Corey (1964) relationships describe only the portion of the SMC for pressure heads less than the bubbling pressure or pressure at which air will enter the soil. In the present study, the relationship proposed by Van Genuchten (1980) is used for SMC.

It is experimentally observed that the SMC exhibits hysteresis, i.e., it has a different relationship when the soil is wetting than when it is drying. hysteresis is caused by entrapment of air in pockets connecting different size pores during wetting (Rawls et al., 1992). Poulovassilis (1962) proposed the concept of independent domains to account for the hysteresis based on pore geometry. Mualem (1974) developed a conceptual hysteresis model, with which all the scanning curves can be derived with the aid of simple functions from the main drying and wetting curves solely. Kool and Parker (1987) developed a hysteretic model based on Van Genuchten's (1980) θ-ψ model and the empirical hysteresis model of Scott et al. (1983). The resulting model yields closed form expressions for hysteretic moisture content, soil moisture capacity and the hydraulic conductivity. Hysteresis can be avoided if one considers either just a wetting cycle or just a drying cycle. For practical applications, hysteresis has mostly been neglected (Rawls et al., 1992).

Brooks and Corey's relationship

$$S_e = \left(\frac{\psi_b}{\psi} \right)^{\lambda} \quad for \ \psi \leq \psi_b$$

$$S_e = 1 \ for \ \psi > \psi_b \tag{2.4}$$

In eqns. (2.4), ψ_b is the bubbling pressure, λ is the pore-size index and S_e is the effective saturation defined as,

$$S_e = \frac{\theta - \theta_r}{\theta_s - \theta_r} \tag{2.5}$$

where, θ_s is the saturated moisture content and θ_r is the residual moisture content of the soil.

Campbell's relationship

$$\frac{\theta}{\theta_s} = \left(\frac{H_b}{\psi} \right)^{\frac{1}{b}} \quad for \ \psi \leq H_b$$

$$\frac{\theta}{\theta_s} = 1 \ for \ \psi > H_b \tag{2.6}$$

where, H_b is the scaling parameter with dimension of length, b is a constant.

Van Genuchten relationship

$$S_e = \left[\frac{1}{1 + (\alpha_v |\psi|)^{n_v}} \right]^{m_v} \qquad \text{for } \psi \leq 0$$

$$S_e = 1 \qquad \text{for } \psi > 0 \tag{2.7}$$

where, α_v and n_v are unsaturated soil parameters with $m_v = 1 - \frac{1}{n_v}$ and $n_v > 1$.

K- θ relationship

The hydraulic conductivity K is a measure of the ability of the soil to transmit water and depends upon both the properties of the soil and fluid. The hydraulic conductivity at or above saturation point ($\psi \geq 0$) is referred to as saturated hydraulic conductivity and for moisture content (θ) below saturation ($\psi < 0$), it is called the unsaturated hydraulic conductivity. The unsaturated hydraulic conductivity K is a nonlinear function of the moisture content θ. Many investigators used the empirical and semi-empirical methods for describing K- θ relationship. Wasseling and Wit (1969) proposed an experimental method based on infiltration, for determination of K- θ characteristics. Campbell (1974) proposed a method for determining unsaturated hydraulic

conductivity from moisture retention data. Dane (1980) compared field and laboratory determined hydraulic conductivity values. Ragab et al. (1981) made a comparative study of numerical and laboratory methods for determining hydraulic conductivity functions of sand. Dane and Hruska (1983) calibrated closed form relation for θ- ψ and K- θ relations in moisture content simulation study of a drainage problem. Hoover and Grant (1983) used least square approach to determine coefficients in the Taylor and Luthin (1969) relations. Ankeny et al., (1991) proposed a new method for determining in situ unsaturated hydraulic conductivities from unsaturated infiltration measurements made at several tensions on the same infiltration surface. Two approaches are generally used for predicting the hydraulic conductivity of unsaturated soils. According to the first approach, the relative hydraulic conductivity K_r is a function of power function of the effective saturation S_e, given by

$$K_r = \frac{K}{K_{sat}}$$

$$= S_e^{\gamma} \tag{2.8}$$

where, K_{sat} is the saturated hydraulic conductivity of the soil. For a wide range of soils, γ = 3.5 leads to a better agreement with experimental observations (Brooks and Corey (1964), Boreli and Vachaud, (1966) and Campbell (1974)).

The second approach makes use of the measured SMC to derive the hydraulic conductivity in the unsaturated state. The most popular among these are: Childs and Collis George (1950) and Burdine (1953) equations, which are given as follows.

Burdine equation

$$K_r(\theta) = S_e^{\,2}\left[\frac{\int_{\vartheta=0}^{\theta} \frac{d\theta}{\psi^2}}{\int_{\vartheta=0}^{\theta_{sat}} \frac{d\theta}{\psi^2}}\right] \tag{2.9}$$

Childs-Collis George equation

$$K_r(\theta) = S_e^{\varsigma} \frac{\sum_{i=1}^{l} \frac{[2(l-i)+1]}{\psi^2}}{\sum_{i=1}^{s} \frac{[2(s-i)+1]}{\psi^2}} \tag{2.10}$$

In Childs-Collis George equation, s represents the total number of intervals into which θ domain is divided; l is the number of intervals up to a prescribed value of θ and ς is the exponent whose value ranges between 0 and 4/3.

Mualem (1976) derived an expression for the relative hydraulic conductivity which is similar to Childs-Collis George equation and which is in better agreement with experimental observations. The Mualem's equation is given as

$$K_r(\theta) = S_e^{1/2} \frac{\int_{\theta=0}^{\theta} \frac{d\theta}{\psi}}{\int_{\theta=0}^{\theta_{sat}} \frac{d\theta}{\psi}} \tag{2.11}$$

Van Genuchten (1980) derived an expression for K_r by combining Mualem equation and the θ- ψ relationship, as

$$K_r = S_e^{1/2}\left[1-(1-S_e^{1/m_v})^{m_v}\right]^2 \tag{2.12}$$

In the present study Van Genuchten relationship for θ- ψ and K- θ relationship are used. These $K - \theta - \psi$ relationships have been very extensively used in the unsaturated flow literature (Paniconi et al., (1991), Celia et al., (1990) and El-Kadi and Ge ling (1993)).

2.3.2.1 Solution of Richards equation

Analytical Models

The Richards equation is highly nonlinear in nature; hence analytical solutions can be obtained only for simple boundary conditions and simple $K - \theta - \psi$ relationships. Most of the Analytical methods make use of relaxation techniques such as linearization quasilinearization and transformation to steady state [Philip (1969), Parlange (1972), Pullan (1990), Warrick et al., (1991)]. Philip (1969) discussed the quasi analytical and analytical solutions for unsaturated flow equation for multidimensional cases and for steady state cases. Parlange (1972) developed an analytical solution for infiltration from cylindrical cavities. He presented expression applicable for both very short and very long times and also provided a proper interpolation for moderate times. Broad-Bridge and White (1988) presented analytical solution for Richards' equation under constant rate rainfall infiltration. They assumed the soil moisture diffusivity and hydraulic conductivity to be simple functional forms of a single parameter which yield physically reasonably analytical moisture characteristics. Warrick et al., (1991) extended the analytical solution of Broad-Bridge and White (1988) to be applicable for time varying infiltration. The solution is expressed as a sum of two terms; the first is a function of the instantaneous infiltration and second an integral which accounts for the moisture distribution within the profile for the previous infiltration event. Pullan (1990) reviewed the quasilinear approximation techniques used for solving Richards' equation. Most of these techniques assumed an exponential relationship between the hydraulic conductivity and the moisture content which reduce the highly nonlinear Richards' equation under steady state regimes to a linear equation which can be solved analytically. Barry et al., (1993) derived an analytical solution for Richards' equation under ponded

infiltration. The solution is obtained by assuming that the form of soil moisture characteristic is a particular weighted integral of the gradient of the hydraulic conductivity.

Numerical Models

To obtain the analytical solutions for problems involving non homogeneous and realistic boundary conditions is extremely difficult. In such situations one has to resort to numerical techniques. Since 1980's numerous models have been developed based on finite element, finite difference and finite analytical methods for solving Richards' equation. Rubin (1968) presented the theoretical analysis of two dimensional flow of water in unsaturated soil using implicit finite difference method. Brutsaert (1971) solved the two dimensional Richards' equation using an implicit finite difference scheme with Newton's iteration technique. The results of his study showed that divergence or instability of the solution has greatly reduced even though the time taken for simulation is more. Neumann et al., (1975) used the finite element method for the analysis of two dimensional flows in unsaturated soils considering water uptake by roots. Feddes et al. (1978) provided the solution of suction head based form of the Richards equation using Crank-Nicolson finite difference scheme. Narsimhan et al., (1978) presented the solution of problems in subsurface hydrology using a finite element based mixed explicit-implicit scheme. Cooley (1983) used the sub domain finite element method to solve the Richards' equation. The method has advantage over finite difference methods in accomplishing a greater amount of nodal averaging of nonlinear quantities to improve stability. He also outlined new procedures for solving the nonlinear matrix equations and for locating positions of seepage faces. Huyakorn et al., (1986) developed two dimensional Galerkin finite element models for solving Richards equation. In their study the element matrices are evaluated in a simple

and efficient manner using influence coefficient technique. This technique avoids numerical integration and leads to a substantial saving of computational cost. Kaluarachchi and Parker (1987) developed a two dimensional Galerkin finite element model for flow through unsaturated soil. They employed forth order Runge Kutta time integration method which allows use of time steps at least two times greater than for a traditional finite difference approximation of time derivatives. This method has advantage of requiring less computational effort while simulating problems having large time duration. Feddes et al. (1988) reviewed the developments in modeling soil moisture movement in the unsaturated zone. Ross (1990) developed two efficient finite difference methods namely fixed grid method and advancing front method. He demonstrated that large time steps are possible when mass conservative mixed form of Richards' equation is combined with an implicit scheme, while a hyperbolic sine transform for the matrix potential allows large spatial increments even in a dry inhomogeneous soil. Celia et al., (1990) proposed a mixed form of Richards' equation which combines the benefits of both θ based and ψ based formulations for improving the poor mass balance and associated poor accuracy in ψ based formulation. However, they pointed out that this mixed form of Richards' equation is not sufficient to guarantee accurate solutions while simulating infiltration in dry soils. Paniconi et al., (1991) evaluated the performance of iterative and non iterative techniques while solving the Richards' equation. They evaluated the accuracy of two first order accurate non iterative methods and two second order accurate non iterative methods along with the standard Picard and Newton iterative methods. They found that the second order accurate non iterative schemes can be used as an alternative for iterative methods. Vogel and Hopmans (1992) presented a two dimensional finite element transient model to simulate infiltration by furrow irrigation with a shallow water table. Gottardi and

Venutelli (1992) developed a moving finite element model for solving one dimensional infiltration in to an unsaturated soil. In this method the grid points are moved during computation along the wetting front so that accuracy can be maintained by using smaller number of nodes, thus saving a lot of computational time. But the limitations of this method are that it can't be used to simulate unsaturated flow behaviour in layered soils or problems in which the top boundary condition is variable in time so that multiple wetting fronts occur. Kirkland et al., (1992) proposed algorithms for solving θ based formulation results an improved computational efficiency over ψ based formulation. However, the usefulness of θ based formulation is limited since it can't be applied to saturated soils. They defined a new variable for the transformed Richards equation which has the characteristics of water content when soil is unsaturated and of pressure head when the soil is at or near saturation. Tasi and Chen, (1993) developed a finite analytical numerical model for analyzing unsaturated flow with irregular boundaries. This method involves evaluating analytical solutions at each interior node of the flow domain which is written in terms of the nodal head values of the adjacent nodes. These analytic functions are solved simultaneously to get the solution for the entire domain. El-Kadi and Gi ling, (1993) proposed courant and peclet number criteria for estimating spatial and temporal mesh sizes while solving the Richards' equation numerically. They argued that, in the absence of criteria for mesh design, acceptance of a solution based on mass conservation and the rate of convergence may no guarantee accurate solutions. Huang et al., (1994) used the Eulerian–Lagrangian approach for simulating flow through an unsaturated soil. The method separates the governing flow equation into convective and diffusion parts which can be solved with the method of characteristics and the conventional finite element method respectively. The method is mass conservative, virtually oscillation free and computationally quite efficient.

Clement et al., (1994) developed a physically based two dimensional finite difference algorithm based on mixed form of Richards' equation proposed by Celia et al., (1990). The finite difference equations are solved by computationally efficient preconditioned conjugate gradient method. Rathfelder and Abriola, (1994) developed efficient conservative solutions of the head based form of the Richards' equation. They have demonstrated that the proper evaluation of specific moisture capacity term improves the mass conservation of the numerical schemes. Letha and Elango, (1994) compared the performance of Brooks and Corey (1964) and Van Genuchten (1980) θ- ψ and K- θ relationships by simulating numerically a furrow irrigation problem using Galerkin finite element method. They suggested that a weighted least square procedure improves the fit of the Brooks and Corey θ- ψ relationship at mild unsaturated range which is a commonly observed while irrigating a course soil. Their study also indicated that a numerical integration procedure improves the fit of Van Genuchten characteristic function for K- θ relationship. Clemente et al., (1994) compared three unsaturated soil water flow models in agricultural water management. Janz and Stonier (1995) used θ-based Richards equation with a macroscopic sink term to produce soil water content profiles at any time. They employed Crank-Nicolson finite difference scheme and solved it by using implicit central difference approximation. Singh and Bhallamudi (1996) developed a numerical model based on Mac Cormack finite difference scheme to study the effect of overland flow depth on infiltration in coupled overland subsurface flows. Singh and Bhallamudi (1998) developed a conjunctive surface-subsurface numerical model for the simulation of overland flow. They solved the complete Saint-Venant equations using explicit essentially non oscillating (ENO) finite-difference scheme for surface flow and two-dimensional Richards equation in the mixed form for subsurface flow simulation. Zhu and Satish, (1999) studied the effect of stochasticity in

soil properties on flow and transport in porous media. Hari Prasad et al. (2001) developed a numerical model to perform the sensitivity analysis of gravity drainage and infiltration process on unsaturated soil parameters. Sato et al. (2003) investigated the importance of soil texture properties and water content on pore water velocity and associated solute dispersion in unsaturated zone. Ojha et al., (2003) studied the effect of soil propertied in soil piping during a levee failure. Hari Prasad et al., (2005) developed a simple numerical model to estimate groundwater recharge from unsaturated flow measurements. Dogan and Motz (2005a, b) solved finite difference formulation of mixed form of Richards equation with volumetric source or sink term using modified picard iteration scheme. They developed a new saturated-unsaturated 3-D rainfall driven groundwater flow model (SU3D) to simulate most of the important elements of the hydrological cycle. They used the preconditioned conjugated gradient method which has advantage over other iterative methods in terms of computer memory requirements and faster convergence to solve the linear system of the equations.

2.3.3 Estimation of Infiltration Parameters

Accurate prediction of surface irrigation events requires the knowledge of system parameters such as Mannings' roughness coefficient n and infiltration parameters: saturated hydraulic conductivity K_{sat}, water retention parameters α_v, n_v, θ_s and θ_r. Among these, the estimation of infiltration parameters at field level is one of the difficult tasks (Walker and Skogerboe, 1987). For a relatively big field, estimation of infiltration parameters using infiltrometers requires that the test be conducted at many places. Further, these parameters may not represent the infiltration phenomenon at field scale. An alternative to these direct measurement techniques is to employ inverse techniques for parameter estimation. In such an approach, the infiltration parameters are estimated by minimizing the deviations between the model predicted and field

observed flow attributes such as irrigation advance, recession, flow depth and wetting front movement. In the following sections literature review regarding the estimation of infiltration parameters (k_{sat}, α_v, n_v) using inverse procedure is presented.

Inverse Problem

Numerical Models for surface irrigation produce results that depend heavily on the field parameters supplied to the models as input. Many investigations have been conducted attempting either to measure directly or estimate the coefficients appearing in the resistance and infiltration formulas used in surface irrigation models. Direct measurement is technically preferable, but the spatial and temporal variability of the field parameters, the difficulty and expense of the required instrumentation, and the variety of alternative formulas have limited the use of such studies to the supply of the data for verification of mathematical models (Roth, et. al., 1974). It is therefore more realistic to evaluate indirectly the resistance and infiltration parameters by monitoring physically measurable variables, such as the rate of advance and the depth of flow.

Parameter estimation using inverse procedures have become an alternative to direct inversion methods (Kool and Parker, 1988). In such a procedure, the parameters are estimated by minimizing the deviations between the observed and model predicted output for prescribed, but arbitrary initial and boundary conditions. Contrary to the direct inversion methods, the optimization approach does not put any inherent constraint on the form or complexity of the model, on the stipulation of the initial and boundary conditions, on the constitutive relationships, or on the treatment of inhomogeneities via deterministic or stochastic representations. Thus, a major advantage is that experimental conditions can be selected on the basis of convenience and expeditiousness, rather than by a need to simplify the mathematics of the direct inversion process.

2.3.3.1 Posedness, Identifiability, Uniqueness and Stability

Three important factors which, need attention while estimating parameters using inverse procedure are i) identifiability ii) uniqueness and iii) stability (Russo et al., 1991). Consider a functional relationship between the response $\boldsymbol{R}$ and the set of parameters $\boldsymbol{p}$, i.e. $\boldsymbol{R=F(p)}$. The inverse relationship i.e. $\boldsymbol{p=I(R)}$ determines the parameters which is known as inverse problem. This problem is properly posed if and only if i) a solution exists; ii) the solution is unique for any given $\boldsymbol{R}$; and iii) the solution is stable (Russo et al., 1991). The illposedness may sometimes be due to nonuniqueness, sometimes due to nonidentifiability or sometimes due to stability (Carrera and Neumann, 1986). If the inverse problem fails to satisfy one or more of these requirements, it is then referred to as being ill posed. Uniqueness refers to the inverse relationships $\boldsymbol{I}$. When $\boldsymbol{I}$ represents the minimization of an estimation criterion (such as the deviation between observed and predicted concentration), the inverse solution is nonunique whenever the criterion to be minimized is nonconvex, i.e. it has local minima or global minimum at more than one point in the parameter space. In other words, if a given response $\boldsymbol{R}$ leads to more than one set of parameter values $\boldsymbol{p}$, the inverse solution is nonunique. If more than one parameter set $\boldsymbol{p}$ leads to a given response $\boldsymbol{R}$, the parameters are unidentifiable. In contrast Stability means that small errors in the response data must not result in large changes in the estimated parameters. Instability may arise from a lack or poor degree of identifiability and it is generally associated with an estimation criterion that is flat near minimum.

2.3.3.2 Classification of Parameter Identification Methods

Newman (1973) classified the inverse problem of parameter estimation into two different approaches, namely direct and indirect. The direct approach treats the model parameters as dependent variables in a formal inverse boundary value problem. The

indirect approach is based upon an output error criterion where an existing estimate of the parameters is iteratively improved until the model response is sufficiently close to that of the measured output (Yeh, 1986). Kubrusly (1977) classified the distributed parameter estimation procedures into three categories. i) direct method which consists of those methods that use optimization techniques directly to the distributed model ii) reduction to a lumped parameter system, which consists of those methods that reduce the distributed parameter system to a continuous or discrete-time lumped parameter system which is described by ordinary differential equation and iii) reduction to an algebraic equation which consists of those methods that reduce the partial differential equation to an algebraic equation.

2.3.3.3 General Formulation of the Estimation Problem

Many parameter estimation problems can be formulated as a weighted least-squares minimization problem.

$$\min_{\boldsymbol{b}} \phi(\mathbf{b}) = \frac{1}{2}(L_b^* - L_b)^T W (L_b^* - L_b) \tag{2.13}$$

where the objective function, $\phi(\boldsymbol{b})$, is a function of the model parameters $\boldsymbol{b}$, $\mathbf{b} = (b_1, b_2 - - - - - b_m)^T; \mathbf{L}^* = (L_1^*, - - - L_n^*)^T$ is the observation vector whose elements represent measured concentrations; $\mathbf{L}(\mathbf{b}) = \{L_1(b), - - - L_n(b)\}^T$ represents the predicted response for a given parameter vector $\boldsymbol{L}$, and $\boldsymbol{W}$ is symmetric weighting matrices. The coefficient 1/2 in above equation is purely for notational convenience. The objective is to find the parameter vector $\boldsymbol{L}$ that minimizes the Eq (2.24) or in other words, results in a best fit between the model predicted and observed data. The weighting matrices $\boldsymbol{W}$ contain information about measurement accuracy, as well as possible correlations between measurement errors and between parameters. In the

absence of any additional information besides the observations L^*, the simplest and recommended approach is to set W equal to the identity matrix, i.e, W =1. In this case the Eq (2.24) reduces to the well known ordinary least squares (OLS) problem.

$$\min_{\mathbf{b}} \phi(\mathbf{b}) = \frac{1}{2}(L_b^* - L_b)^T (L_b^* - L_b) = \frac{1}{2}\sum_{i=1}^{N} (L_b^* - L_b)^2 \qquad (2.14)$$

The OLS formulation has probably been the most popular one for parameter estimation problems. Its attraction is due to its simplicity and because it requires a minimum amount of information. When observation errors are normally distributed, are uncorrelated and have a constant variance, the OLS estimates possess optimal statistical properties. When these conditions are not met, the OLS method will no longer yield optimal parameter estimates in terms of precision and minimum variance. More serious difficulties arise due to violation of the constant variance and uncorrelated errors assumptions. These situations often occur in practical problems. For instance, error variances are commonly found to increase with the magnitude of the property being measured.

2.3.3.4 Studies on Estimation of Parameters using Inverse Procedure

Few studies have been reported in estimating/identifying infiltration parameters using inverse procedure in the literature. Norum and Gray (1970) and Merriam (1985) estimated the parameters of power-law models of surface irrigation system from irrigation advance. However, the parameters so obtained may not be useful for other models, thus provide lumped estimates of field coefficients as opposed to true parameters describing the field conditions. Katopodes (1990) examined the conditions of observability and parameter identifiability for surface irrigation advance using analytical techniques and the linearized zero-inertia model. His study showed that linearized zero-inertia model is conditionally observable and the roughness and two

infiltration parameters can't be identified from measurements of the rate of advance alone. However, these three parameters can be identified from measurement of the surface water profile. Katopodes et al., (1990) estimated the surface irrigation parameters by minimizing the deviations between field observations and linearized zero-inertia model predictions. The minimization was carried out using conjugate gradient and variable metric techniques. They concluded that formulation of the direct problem and its numerical solution plays a key role in the optimization and the search converges quickly when the influence of independent parameters can be decoupled during construction of the objective function. Bautista and Wallender (1993) studied the identification of furrow infiltration parameters by minimizing the squared difference of observed and model predicted advance times as a function of distance. They also investigated the identifiability using an alternative objective function in terms of velocity of the advancing wave. Marquardt algorithm was used in the optimization. Their study indicated that faster convergence and larger radius of convergence is achieved when velocities are used in objective function rather than advance times. Their study also showed that measurement errors and system perturbations impede the identification process.

2.4 OBJECTIVES OF THE PRESENT STUDY

The present study is concerned with the numerical modeling of surface and subsurface flow and estimation of infiltration parameters. Keeping this in view, the following objectives are considered.

1. To develop a numerical model for the analysis of different phases of border strip irrigation system by solving coupled differential equations governing both overland (Saint-Venant equations) and subsurface (Richrads equation) flows.

2. To validate the numerical model by comparing the model results with experimentally observed advance and recession phases of irrigation events reported in literature.
3. To conduct field experiments to study the performance of the numerical model in predicting the advance and recession phases of border strip irrigation and soil moisture movement in subsurface.
4. To develop a parameter estimation model for the estimation of infiltration parameters from the measured irrigation advance, flow depth and moisture content data.
5. To address the issue of identifiability of model parameters from the irrigation advance, flow depth and moisture content data.

CHAPTER 3

MODEL DEVELOPMENT

3.1 INTRODUCTION

The present chapter discusses the development of a hydrodynamic numerical model for the simulation of overland and subsurface flow for border strip irrigation. A numerical model is developed for solving the differential equations governing overland flow (Saint Venants equations) and subsurface flow (Richards equation). MacCormack scheme is used to solve the Saint Venants equations while the Richards equation is solved using a mass conservative fully implicit finite difference method. The model performance is assessed by comparing model predicted irrigation advance and recession with the data reported in literature. Fig. 3.1 shows the schematic diagram of border strip irrigation.

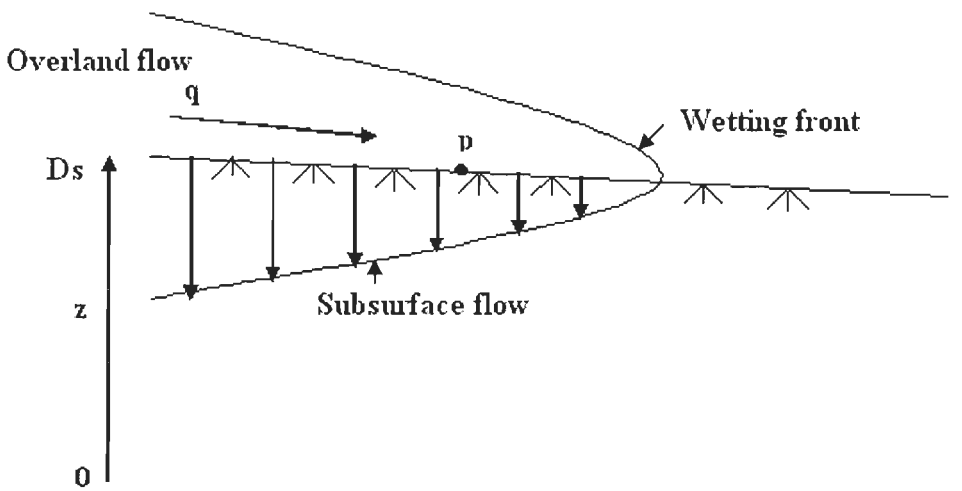

Fig. 3.1: Schematic diagram of border strip irrigation

In Fig. 3.1, water is applied at the upstream end of the border strip, which has a slope of S_0. As the water flows downstream, it gets percolated into subsurface soil as shown in Fig. 3.1. Modelling such an irrigation system, requires governing equations for both overland and subsurface flows.

3.2 MODEL DEVELOPMENT

Fig. 3.1 shows the schematic diagram depicting overland and subsurface flow in border strip irrigation. Irrigation water is applied at the upstream end of the border strip which has a slope. As the water flows on the ground surface it starts infiltrating into the subsurface. Mathematical analysis of such a flow requires the solution of coupled partial differential equations governing overland and subsurface flows.

3.2.1 Governing Equations for Overland Flow

The partial differential equations governing overland flow in a wide rectangular border strip in Cartesian co-ordinates (Singh & Ballamudi, 1996) are

$$\frac{\partial h}{\partial t}+\frac{\partial q}{\partial x}+q_s=0 \tag{3.1}$$

$$\frac{\partial q}{\partial t}+\frac{\partial}{\partial x}\left[\frac{q^2}{h}+\frac{gh^2}{2}\right]=gh\left(S_0-S_f\right) \tag{3.2}$$

where, h is flow depth, q is discharge per unit width, g is acceleration due to gravity, q_s is volumetric rate of infiltration per unit area, S_0 is slope of the border, S_f is friction slope, x is distance along the border strip and t is time. The friction slope S_f in Eq. (3.2) is calculated using the Manning's formula.

$$S_f=\frac{q^2n^2}{h^{10/3}} \tag{3.3}$$

where, n is Manning's roughness coefficient.

3.2.1.1 Initial and Boundary Conditions:

Initial condition:

Although dry-bed conditions occur before the start of irrigation in the border, however, to start the computations, a small uniform initial flow depth is specified at all the nodes at initial time (i.e. t = 0). Correspondingly, a uniform discharge computed using the Manning's equation is specified as initial discharge throughout the length of the border strip. The value of initial flow depth is chosen such that it is as small as possible and at the same time provides numerically stable results.

i.e. $t = 0; \quad h = h_{ini}, \quad q = q_{ini} \quad 0 < x < L$ (3.4)

Boundary conditions:

The boundary conditions at the upstream and downstream of the border strip depend on the irrigation phases such as advance, storage and depletion and recession phase. These conditions are described in detail as below.

Advance phase

The advance phase starts from the instant water is released at the upstream end of the border and continues till the irrigation front reaches the downstream end. The boundary is written as

$0 \le t \le t_{ds} \quad x = 0, \quad q = q_{us}$ (3.5a)

$x = L, \quad q = q_{ini}$ (3.5b)

where, t_{ds} is the time taken for the irrigation front to reach the downstream end, q_{us} is the inlet discharge per unit width. The flow depth at the upstream end is obtained using the negative characteristic equation of the Eqs. (3.1) and (3.2). The flow depth at the downstream is set equal to initial flow depth h_{ini}.

Storage phase

Storage phase starts when the irrigation front reaches the downstream end (t_{ds}) and continues up to the instant at which the irrigation supply is cutoff. The upstream boundary condition remains the same as in the case of advance phase, since the discharge q flows continuously into the border at the upstream end during this phase. The boundary is written as

$$t_{ds} < t < t_c; \qquad x = 0, \qquad q = q_{us} \tag{3.6}$$

where, t_c is the time of cutoff of water supply. It is assumed that the flow leaves the border at downstream at normal condition. To determine the flow depth and discharge at the downstream boundary, the positive characteristic equation of the governing equations (Eqs. 3.1 and 3.2) and Manning equation are solved simultaneously.

Depletion and Recession phase

During these phases, the discharge at the upstream end is stopped and hence, the discharge at the upstream becomes zero. As a consequence, the flow depth at the upstream tends to become zero. It is assumed that recession reaches at a point when the flow depth becomes less than or equal to initial flow depth. Here also, to avoid numerical difficulties, the flow and flow depth is kept as initial flow q_{ini} and flow depth. The boundary is written as below.

h_{ini}. i.e. $t \geq t_c$ $x = 0$; $q = q_{ini}$, $h = h_{ini}$ (3.7)

However, the boundary condition at the downstream end is kept same as in the storage phase.

3.2.2 Governing Equation for Subsurface Flow

To compute the sink term q_s present in continuity equation (Eq. 3.1), one needs to know the amount of water infiltrated into the ground. Now days, in most of the studies of unsaturated zone, the fluid motion is assumed to obey the classical Richards

equation (Celia et al., 1990). The Richards equation (1931) embodies the mechanism by which moisture redistributes within a particular soil. This equation is a combination of Darcy's law and the continuity equation. In this study, for the analysis of infiltration process, one dimensional Richards equation is used.

The mixed form of the Richard's equation (Celia et al., 1990) for one-dimensional vertical flow can be written as

$$\frac{\partial}{\partial z}\left[K(\psi)\left(\frac{\partial \psi}{\partial z} + 1 \right) \right] = \frac{\partial \theta}{\partial t} \tag{3.8}$$

where ψ is the pressure head, θ is the volumetric moisture content, K is hydraulic conductivity, z is the vertical co-ordinate taken positive upwards, and t is the time co-ordinate. The Eq. (3.8) is highly nonlinear in nature, since, both the flow and storage properties (K and θ) are functions of the dependent variable ψ and its solution requires constitutive relationships.

3.2.2.1 Constitutive Relationships

In the present study, the relationships proposed by Van Genuchten (1980) are adopted for θ-ψ and K-θ relationships, which are described as follows.

$\theta - \psi$ Relationship

$$S_e = \left[\frac{1}{1 + (\alpha_v |\psi|)^{n_v}} \right]^{m_v} \qquad \text{for } \psi < 0$$

$$S_e = 1 \qquad \text{for } \psi \geq 0 \tag{3.9}$$

where α_v and n_v are unsaturated soil parameters with $m_v = 1-(1/n_v)$, $n_v > 1$ and S_e is the effective saturation defined as

$$S_e = (\theta - \theta_r)/(\theta_s - \theta_r) \tag{3.10}$$

where θ_s and θ_r are saturated moisture content and residual moisture content of the soil respectively.

$K-\theta$ Relationship

$$K = K_s S_e^{1/2}\left[1-\left(1-S_e^{1/m_v}\right)^{m_v}\right]^2 \qquad \text{for } \psi < 0$$

$$K = K_s \qquad \text{for } \psi \geq 0 \qquad (3.11)$$

where, K_s is the saturated hydraulic conductivity of the soil.

3.2.2.2 Initial and Boundary conditions:

Initial condition

Before the start of an irrigation event, the subsurface soil in the border is assumed to be very dry, therefore a very high negative pressure head is assumed as initial condition throughout the length of subsurface soil considered.

$$t = 0; \qquad 0 < z < D_s, \qquad \psi = \psi_{ini} \qquad (3.12)$$

where, D_s is the vertical depth of the subsurface considered and ψ_{ini} is the initial pressure head in the subsurface before irrigation.

Boundary conditions:

The top and bottom boundary conditions are described as follows.

Top boundary condition:

The water starts infiltrating into the subsurface soil at a point 'p' (Fig. 3.1) along the border strip only after the irrigation front reaches that point and continues to infiltrate till the recession front passes through that point. Denoting $t_{adv,p}$ and $t_{rec,p}$ as the times at which the irrigation advance and recession fronts arrives at a point 'p' respectively, the top boundary condition is written as

$$t_{adv,p} < t < t_{rec,p}, \qquad z = D_s, \qquad \psi = h \qquad (3.13)$$

where, h is the flow depth obtained by solving the Eqs. (3.1) and (3.2) governing overland flow. At all other times, it is assumed that infiltration is zero at point 'p'.

Bottom boundary condition:

It is assumed that the water flows freely due to gravity at the bottom of the solution domain. Hence, a gravity drainage boundary condition is specified at bottom boundary as given below.

$$t_{adv,p} < t < t_{rec,p}, \qquad z = 0, \qquad \frac{\partial \psi}{\partial z} = 0 \tag{3.14}$$

3.2.3 Numerical Scheme

The differential Eqs. (3.1), (3.2) and (3.8) are nonlinear partial differential equations and are coupled by the sink term q_s in Eq. (3.1). These three equations have to be solved simultaneously to obtain the solution. In the present study, MacCormack finite-difference scheme is used for solving overland flow equations and a mass conservative implicit finite difference scheme is used for solving subsurface flow equation.

Fig. 3.2 shows a finite difference numerical grid imposed over the solution domain. The length of the border strip is divided into uniform segments of length Δx along the x-direction. The overland flow equations (Eqs. 3.1 and 3.2) are solved numerically to obtain the flow depth at each surface nodal point. Having obtained the flow depths at each of the surface nodal points, this depth is imposed as the driving head to analyse the moisture flow through the subsurface by solving the subsurface flow equation (Eq. 3.8) along each vertical below the surface nodal points. Each vertical is divided into uniform segments of length Δz along z-direction. The development of the numerical model is discussed in detail in the following sections.

3.2.3.1 Numerical Scheme for Overland Flow:

MacCormack scheme (Singh & Ballamudi, 1996) is used to solve Eqs. (3.1) and (3.2). In Fig. 3.2, the index i refers to a typical surface node in x-direction. The index k refers to the discrete time at which solution is known and index k+1 refers to the

discrete time at which solution is sought with'Δt' being the time increment between time levels k and k+1.

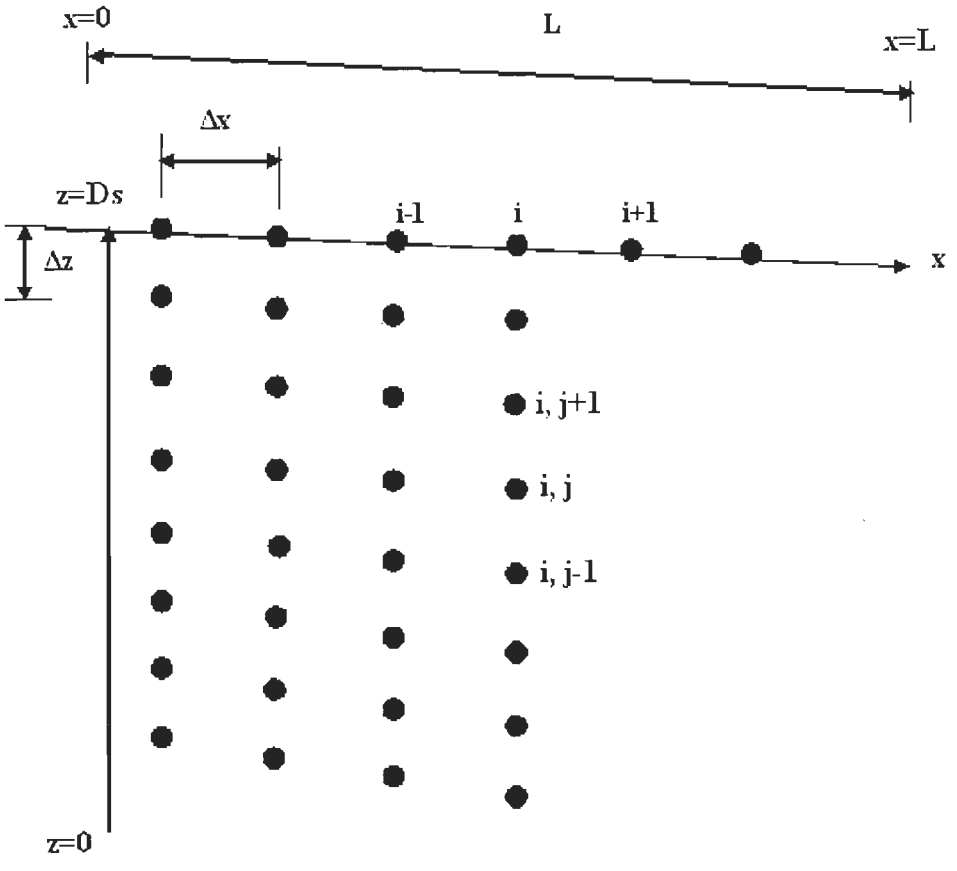

Fig. 3.2: Finite–Difference grid for numerical solution

3.2.3.1.1 Finite Difference (FD) Approximation:

The discrete values of continuous variables appearing in the differential Eqs. (3.1 and 3.2) are denoted as follows:

i. Flow depth at node i, at time level k: h_i^k

ii. Flow depth at node i, at time level k+1: h_i^{k+1}

iii. Discharge at node i-1, at time level k: q_{i-1}^k

iv. Discharge at node i, at time level k: q_i^k

v. Discharge at node i+1, at time level k: q_{i+1}^k

vi. Cumulative infiltration at node *i*, at time level *k*: I_i^k

vii. Cumulative infiltration at node *i*, at time level *k*+1: I_i^{k+1}

viii. Friction slope at node *i*, at time level *k*: $S_{f(i)}^k$

3.2.3.1.2 Predictor part:

Forward finite-difference approximations are used in the predictor part to convert Eqs. (3.1) and (3.2) into algebraic equations. Accordingly, Eq. (3.2) gets transformed into an explicit equation for predicted discharge q_i^p at node *i* as

$$q_i^p = q_i^k - \frac{\Delta t}{\Delta x}\left[\frac{(q_{i+1}^k)^2}{h_{i+1}^k} - \frac{(q_i^k)^2}{h_i^k} + \frac{g}{2}((h_{i+1}^k)^2 - (h_i^k)^2)\right] + g dt h_i^k \left[S_0 - S_{f(i)}^k\right] \quad (3.15)$$

Similarly, Eq. (3.1) results into a finite difference equation involving the predicted flow depth h_i^p and the cumulative infiltration at unknown time level *k*+1 as

$$h_i^p + I_i^{k+1} = h_i^k + I_i^k - \frac{\Delta t}{\Delta x}\left(q_{i+1}^k - q_i^k\right) \quad (3.16)$$

The cumulative infiltration at the known time level I_i^k as well as at the unknown time level I_i^{k+1} are equal to zero if the wetting front has not arrived at node *i*. The cumulative infiltration I_i^{k+1} is equal to I_i^k if the recession front has already arrived at node *i*. In the present study, the cumulative infiltration at the unknown time level I_i^{k+1} is computed by solving the subsurface flow Eq. (3.8) which is discussed in detail later. Knowing the cumulative infiltration I_i^{k+1}, predicted flow depth h_i^p can be computed explicitly using Eq. (3.16).

3.2.3.1.3 Corrector part:

The corrector part is similar to the predictor part except that backward finite differences are used to approximate the spatial differential terms and the predicted values obtained from the predicted part are used instead of the values at the known time

level. Accordingly, Eq. (3.2) gets transformed into an explicit equation for corrected discharge q_i^c at node i as

$$q_i^c = q_i^k - \frac{\Delta t}{\Delta x}\left\{\frac{(q_{p(i)}^k)^2}{h_{p(i)}^k} - \frac{(q_{p(i-1)}^k)^2}{h_{p(i-1)}^k} + \frac{g}{2}\left[(h_{p(i)}^k)^2 - h_{p(i-1)}^k)^2\right]\right\} + gdth_{p(i)}^k(S_0 - S_{f(i)}^k) \tag{3.17}$$

Similarly, Eq. (3.1) results into a finite difference equation involving the corrected flow depth h_i^c and the cumulative infiltration at unknown time level k+1 as

$$h_i^c + I_i^{k+1} = h_i^k + I_i^k - \frac{\Delta t}{\Delta x}\left(q_{p(i)}^k - q_{p(i-1)}^k\right) \tag{3.18}$$

Finally, the values of flow depth and discharge at the new time level are determined by taking the average of predicted and corrected values.

$$h_i^{k+1} = 0.5(h_i^p + h_i^c) \tag{3.19}$$

$$q_i^{k+1} = 0.5(q_i^p + q_i^c) \tag{3.20}$$

3.2.3.2 Numerical Scheme for Subsurface Flow

A mass conservative fully implicit finite difference numerical scheme proposed by Celia et al. (1990) is used for solving Eq. (3.8).

3.2.3.2.1 Discretization in space and Time

The spatial index j below each surface node i in the z-direction increases from bottom to top (Fig. 3.2) and the corresponding node is denoted by i,j.

The time domain has been discretized by finite number of discrete times of size, Δt. Due to high non-linear nature of Richards' equation, very small time step is used in the simulation. k denotes the discrete time level where the solution is known, k+1 denotes the discrete time level where the solution is unknown. The previous and current Picard iteration levels are denoted as m and m+1 respectively.

3.2.3.2.2 Finite Difference (FD) Approximation

The discrete values of continuous variables appearing in the differential equation (Eq. 3.8) are denoted as follows.

i. Pressure head ψ at node i,j, at time level k+1 and at Picard iteration level m: $\psi_{i,j}^{k+1,m}$

ii. Pressure head ψ at node i,j, at time level k+1 and at Picard iteration level m+1: $\psi_{i,j}^{k+1,m+1}$

iii. Hydraulic conductivity K at node i,j, at time level k+1 and at Picard iteration level m : $K_{i,j}^{k+1,m}$

iv. Moisture content θ at node i,j, at time level k+1 and at Picard iteration level m: $\theta_{i,j}^{k+1,m}$

v. Soil moisture capacity C at node i,j, at time level k+1 and at Picard iteration level m: $C_{i,j}^{k+1,m}$

3.2.3.2.3 Spatial Approximation

For a typical interior node i,j (Refer Fig. 3.2), a fully implicit, finite difference approximation of the non-linear spatial terms on left hand side of the Eq. (3.8), using Picard iteration scheme (Clement et al., 1994) is written as:

$$\frac{1}{\Delta z}\left[\left\{\frac{K_{i,j}^{k+1,m}+K_{i,j+1}^{k+1,m}}{2}\right\}\left\{\frac{\psi_{i,j+1}^{k+1,m+1}-\psi_{i,j}^{k+1,m+1}}{\Delta z}\right\}-\left\{\frac{K_{i,j}^{k+1,m}+K_{i,j-1}^{k+1,m}}{2}\right\}\left\{\frac{\psi_{i,j}^{k+1,m+1}-\psi_{i,j-1}^{k+1,m+1}}{\Delta z}\right\}\right]$$
$$+\frac{1}{\Delta z}\left[\left\{\frac{K_{i,j}^{k+1,m}+K_{i,j+1}^{k+1,m}}{2}\right\}-\left\{\frac{K_{i,j}^{k+1,m}+K_{i,j-1}^{k+1,m}}{2}\right\}\right] \qquad (3.21)$$

3.2.3.2.4 Temporal Approximation

The temporal variation in moisture content owing to changes in pressure is approximated using a backward Euler approximation coupled with a Picard iteration scheme. The discretization of the temporal term on right hand side of the Eq. (3.8), containing the time derivative of the moisture content (Clement et al., 1994) is written as:

$$\frac{\partial \theta}{\partial t} \approx \frac{\theta_{i,j}^{k+1,m+1} - \theta_{i,j}^{k}}{\Delta t} \tag{3.22}$$

After Celia et al., (1990), the term $\theta_{i,j}^{k+1,m+1}$ in Eq. (3.22) is expanded using a first-order, truncated Taylor series, in terms of the pressure-head perturbation arising from Picard iteration, about the expansion point $(\theta_{i,j}^{k+1,m}, \psi_{i,j}^{k+1,m})$, neglecting all higher order terms and is written as:

$$\theta_{i,j}^{k+1,m+1} \approx \theta_{i,j}^{k+1,m} + \left(\frac{\partial \theta}{\partial \psi}\right)_{i,j}^{k+1,m} \left(\psi_{i,j}^{k+1,m+1} - \psi_{i,j}^{k+1,m}\right) \tag{3.23}$$

The specific moisture capacity of a soil (L^{-1}) is defined as

$$C(\psi) = \frac{\partial \theta}{\partial \psi} \tag{3.24}$$

Using Eqs. (3.22)-(3.24), the partial time derivative of water content is approximated as

$$\frac{\partial \theta}{\partial t} \approx \left(\frac{\theta_{i,j}^{k+1,m} - \theta_{i,j}^{k}}{\Delta t}\right) + C_{i,j}^{k+1,m} \left(\frac{\psi_{i,j}^{k+1,m+1} - \psi_{i,j}^{k+1,m}}{\Delta t}\right) \tag{3.25}$$

The first term on the right side of Eq. (3.25) is an explicit estimate for the partial time derivative of the moisture content, based on the Picard level *m*, estimates of pressure head. In the second term of the right side of Eq. (3.25), the numerator is an estimate of the error in the pressure head at node *i,j*, between two successive Picard iterations. Its value diminishes as the Picard iteration process converges. As a result,

when the Picard procedure proceeds, the contribution of the specific moisture capacity $C(\psi)$ is diminished. This behavior, coupled with the fact that the specific moisture capacity is used only in the derivative term of the Taylor series expansion of the temporal derivative of the moisture content, distinguishes this numerical solution of the mixed form of the variably saturated equation from that of pressure-based form (Celia et al., (1990).

Interior Nodes

The finite-difference expressions for the spatial and temporal derivative in Eqs. (3.21) and (3.25) at a typical node *i,j* are rearranged by collecting all the unknowns on the left side and all the knowns on the right in agreement with Eq. (3.8) and the following expression is obtained.

$$\left(\frac{K_{i,j}^{k+1,m}+K_{i,j-1}^{k+1,m}}{2(\Delta z)^2}\right)\psi_{i,j-1}^{k+1,m+1}-\left(\frac{K_{i,j-1}^{k+1,m}+2K_{i,j}^{k+1,m}+K_{i,j+1}^{k+1,m}}{2(\Delta z)^2}+\frac{C_{i,j}^{k+1,m}}{\Delta t}\right)\psi_{i,j}^{k+1,m+1}$$
$$+\left(\frac{K_{i,j}^{k+1,m}+K_{i,j+1}^{k+1,m}}{2(\Delta z)^2}\right)\psi_{i,j+1}^{k+1,m+1}=-\left(\frac{K_{i,j+1}^{k+1,m}-K_{i,j-1}^{k+1,m}}{2(\Delta z)}\right)+\left(\frac{\theta_{i,j}^{k+1,m}-\theta_{i,j}^{k,m}}{\Delta t}\right)-\left(\frac{C_{i,j}^{k+1,m}\psi_{i,j}^{k+1,m}}{\Delta t}\right) \tag{3.26}$$

Using the above fully implicit finite difference approximation, the pressure heads at the time level (k+1) and Picard level (m+1) are obtained from the solution of the following system of simultaneous linear algebraic equation.

$$A\psi_{i,j-1}^{k+1,m+1}+B\psi_{i,j}^{k+1,m+1}+C\psi_{i,j+1}^{k+1,m+1}=R_{i,j}^{k+1,m} \tag{3.27}$$

where, coefficients A, B, C and R are defined as

$$A=\left(\frac{K_{i,j}^{k+1,m}+K_{i,j-1}^{k+1,m}}{2(\Delta z)^2}\right) \tag{3.28a}$$

$$B=-\left(\frac{K_{i,j-1}^{k+1,m}+2K_{i,j}^{k+1,m}+K_{i,j+1}^{k+1,m}}{2(\Delta z)^2}+\frac{C_{i,j}^{k+1,m}}{\Delta t}\right) \tag{3.28b}$$

$$C = \left(\frac{K_{i,j}^{k+1,m} + K_{i,j+1}^{k+1,m}}{2(\Delta z)^2} \right) \tag{3.28c}$$

$$R = \left(\frac{\theta_{i,j}^{k+1,m} - \theta_{i,j}^{k,m}}{\Delta t} \right) - \left(\frac{K_{i,j+1}^{k+1,m} - K_{i,j-1}^{k+1,m}}{2(\Delta z)} \right) - \left(\frac{C_{i,j}^{k+1,m} \psi_{i,j}^{k+1,m}}{\Delta t} \right) \tag{3.28d}$$

Eq. (3.27) applies to all interior nodes. At the boundary nodes the equation is modified to take into account the appropriate boundary conditions. The resulting set of linear algebraic equations for the unknown pressure head values is written in matrix notation as:

$$\mathbf{T}\hat{\psi} = \hat{\mathbf{R}} \tag{3.29}$$

where, $\hat{\psi}$ is the vector of unknown pressure heads, $\hat{\mathbf{R}}$ is the forcing vector. **T** is a square matrix consisting of the coefficients of the finite difference equation (eqn. 3.27). The system of finite difference equations is tridiagonal in nature and is solved using Thomas Algorithm (Remson et al., 1971). The iterative process is carried out till the difference in pressure head values between two successive iterations is less than a specified tolerance limit.

3.3 COMPUTER CODE

A computer code is written in FORTRAN 77 to implement the numerical scheme and is presented in Appendix-I. The salient features of the comp uter code are described in the following sections.

3.3.1 Main Program

The following tasks are performed

(A) Reading of input data. The details of READ statements are as follows:

hini: Initial water depth applied over the dry border (L), S_0**:** Longitudinal border slope (LL^{-1}), **rn:** Manning's roughness coefficient, **crn:** Courant

Number, **lmax:** Border length (L), **quns:** Discharge rate at upstream end per meter width (L^3S^{-1}), **g:** Acceleration due to gravity (LS^{-2}), **dx:** Nodal spacing in horizontal direction in surface flow (L), **tmax:** Maximum simulation time, **slength:** Length of the unsaturated soil column (L), **nnodes:** Number of nodes in the considered unsaturated soil length, **sini:** Initial pressure head in the soil of solution domain, **alpha (L^{-1})** Van Genuchten's parameter, **en:** Van Genuchten's parameter, **satk:** Saturated hydraulic conductivity of the soil (LT^{-1}), **thetas:** Saturated moisture content (L^3L^{-3}), **thetar:** Residual moisture content (L^3L^{-3}), **maxiter:** Number of maximum iteration, **epsilon:** Convergence factor for Picard's implicit iteration, **nprint:** Number of times the output required, **tprint:** The times at which the output is required.

(B) Preliminary computations carried out before the time loop starts:

Computation of initial discharge using initial water depth, computation of number of sections and number of nodes in horizontal direction, computation of space discretization in the vertical direction, computation of Van Genuchten parameter.

(C) Computation of discrete time step using Courant-Friedrichs-Lewy stability condition and total time, computation of upstream boundary head using negative characteristic equation and known value of discharge qups, computation of downstream boundary head and discharge using positive characteristic equation and Mannings equation.

(D) Computation of water depth and discharge at interior nodes using MacCormack explicit scheme, computation of infiltration by Richards equation using implicit scheme, computation of average values of the variables i.e., water depth h, discharge q, and infiltration f, at all nodes.

3.3.2 Functions

F2 Computes unsaturated hydraulic conductivity at every nodal points of the solution domain, during each iteration, by Mualem's equation using Van Genuchten relationship of moisture content and pressure head. The data supplied are effective saturation, Van Genuchten parameter values and saturated hydraulic conductivity.

F3 Computes specific soil moisture capacity at every nodal points of the solution domain, during each iteration, corresponding to the effective saturation value using Van Genuchten relationship for moisture content and pressure head. Other supplied data are saturated moisture content, residual moisture content, and Van Genuchten parameters, alpha, em.

F7 Computes effective saturation at every nodal of the solution domain, during each iteration, corresponding to pressure head value. Other data supplied are Van Genuchten parameters, alpha, en, and em.

3.3.3 Subroutines

Subroutine Infiltration

This assigns the old value of pressure head for first iteration and new value of pressure head for subsequent iterations for all the nodes in the unsaturated zone, till the maximum iteration number. This provides the call statements, viz. call coeff, call solve, call convergence, to return the values from the subroutine coeff, subroutine solve and subroutine convergence up to maximum iteration number. This also provides the call statement, call fp computation, to return the infiltration from subroutine fp computation for each time step. This also provides the functions, F2, F3, and F7.

Subroutine Coeff

In this subroutine, the coefficients of the matrix generated by the finite difference approximation are computed.

Subroutine Solve

In this subroutine, pressure head values are computed using the Thomas Algorithm for all the nodes for each time step.

Subroutine Convergence

In this subroutine, the maximum value of the difference between simulated pressure head values at each node in successive iterations is computed. This is essential to check and satisfy the convergence criterion.

Subroutine fpcomputation

In this subroutine, the infiltration at each surface node is computed using Darcy's law.

3.4 MODEL VALIDATION:

The numerical model developed in section 3.4 is validated by comparing model predictions with the reported results (both numerical and experimental). The validation is done in two steps. In the first step, the subsurface flow model is validated with the reported numerical results from literature. In the second step, the coupled overland subsurface flow model is validated by comparing model predicted advance and recession with experimentally observed data.

3.4.1 Validation of Subsurface Flow model

The Subsurface flow model is validated by comparing model results for three different problems accounting for diverse boundary conditions chosen from literature.

3.4.1.1 Infiltration into a very dry soil with Dirichlet type boundary condition at top

Problem of infiltration into a very dry soil solved by Celia et al. (1990) is taken here for model validation. This problem considers infiltration into a homogeneous soil column, which is initially dry. The soil parameters are $\alpha_v = 0.0335$ cm^{-1}, $\theta_s = 0.368$, $\theta_r = 0.102$, $n_v = 2$, $m_v = 0.5$, $K_s = 0.00922$ cm/s. Length of the soil sample is 100 cm. The initial and boundary conditions are;

$$\psi(z,0) = -1000 \text{ cm}, \quad 0 \leq z \leq 100 \text{ cm}$$

$$\psi(0,t) = \psi_{bottom} = -1000 \text{ cm}$$

$$\psi(100, t) = \psi_{top} = -75 \text{ cm}$$

Celia et al. (1990) obtained finite element as well as finite difference solution using coarse and dense grid. For the dense grid consideration, the over all soil domain length L is divided into 101 grids such that the distance between two grids will be 1.0 cm. The problem is simulated using the present model with Δt = 20 sec. Fig. 3.3 compares the model predicted pressure head after one day of simulation with Celia et al. (1990) dense grid simulation. It is clear from Fig. 3.3 that the model predictions are in excellent agreement with the reported predictions.

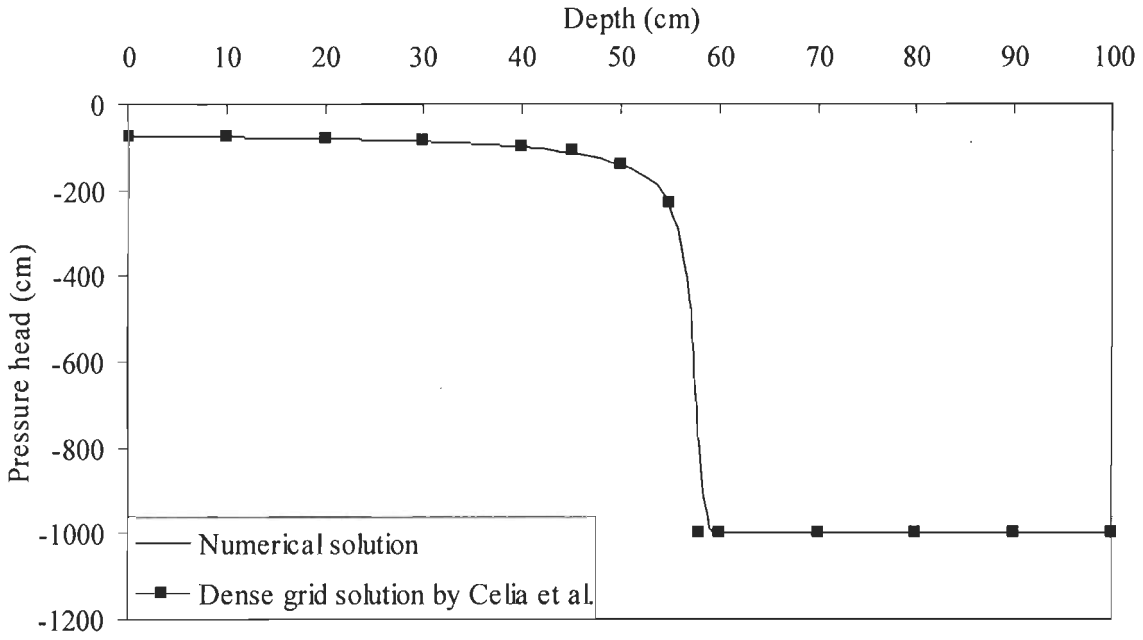

Fig. 3.3: Model validation for infiltration into a very dry soil: Dirichlet boundary condition at top

3.4.1.2 Gravity drainage from an initially saturated soil

Dane and Hruska (1983) simulated gravity drainage from a hypothetical soil with the following set of soil parameters. $\alpha_v = 0.02912$ cm^{-1}, $n_v = 3.57168$, $K_s = 0.00305$ cm/sec, $\theta_s = 0.365$ and $\theta_r = 0.069$. The problem involves allowing a soil column of length (L) = 1.4m, which is at an initial moisture content of 0.3 throughout, to drain due to gravity at the lower boundary. The Darcy's flux at the top is zero. The initial and boundary conditions for the problem are as follows

$t = 0$: $\theta = 0.30$ $\quad 0 \le z \le 1.4$m

$t > 0$: $q_{bottom} = -K$ $\quad z = 0$

$q_{top} = 0$ $\quad z = 1.4$ m

The problem is simulated using the present model with Δz = 2 cm. Fig. 3.4 shows a comparison between the moisture contents obtained after 12 hours of simulation by Dane and Hruska and the present model. It can be seen from Fig. 3.4 that

results are in excellent agreement with those of Dane and Hruska.

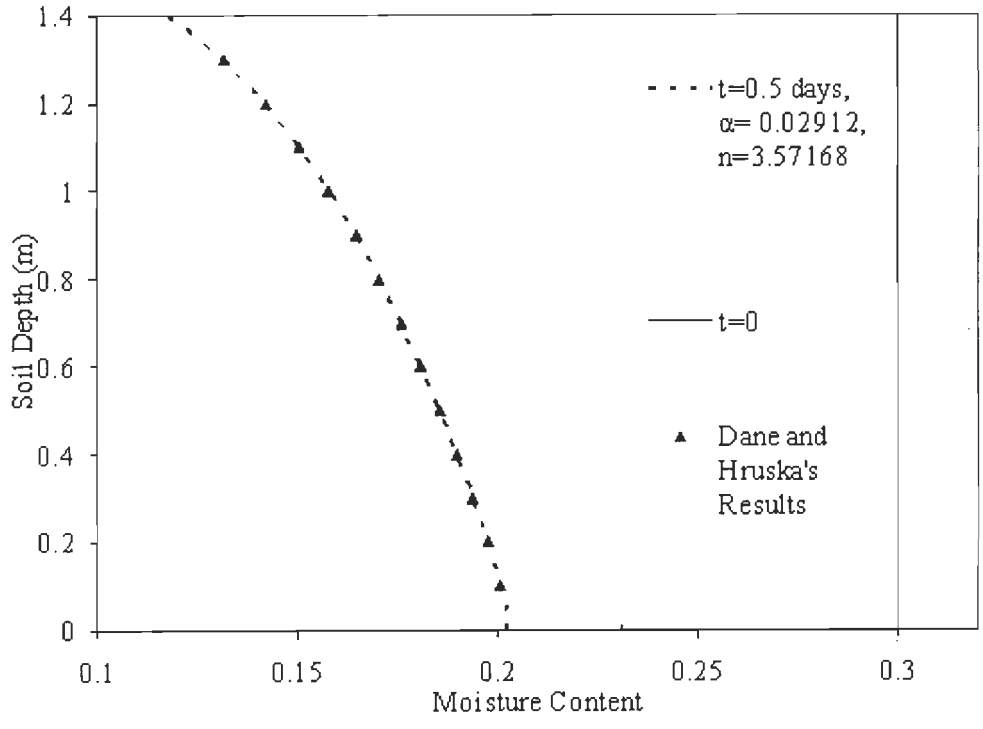

Fig. 3.4: Model validation for gravity drainage from an initially saturated soil

3.4.1.3 Infiltration into a very dry soil with Neuman type boundary condition at top

Problem 3 considers infiltration into an initially dry, producing sharp moisture fronts and a four order of magnitude change in relative hydraulic conductivity across the wetting front (Paniconi et al., 1991). The parameter values for sharp front infiltration are, K_s = 1.11 × 10^{-5} cm/sec, θ_s = 0.38, θ_r = 0.15, n_v = 4.0 and L =1.25m. The initial and boundary conditions are

$t = 0$: ψ = -3.0 m	$0 \leq z \leq 1.25$ m
$t > 0$: ψ = -3.0m	$z = 0$
$t > 0$: q = 0.0008 m^3/hr	z = 1.25m

The problem is simulated using the present model with Δz = 0.004167 m and Δt = 0.01hr. Figs. 3.5 and 3.6 show a comparison between pressure head and moisture content obtained after 120 hours of simulation by Paniconi et al. (1991) and the present

model. It is evident from Figs. 3.5 and 3.6 that the results of the present model are in excellent agreement with those of Paniconi et al. (1991).

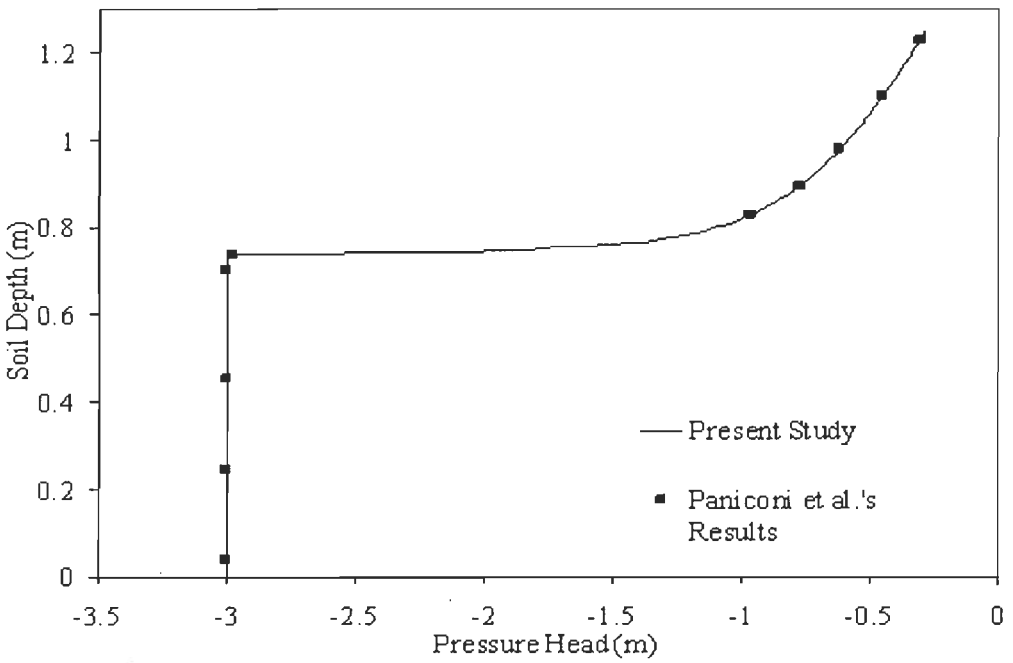

Fig. 3.5: Model validation for infiltration into a dry soil- Neuman boundary condition: Comparison of Pressure heads

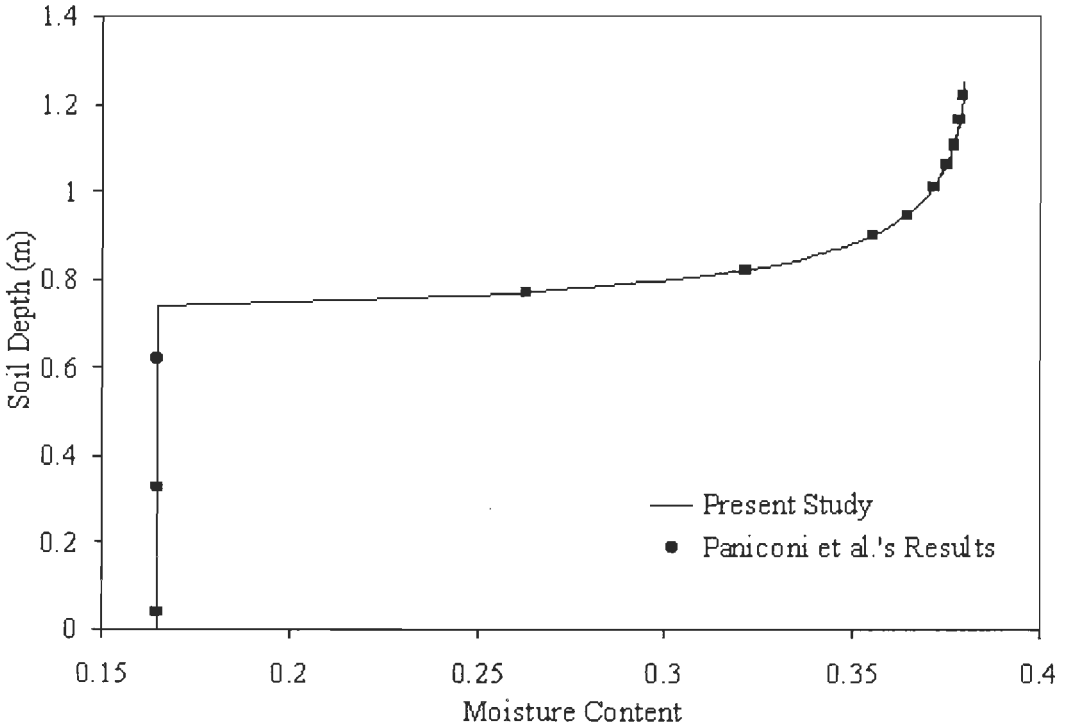

Fig. 3.6: Model validation for infiltration into a dry soil- Neuman boundary condition: Comparison of moisture content

3.4.2 Validation of Surface Flow model

The coupled overland subsurface flow model is validated by comparing model predicted advance and recession with experimentally observed data. Walker and Humpherys (1983) provided field geometry and advance and recession field data from three Colorado, Utah and Idaho sites. Due to nonavailability of the unsaturated soil parameters (K_{sat}, α_v, n_v, θ_s, and θ_r) for these soils, these data is obtained by the unsaturated soil data bank given by Carsel and Parish (1988). Table 3.1 provides the relevant soil, field geometry and flow data for these three fields.

Table 3.1: Input data for model validation

Sl.No.	Model Parameters	Field 1	Field 2	Field 3
1	Soil type	Sandy loam	Silty-Clay loam	Loamy sand
2	Inflow (m^3/s)	0.002	0.0015	0.00349
3	Field length (m)	360	360	350
4	Field slope (m/m)	0.008	0.0104	0.0025
5	Manning's roughness Coefficient (n)	0.04	0.04	0.02
6	Time of cutoff (min)	400	200	110
7	Hydraulic Conductivity K_{sat} (m/s)	3.50×10^{-6}	2.50×10^{-6}	4.05×10^{-6}
8	Van Genuchten Parameter (α_v) (m^{-1})	2.0	1.0	12.4
9	Van Genuchten Parameter (n_v)	1.45	1.23	2.28
10	Saturated Water Content (θ_s)	0.39	0.43	0.41
11	Residual Water Content (θ_r)	0.04	0.089	0.057

Figs. 3.7, 3.8 and 3.9 show the comparison of model predicted irrigation advance and recession with the field observed values for three fields of different soil types respectively. It can be seen from figs. 3.7 to 3.9 that model predictions are in good agreement with the experimental results.

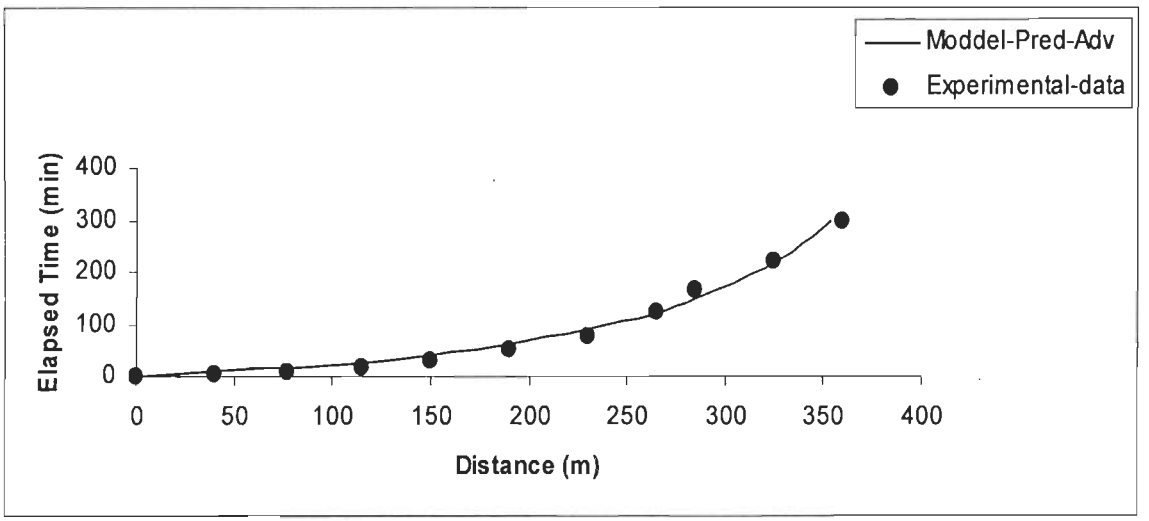

Fig. 3.7: Comparison of model predicted and experimental advance for field 1

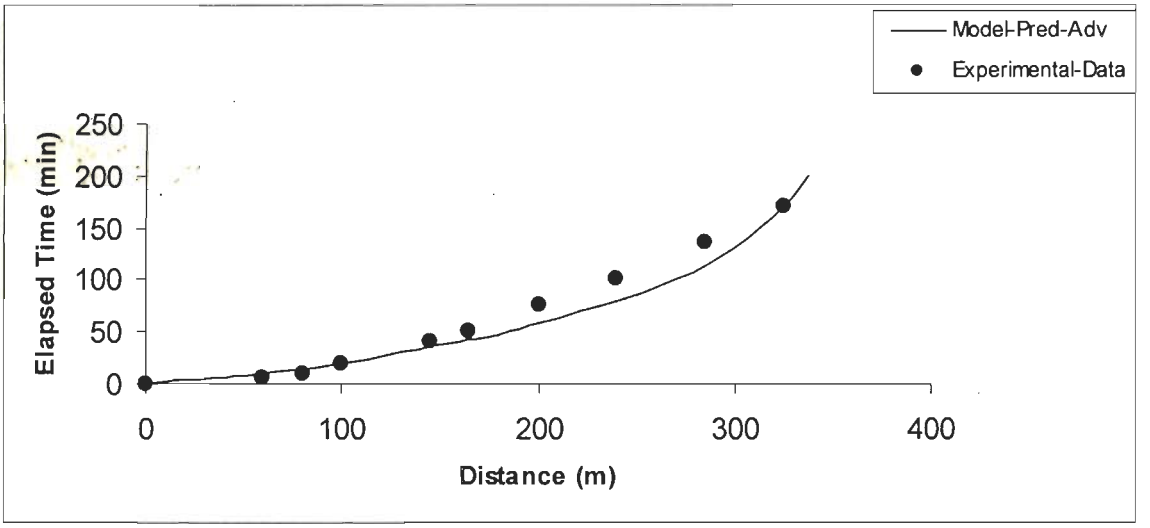

Fig. 3.8: Comparison of model predicted and experimental advance for field 2

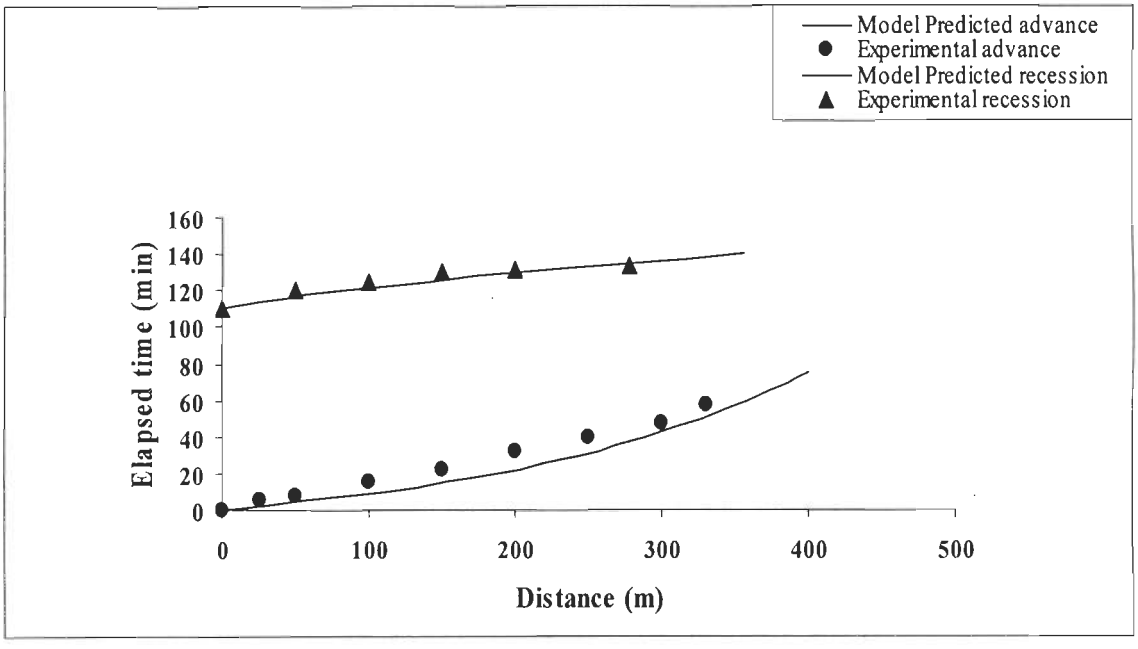

Fig. 3.9: Comparison of model predicted and experimental advance and recession field 3

3.5 CLOSURE

In the present Chapter a complete hydrodynamic numerical model is developed for the simulation of overland and subsurface flow for border strip irrigation. The numerical model involves the solution of the differential equations governing overland flow (Saint Venants equations) and subsurface flow (Richards equation). The explicit finite difference MacCormack scheme is used to solve the Saint Venants equations while the Richards equation is solved using a mass conservative fully implicit finite difference method. The model is validated by comparing model predictions with the reported numerical and experimental results. The validation is done in two steps. In the first step, the subsurface flow model is validated with the reported numerical results from literature. In the second step, the coupled overland subsurface flow model is validated by comparing model predicted advance and recession with the data reported in literature.

CHAPTER 4

EXPERIMENTAL PROGRAMME

4.1 INTRODUCTION

In chapter 3, a numerical model is developed for the analysis of water flow through a border strip during irrigation. The model is validated by comparing model predicted irrigation advance and recession with experimental data. A review of literature suggests that most of the experimental data consists of overland measurements such as advance and recession (Walker and Humpherys, 1983, Playan et al., 1994, Singh and Ballamudi, 1996). Very few experimental programmmes involved soil moisture measurements in addition to advance and recession data. (Bali and Wallender, 1987, Wohling and Mailhol 2007). Hence, a detailed irrigation field experiments are conducted involving both overland and subsurface measurements to asses the performance of the numerical model developed in chapter 3 in predicting both overland and subsurface flow variables. A detailed experimental programmme is described in the following sections.

4.2 EXPERIMENTAL SITE

The experiments were conducted at the field experimental station of Civil Engineering Department, Indian Institute of Technology Roorkee, Uttrakhand, India, from July 2008 to July 2009. Prior conducting irrigation experiments, various laboratory and field tests are carried out to obtain various soil parameters needed for the analysis. To obtain the soil parameters, soil samples are collected form four locations selected in the experimental station, at each location two samples are taken consisting of 0-30 cm and 30-60 cm depths.

4.3 CALIBRATION OF THE EQUIPMENTS USED

In this study, standard equipments and methods have been used for conducting field and laboratory experiments. The details of equipments used for determining different variables are given in Table 4.1. Most of the equipments used for laboratory tests were pre-calibrated. However, some instruments used in the field needed to be calibrated for the actual field conditions and soil type. The details of the equipments and their calibration are given in the following sections. The various soil physical parameters determined and their method of analysis are presented in Table 4.1.

Table 4.1: Different variables and equipment/methods of analysis

Sl. No.	Parameter	Method/Equipments
1	Texture (%)	Sieve analysis, Hydrometer (Lab test)
2	Bulk Density (gm/cm^3)	Core Samplers (Lab test)
3	Particle Density (gm/cm^3)	Pycnometer Analysis (Lab test)
4	Porosity, θ_s (%)	Core Samplers (Lab test)
5	Saturated Hydraulic Conductivity, *Ks* (m/sec)	Guelph type permeameter (field test)
6	Soil Moisture Characteristics	Pressure plate Extractor
6	Soil Moisture Content	Soil moisture meter (TDR)
7	Pressure head	Sensors
8	Mannings coefficient (n)	Strickler's formula
9	Field slope (S_0)	Dumpy level

4.3.1 Soil Moisture Meter (TDR)

Soil moisture is a critical and potentially highly variable component of the soil environment. Time domain reflectometry is a proven technology for quickly and accurately determining volumetric content (VMC) in soil. TDR 300, soil moisture meter (Fieldscout, Spectrum Technologies, Inc., Plainfield, IL,USA) provided with shaft-mounted probes has been used for easy and rapid measurements of soil moisture

at ground surface and at various depths. The instrument measures percent volumetric water content, with a resolution of 0.1 % and accuracy of ± 3.0% volumetric water content having range from 0% to saturation (saturation is dependent on soil type). Volumetric moisture content (VMC) can be measured in standard or high clay mode and relative moisture content (RMC) up to 2 RWC modes can be established. Probes in different lengths i.e. short (7.6cm), Medium (12cm) and long (20cm), 0.5cm diameter and 3.3cm spacing are specified. The volumetric water content displayed is the average moisture content of the soil depth equal to probe length into which the probe is inserted. The VMC measurements are stored in the data logger, which can be transferred to PC using Field-scout software. Plate 4.1 shows the moisture content observations being taken using soil moisture meter (TDR).

The volumetric moisture content is the ratio of the water in a given volume of soil to the total soil volume. At saturation, VMC equals the percent pore space of the soil. The TDR is equipped to measure VMC at standard and high clay modes, however for maximum accuracy soil specific calibration of the instrument has been done. The TDR is kept at standard mode and gravimetric soil moisture measurement is done for the calibration using a well defined procedure for gravimetric sampling. The calibration helps in converting the TDR measured soil moisture content values to representative soil moisture content values for the sandy loam soil of the experimental field.

4.3.2 Volumetric Moisture Content Measurements

The measurement of moisture content in the field is made with Time Domain Reflectometer (TDR). The moisture content is measured up to 0.60m depth at every 0.10m depth at different points along the border before and after irrigation. In the field a number of sites are established to get the soil samples. Some of the sites are wetted to different soil moisture content by adding various amounts of water. At each site a field

scout TDR reading is taken, followed by the extraction of a known volume of soil. Extracted soil samples are stored in plastic bags to avoid evaporation. The wet weight of the each soil sample is determined in lab. The soil is then oven dried (105^0 C for 48 hours) and weighed again. The volumetric water content is calculated as follows:

$$VWC = 100*(M_{wet} - M_{dry})/(\rho_w * V_{tot}) \quad (4.1)$$

where, M_{wet} and M_{dry} are Mass (g) of wet and dry soil respectively, V_{tot} is the total soil volume (ml) and ρ_w is the density of water (1 g/ml)

Plate 4.1: Soil Moisture measurements being done using TDR Soil Moisture Meter

4.3.3 Calibration Curve

The corresponding gravimetrically measured and Field Scout TDR meter measured values of soil moisture content are plotted to obtain calibration curve. To obtain the best fit relationship linear, logarithmic, power and exponential, regression analysis of the data has been performed. The R^2 values in all these cases have been found to be 0.9848, 0.9424, 0.9791 and 0.9494 respectively; among these values, the value corresponding to the linear regression is highest. Hence equation obtained using linear regression has been used to convert the TDR readings to soil type representative VMC values of the field soil. Fig. 4.1 shows the calibration curve and the corresponding linear regression equation for the TDR soil moisture meter corresponding to the soil of the experimental plot. Hence observations of soil moisture content using TDR soil moisture meter are modified using the following equation.

Soil Moisture Content = 1.1794 (TDR moisture meter measured value) -0.0089 (4.2)

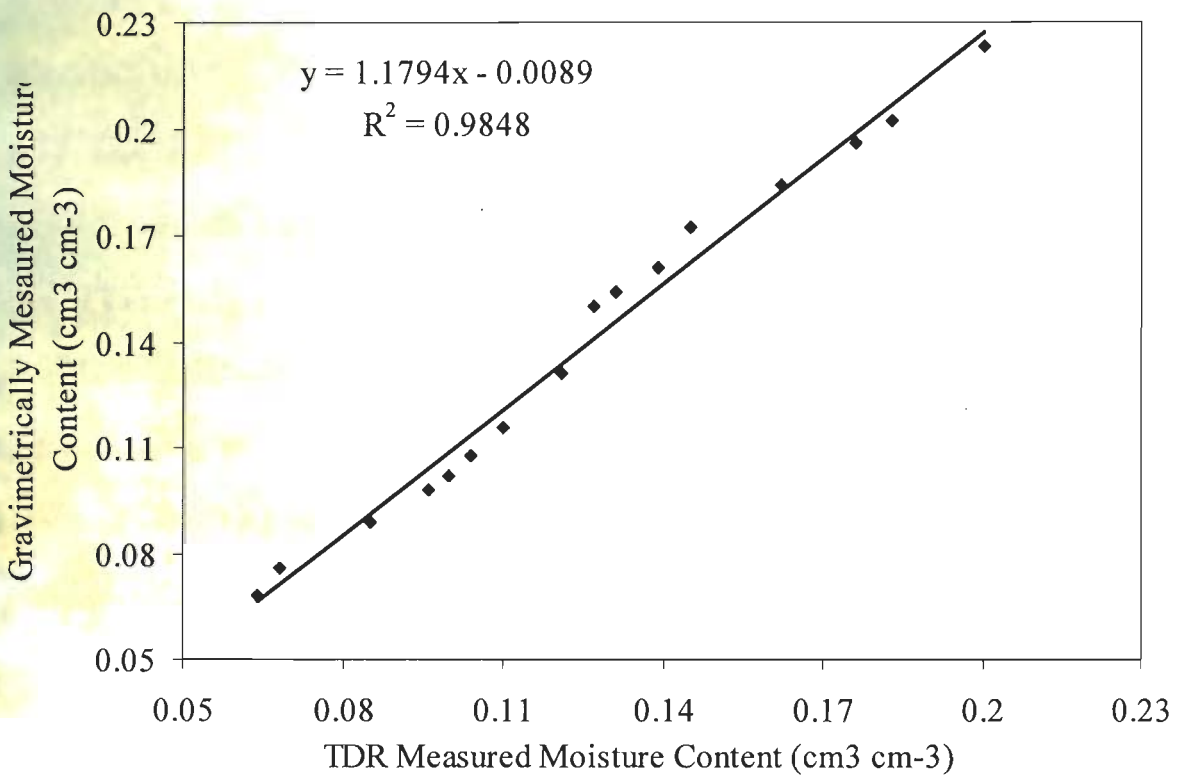

Fig. 4.1: Calibration curve for TDR Soil Moisture Meter

4.3.4 Soil Moisture Measurement Sensors

For wide range of soil suction head observations an advanced system of the soil moisture measurement sensors (Watermark, Irrometer Company, Inc. Riverside CA) has been installed. The sensors can measure soil suction head in a range of 0-199 Centibars. In the experimental plot nine sensing stations have been chosen for better representation of the moisture distribution in the root zone. The sensors have been installed in the field at depth of 0.4, 0.3, 0.2 and 0.1m along the length of the border at spacing of 5m. The sensors are connected with wire lead, which can be connected to the Watermark digital Meter with alligator clips. The digital meter directly gives the soil suction head value and is equipped with temperature adjustment setting. Before installation the sensors as well as the meter has been checked to ensure that both are functioning properly.

For representative results, the sensors are planted wet. Before installation, wetting and drying cycle is repeated two to three times. The sensors are wetted for 30 minutes two days prior to installation, and let dry until evening, wet for 30 minutes, let dry overnight, wet again for 30 minutes the next morning and let dry again until evening. Before the day of installation the sensors are soaked overnight and installed wet in the morning. This wetting and drying improves the sensor response to the soil moisture. To embed the sensors, an assess hole is made at each sensing location with the augur. A suitable length of class 315 PVC pipe is fitted snugly and solvent welded with PVC cement, over each sensor's collar. The sensor is kept in vertical position holding the pipe and soil slurry is poured around the sensor to attain firm contact with the soil. The sensor's wires can be staked up for easy access through the PVC pipe which acts as a conduit for the sensor's wires. At the ground surface the pipe is capped off, so no surface water can infiltrate to the sensor and disturb the sensor reading. The

wire left at the top attached to the pipe and the connecting points are covered with water proof packing to avoid corrosion and destruction of lead during field operations. To take the moisture suction readings a portable digital meter is connected to the sensor wires, which gives the soil suction reading.

Degree of soil moisture reduction at various depths shows soil condition at various depths and gives an idea of irrigation duration needed to rewet the root zone. Plate 4.2 shows the soil moisture sensors being installed in the field. The top of pipe is kept at a height to avoid passage of irrigation water. Plate 4.3 shows the suction head measurements being done by using digital soil moisture meter. The values of suction head observed using sensors are converted to the corresponding moisture contents using field calibrated Van Genuchten's relationships (The estimation of Van Genuchten parameters used here is explained in the later section). To check the consistency of the moisture contents, so obtained, moisture content from the corresponding points is also measured gravimetrically in the laboratory. The data set of moisture content values so obtained has been plotted against each other. Fig. 4.2 shows the gravimetrically obtained values against moisture content values deduced from the soil moisture measurement sensors. The points fall along a 1:1 line, which indicates the sensor measured soil pressure head deduced moisture content values.

Plate 4.2: Soil Moisture Sensor installation in the field

Plate 4.3: Measurement of soil suction head by digital meter in the field

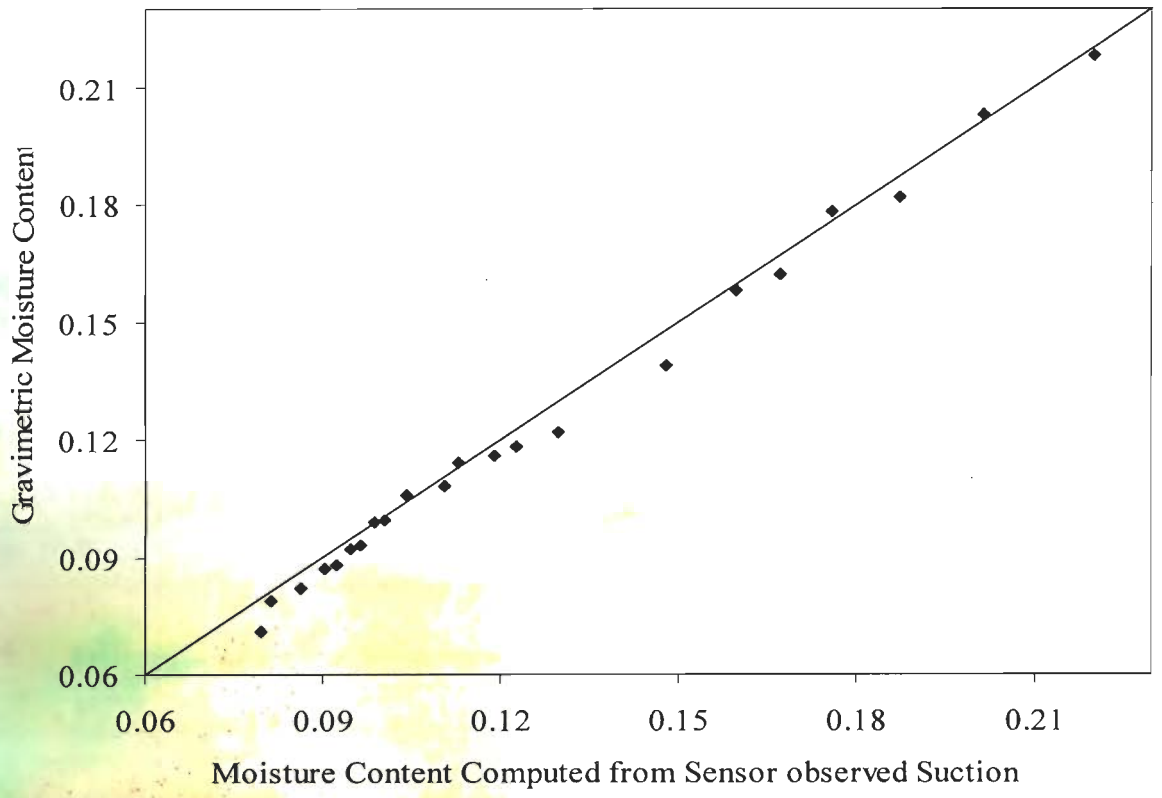

Fig. 4.2: Laboratory and Sensor computed Moisture Content values along 1:1 line.

4.4 SOIL PARAMETERS:

4.4.1 Texture

The soil properties such as permeability, water storage capacity and ability to aggregate depend on its grain size distribution. The grain size analysis of a soil is a procedure to determine the relative proportions of different grain sizes. In this study, soil samples were collected from the 0-0.3m and 0.3-0.6m depth at four locations within the experimental site. At each location, two samples are collected (first sample from 0-30 cm and the second sample from 30-60 cm). The grain size analysis of these samples is done using a set of standard sieves following the methodology suggested by Trout at al. (1982). The cumulative particle size curves so obtained were used to determine the gravel (greater than 2.0mm diameter), coarse sand (0.6-2.0mm diameter), medium sand (0.2-0.6mm diameter), fine sand (0.05-0.2mm), silt (0.002-0.05mm) and

clay (less than 0.002mm) fractions of each sample. For the 0-0.60m depth, mean values of gravel, sand, silt and clay are 0.66%, 74.8%, 17.2% and 7.4% respectively. According to the USDA triangular soil classification system, the soil is classified as sandy loam soil. The individual and average particle size distribution at depths 0-30 cm and 30-60 cm is presented in Table 4.2.

Table 4.2: Depth wise grain size distribution (%)

Soil ingredient	Depth (0-30cm)				
	Location 1	Location 2	Location 3	Location 4	Average
Gravel	0.50	0.25	0.50	1.20	0.61
Sand	72.50	75.50	74.10	72.70	73.70
Silt	20.00	16.25	17.00	19.60	18.21
Clay	7.00	8.00	8.40	6.50	7.50
	Depth (30-60cm)				
Gravel	0.20	0.40	2.00	0.20	0.70
Sand	73.70	72.50	80.90	76.30	75.85
Silt	17.80	18.10	13.00	16.00	16.20
Clay	8.50	9.00	4.10	7.50	7.30

4.4.2 Bulk Density:

The bulk density of a soil is defined as the average mass of dry soil solids per unit volume of soil. It is also sometimes represented as specific gravity (or weight), which is the mass of the soil relative to the mass of an equal volume of water. The bulk density of a soil sample depends upon its state of compaction or aggregation. To determine the bulk density, undisturbed soil samples were collected using core samplers, from the same locations and depths at which the textural fractions were determined. The procedure suggested by Trout et al. (1982) is used to determined bulk density. The bulk density of a soil is determined by collecting a known volume of soil, oven drying it, and determining its mass. The values of bulk density for each sample

shown in the Table 4.3 indicate that the deviation of values for the two layers is insignificant. The average value of bulk density is observed as 1.78g/cm^3.

Table 4.3: Determination of Bulk Density (gm/cm^3)

Depth (m)	Locations				
	Location 1	Location 2	Location 3	Location 4	Average
0-0.30	1.77	1.80	1.73	1.86	1.79
0.3-0.6	1.80	1.78	1.74	1.78	1.78

4.4.3 Particle Density:

The particle density of a soil which represents the density of the soil solids is defined as the mass of soil solids per unit volume of the soil solids. The Pycnometer method as suggested by Trout et al. (1982) is used to determine particle density of the samples collected. To determine the particle density of a soil sample, first, de-aerated water is prepared to be used in the experiment. Weight of dry pycnometer (W_1) was measured using an electronic balance. The pycnometer was filled with about 200 gm of oven dried sieved soil and weighed to obtain (W_2). Sufficient de-aerated water was added to the pycnometer to cover the soil about half full, shaked well and the pycnometer connected to the vacuum pump to remove the entrapped air at least for 10 minutes. Then the pycnometer was disconnected and filled with water about three fourth full and vacuum was reapplied to evacuate the pycnometer until very few bubbles appear on the top of the water. The pycnometer was filled with water up to the mark and weighed after drying it on the outside to obtain (W_3). Then the pycnometer was cleaned by washing thoroughly and filled with water up to its top and weighed after drying it on the outside to obtain (W_4). The particle density is determined as:

$$Particle\ density = \frac{W_2 - W_1}{(W_2 - W_1) - (W_3 - W_4)} \qquad (4.3)$$

where, W_1 is weight of empty pycnometer, W_2 is weight of pycnometer with soil, W_3 is the weight of pycnometer filled with soil and water and W_4 is the weight of pycnometer filled with water. The particle density values determined are shown in Table 4.4. Being the deviation of the particle density values for the two depths insignificant, the average value was obtained as 2.52gm/cm^3.

Table 4.4: Determination of particle Density (gm/cm^3)

Depth (m)	Locations				
	Location 1	Location 2	Location 3	Location 4	Average
0-0.30	2.44	2.52	2.6	2.47	2.51
0.3-0.6	2.61	2.42	2.63	2.44	2.53

4.4.4 Porosity:

The porosity of a soil is defined as the percentage of the total volume of the material that is occupied by pores or interstices. These pores may be completely filled with water if the soil is saturated. The porosity is determined on an undisturbed sample of the soil. The total volume of the undisturbed sample is determined. The sample is oven dried to remove the water (24 hrs at 105^{0}C) and the dry weight is determined. Then dividing the dry weight by the density of the soil, the volume of the solid phase of the sample is determined. The porosity is calculated as.

$$n = \frac{V_t - V_s}{V_t} * 100 \qquad (4.4)$$

where, n is the porosity, V_t is the total volume and V_s is the volume of the solid phase. The porosity of the undisturbed soil sample collected from the experimental site determined is as 0.330009, i.e 33%.

4.4.5 Saturated Hydraulic Conductivity

Hydraulic conductivity is the measure of the ability of a soil to transmit water. Guelph Permeameter, which is an in-hole constant head Permeameter, employing the

Mariotte principle has been used to determine the saturated hydraulic conductivity. The Permeameter is made of high impact polycarbonate and has a 2" diameter soil auger to test to a depth of 15 to 75 cm. The method involves measuring the steady state rate of water recharge in to unsaturated soil from a cylindrical well hole, in which a constant depth (head) of water is maintained.

When a constant well height of the water is established in a cored hole in the soil, a bulb of saturated soil with specific dimension is rather quickly established. This bulb is very stable and its shape depends upon the type of soil, the radius of the well and the head of water in the well. The shape of the bulb is numerically described by the *X*-factor (Reynolds and Elrick, 1986). The *X*-factor is numerically derived shape factor, which is dependent on the well radius and head of water in the well. The Richards analysis of steady state discharge from a cylindrical well in unsaturated soil as measure by the GUELPH Permeameter technique, accounts for all the forces that contribute to three dimensional flow of water into the soil: the hydraulic push of water into the soil, the gravitational pull of the liquid out through the bottom of the well, and the capillary pull of water out of the well into the surrounding soil (Reynolds and Elrick, 1985; Messing and Jarvis, 1990). The Richards analysis is the basis for the calculation of the hydraulic conductivity.

In the present study, for experimental investigations GUELPH Permeameter, radius of the bore hole and well height are kept same as specified in the standard procedure. Hence, the standard value of *X*-factor specified has been used in the calculations. Experiments to determine field saturated hydraulic conductivity are performed at four locations in the experimental field. The standard procedure was followed with combined reservoir mode at 40 cm depth bore hole. Steady state rate of flow from well to the soil is recorded with the height of the water in the well set at 5cm

and 10cm using both the reservoirs of the GUELPH Permeameter. The water level change for these two conditions is denoted by H_1 and H_2 whereas, steady state rate of flow by $\overline{R_1}$ and $\overline{R_2}$. The steady state rate of flow is achieved when the rate is same in three consecutive time intervals. The standard equation used for computation of the saturated hydraulic conductivity is as:

$$K_s = \left(0.0041 * X * \overline{R_2} - 0.0054 * X * \overline{R_1}\right) \quad (4.5)$$

where, *Ks* is the field saturated hydraulic conductivity (cm/s), X is the reservoir constant (35.54, when both the reservoirs are used), $\overline{R_1}$ and $\overline{R_2}$ are the steady state rate of flow corresponding to water level changes H_1 and H_2 respectively. The setup of GUELPH Permeameter at one of the locations during field experiments is shown in Plate 4.4. The observations and calculations for determining field saturated hydraulic conductivity at all the four locations are shown in Table 4.5

Table 4.5: Determination field saturated hydraulic conductivity (K_{sat})

Location	Depth (cm)	Height of water in well =5cm			Height of water in well =10cm			K_{sat} (cm/s) (10^{-4})	K_{sat} (cm/hr)
		Time interval (min)	H_1 (cm)	$\overline{R_1}$ (cm/s)	Time interval (min)	H_2 (cm)	$\overline{R_2}$ (cm/s)		
1	40	2	2.0	0.01667	2	3.3	0.0275	8.08535	2.910726
2	40	2	1.8	0.015	2	3.0	0.025	7.6411	2.750796
3	40	2	1.9	0.015833	2	3.1	0.02583	7.25608	2.61219
4	40	2	2.6	0.021666	2	4.2	0.035	9.4181	3.390516
Average field saturated hydraulic conductivity value								8.10016	2.916057

Plate 4.4: Measurement of Saturated Hydraulic Conductivity in the field using Guelph permeameter

4.4.6 Soil Moisture Characteristics

Soil Moisture Characteristic curve is obtained in the laboratory using Pressure plate extractor. Pressure plate extractor is one of the most commonly used equipment for the determination of soil moisture content in the laboratory. Pressure plate extractor is a modification of the suction procedure, where liquid phase water is mobilized across the porous ceramic using positive pressures. At equilibrium the moisture content is said to be held by an equal but negative force. Hence the moisture content is expressed with respect to negative pressures. At any given pressure in the chamber, soil moisture will flow from around each of the soil particles and out through the ceramic plate until the time at which the effective curvatures of the water films throughout the soil become the

same as at the pores in the membrane. When this occurs, equilibrium is reached and flow of moisture ceases. Water content by weight or by volume can be determined for the sample that was equilibrium with the pressure in the extractor. The soil moisture content of the samples collected is determined in the laboratory using 1500-15 Bar Pressure Plate Extractor (Soil Moisture Equipment Corp. California). To regulate pressure, pressure gauge 0780P0300 with 6-inch diameter with an accuracy of 1% is used for 15 Bar Extractor. The Plates 4.5 and 4.6 show the pressure plate extractor and the pressure gauge set up respectively.

The air dried, 2mm sieve passed, soil samples were used to obtain desorption data using the Pressure Plate Apparatus. Six replicate of a particular sample of about 20g each were prepared for each pressure application and placed on the appropriate ceramic plate using rubber retainer rings (5.5cm diameter, 1cm height). These samples were allowed to saturate on the ceramic plate for about 24 hours. After removing the excess free water with a syringe, the plate was then loaded into the extractor and the appropriate constant pressure applied from an external source. At equilibrium, when no further outflow of water was seen, the pressure was released and soil samples were immediately transferred into air tight container and weighed. These samples were dried for 24 hours at 105^0 C and weighed to calculate the equilibrium moisture content on a dry basis, which are later converted to volume fractions. The soil moisture characteristic data obtained by pressure plate extractor for the eight samples collected from the experimental station is shown in Table 4.6.

Table 4.6: Pressure Plate Extractor Data

Suction Pressure (bars)	Moisture content (%)							
	Location 1		Location 2		Location 3		Location 4	
	Depth (cm)		Depth (cm)		Depth (cm)		Depth (cm)	
	0-30	30-60	0-30	30-60	0-30	30-60	0-30	30-60
0.1	15.5	14.2	15.8	15.6	15.7	14.5	13.8	21.8
0.3	9.8	10.5	10.5	10.3	10.0	9.2	9.0	15.0
0.5	8.2	8.4	8.7	8.4	8.4	7.4	7.2	13.5
0.7	7.3	7.2	7.9	7.6	7.2	6.5	6.5	12.4
0.9	6.5	6.5	6.8	6.8	6.7	6.0	6.0	11.5
1.0	6.3	6.0	6.6	6.3	6.4	5.7	5.6	11.3

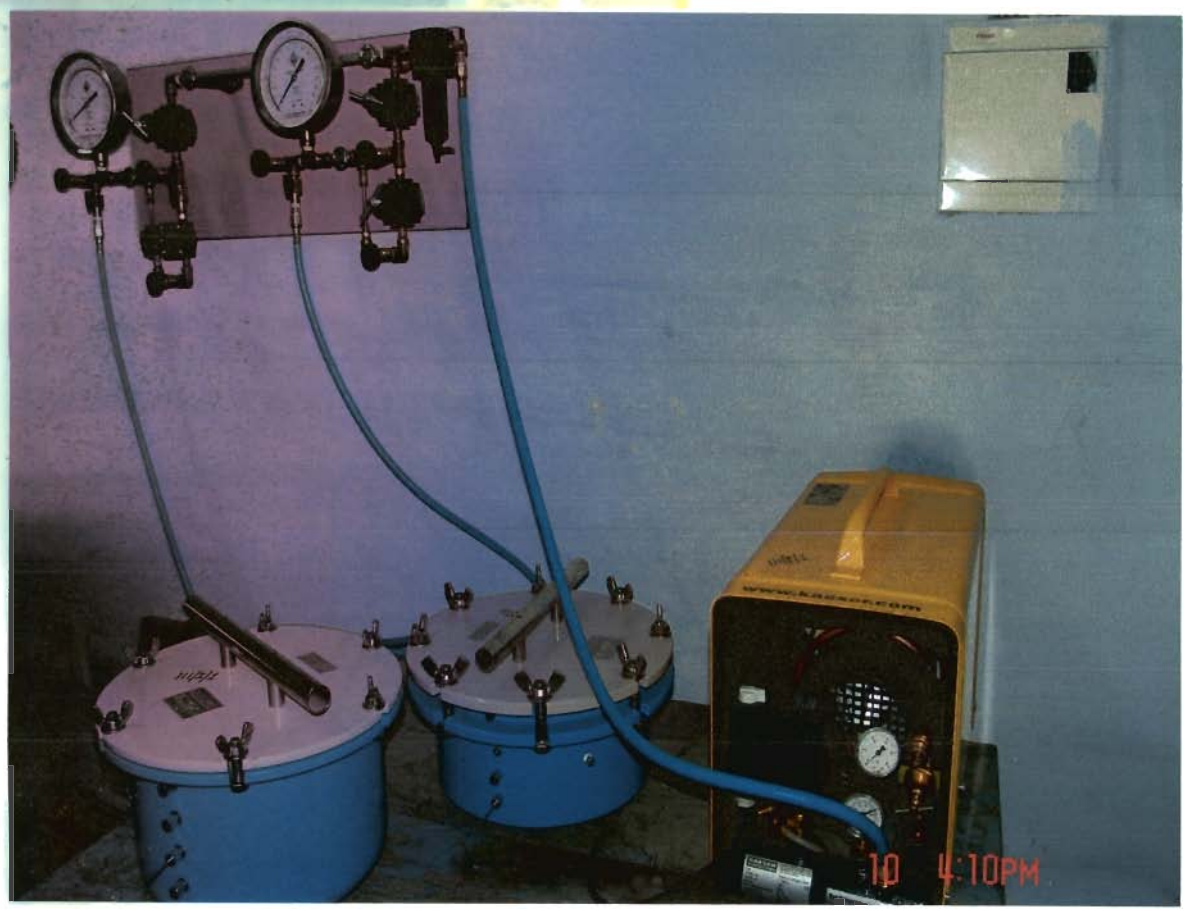

Plate 4.5: Pressure Plate Extractor

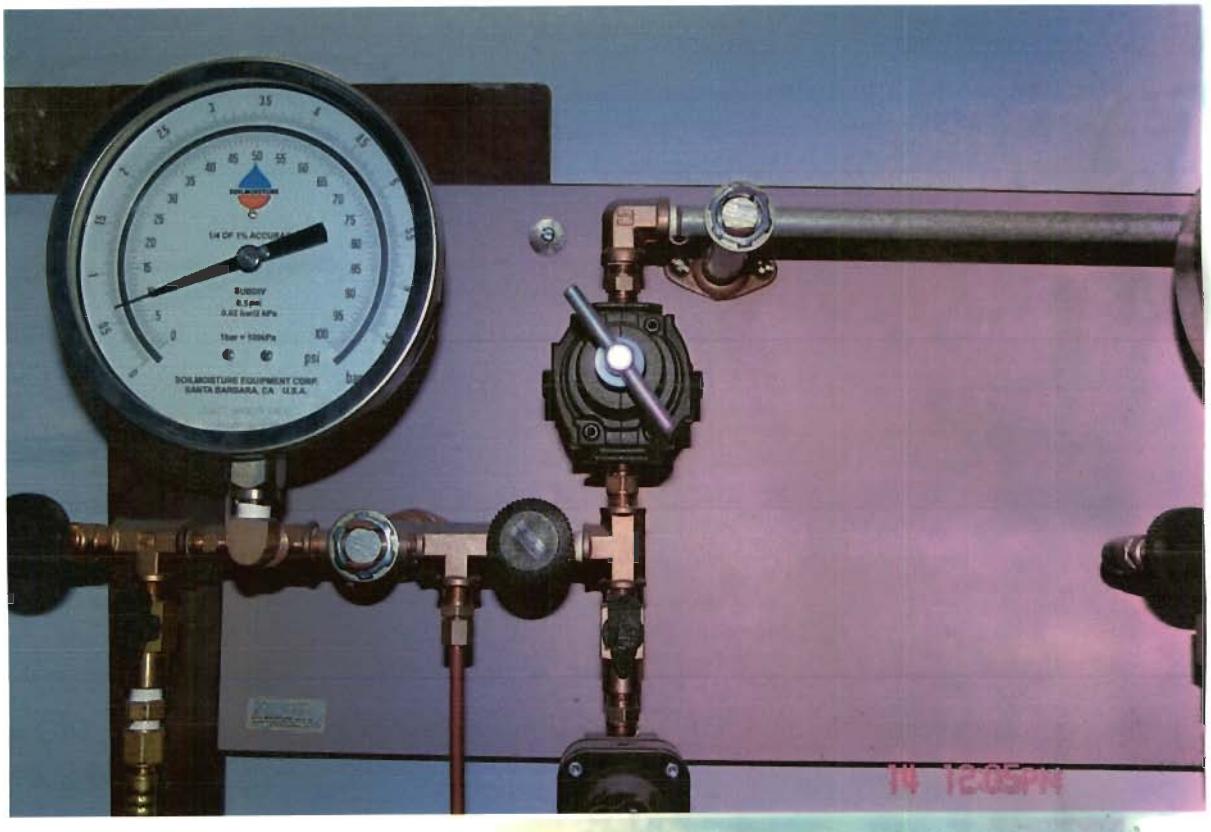

Plate 4.6: Pressure gauge set up during experiment

Fig. 4.3 to 4.6 show the Van Genuchten model fit for soil moisture data obtained by pressure plate extractor at four locations. Table 4.7 shows the optimum Van Genuchten retention parameters α_v and n_v obtained by nonlinear regression. It can be seen from the Table 4.7 that the variation in α_v and n_v among the eight sample is very minimal. The range of α_v is between 0.05 to 0.065cm^{-1} and the range of n_v is between 1.3 to 1.5. An average value of 0.056cm^{-1} for α_v and 1.44 for n_v are used in the border strip irrigation analysis.

Table 4.7: Van Genuchten Model fit Parameters

Locations	Depth (cm)	Van Genuchten Model fit Parameters	
		α_v (cm^{-1})	n_v
1	0-30	0.055	1.45
	30-60	0.060	1.45
2	0-30	0.05	1.45
	30-60	0.065	1.42
3	0-30	0.051	1.46
	30-60	0.058	1.48
4	0-30	0.056	1.50
	30-60	0.05	1.30
Average value		0.056	1.44

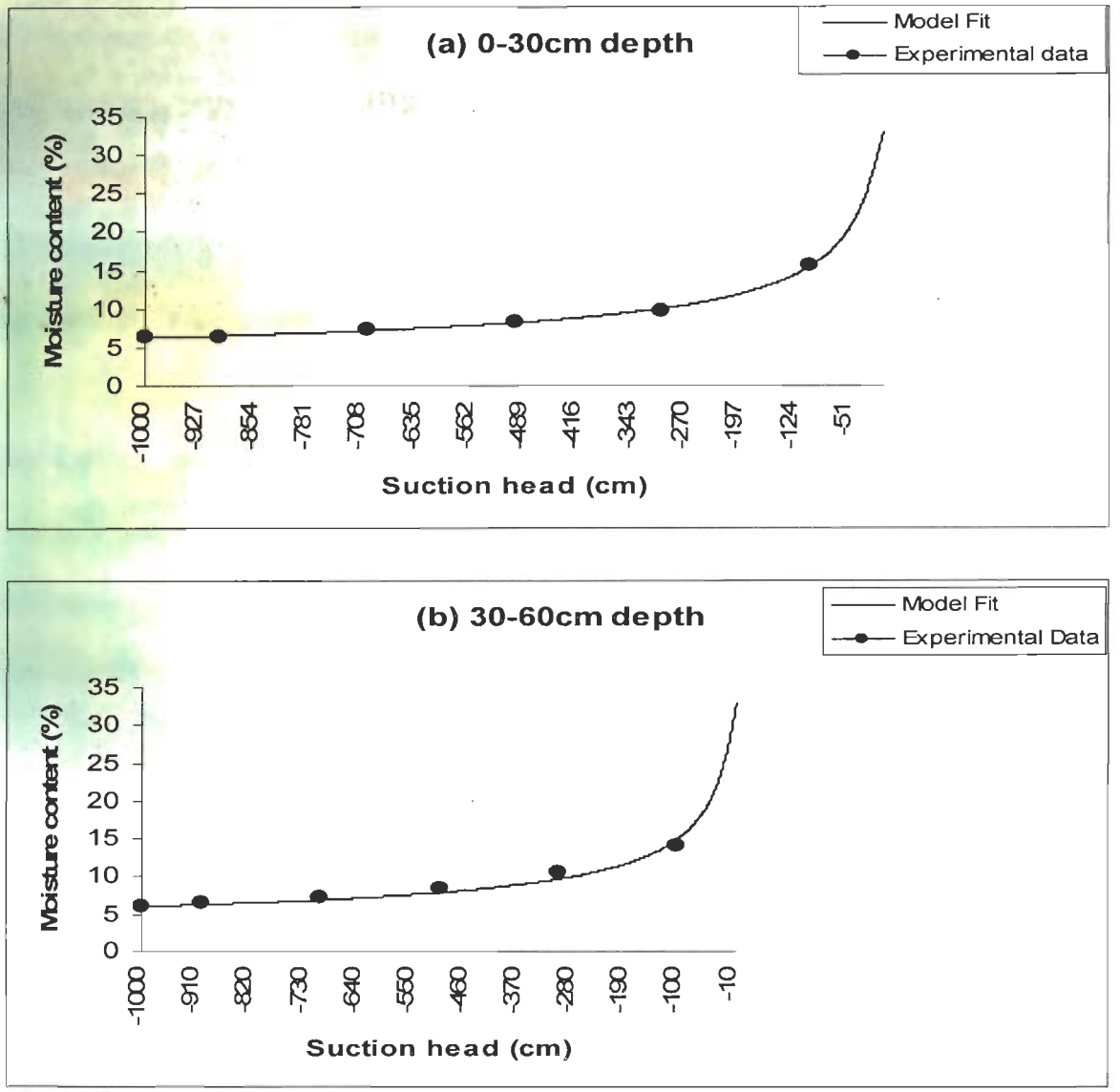

Fig. 4.3: Van Genuchten model fit for soil moisture data at location 1

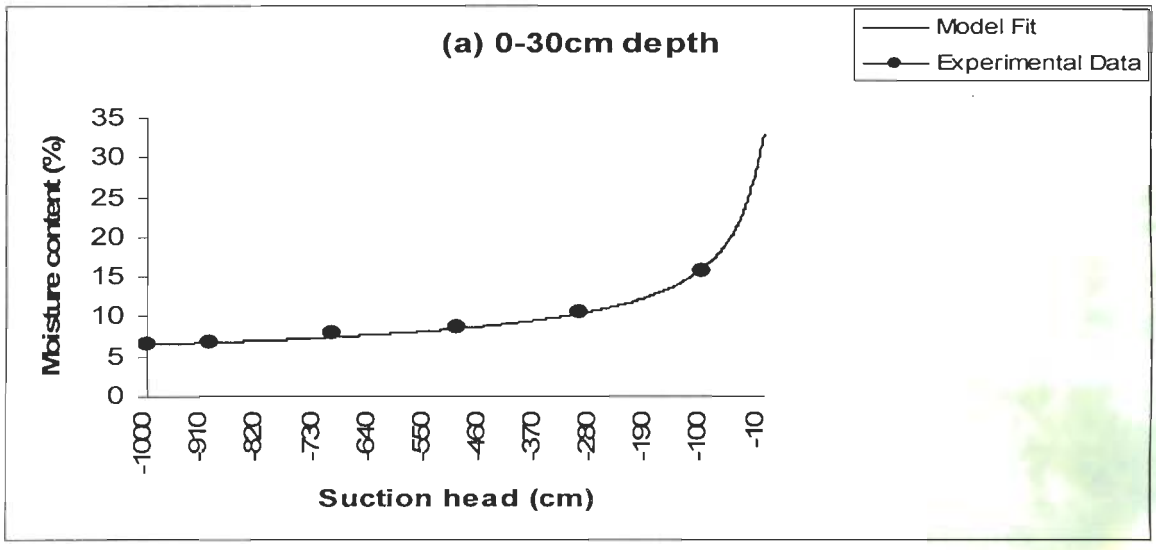

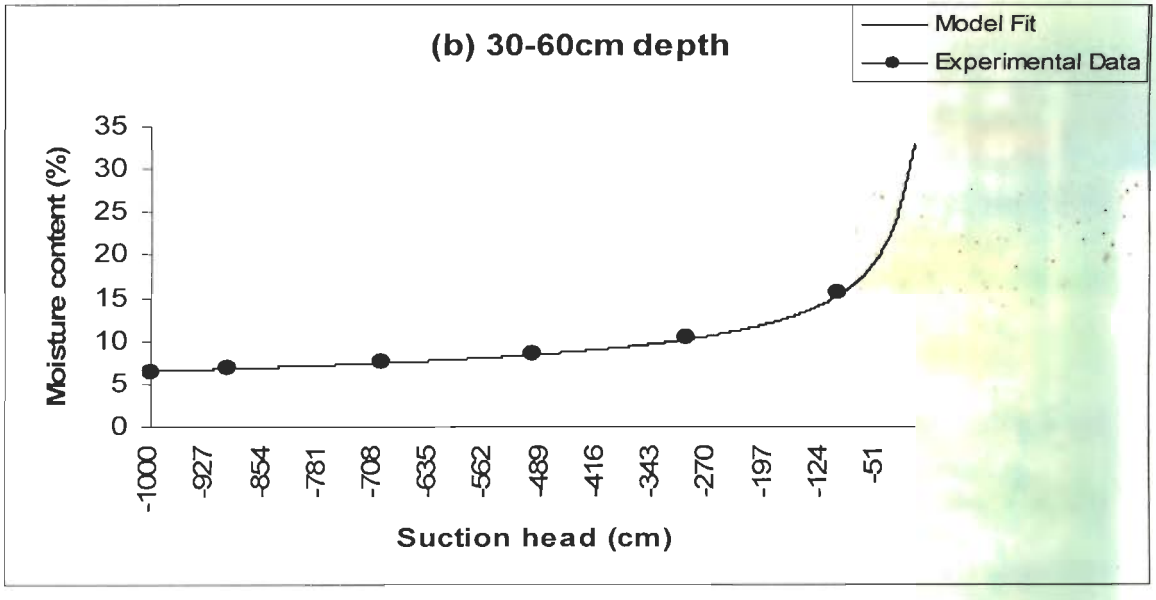

Fig. 4.4: Van Genuchten model fit for soil moisture data at location 2

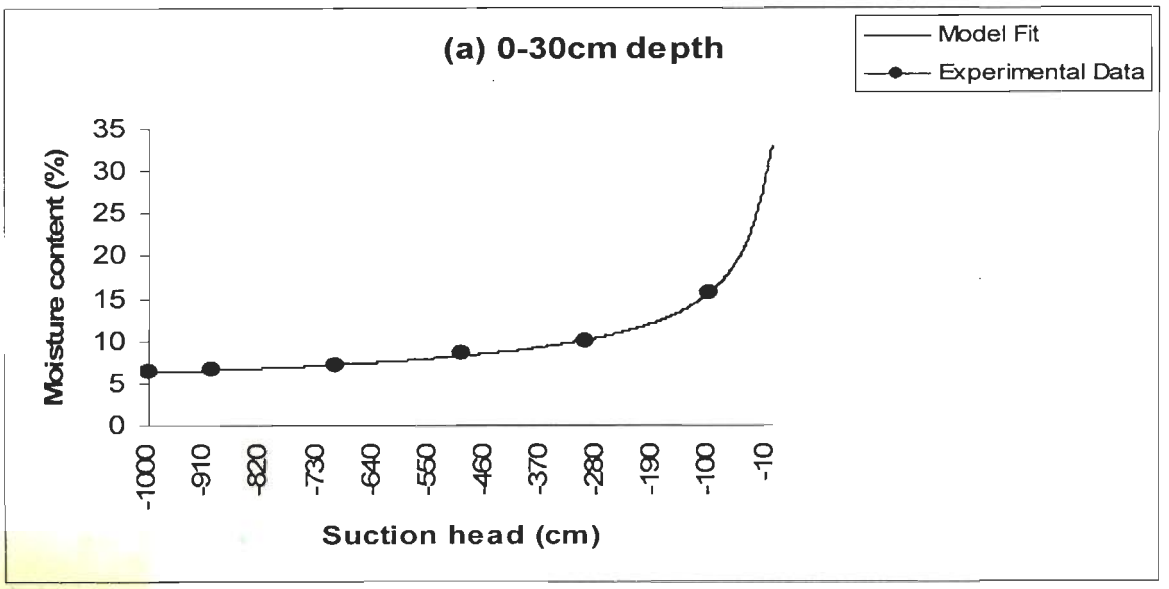

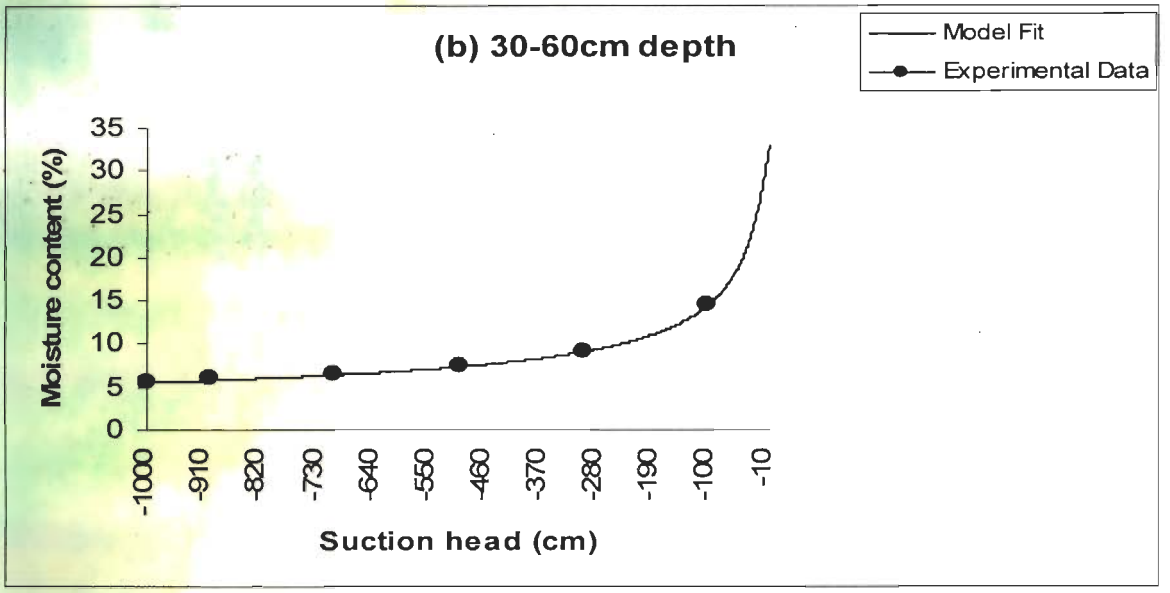

Figs. 4.5: Van Genuchten model fit for soil moisture data at location 3

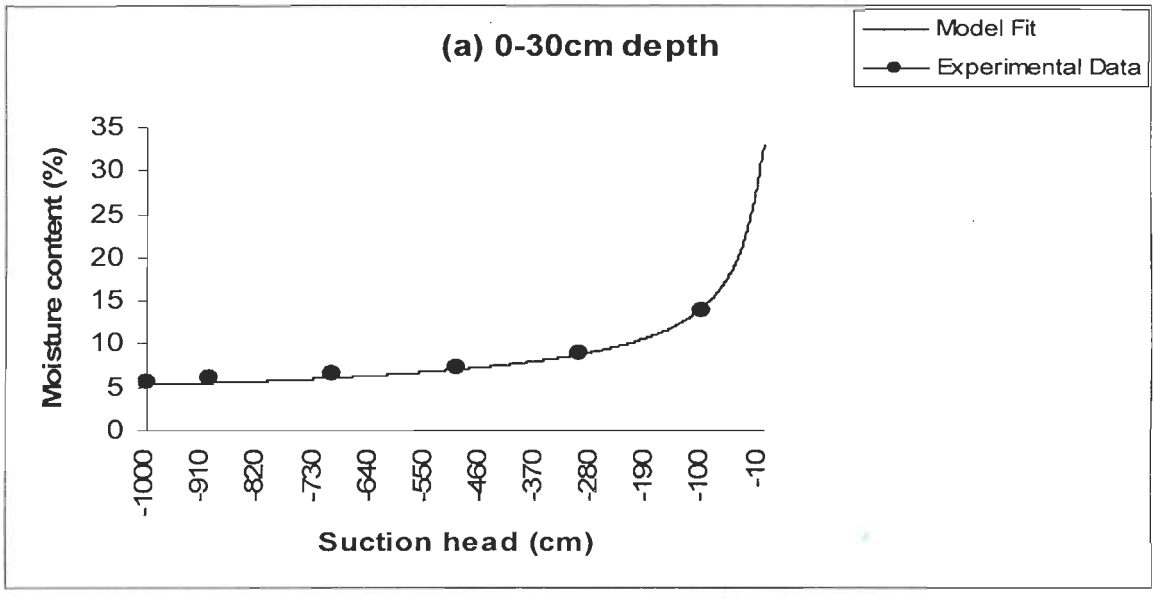

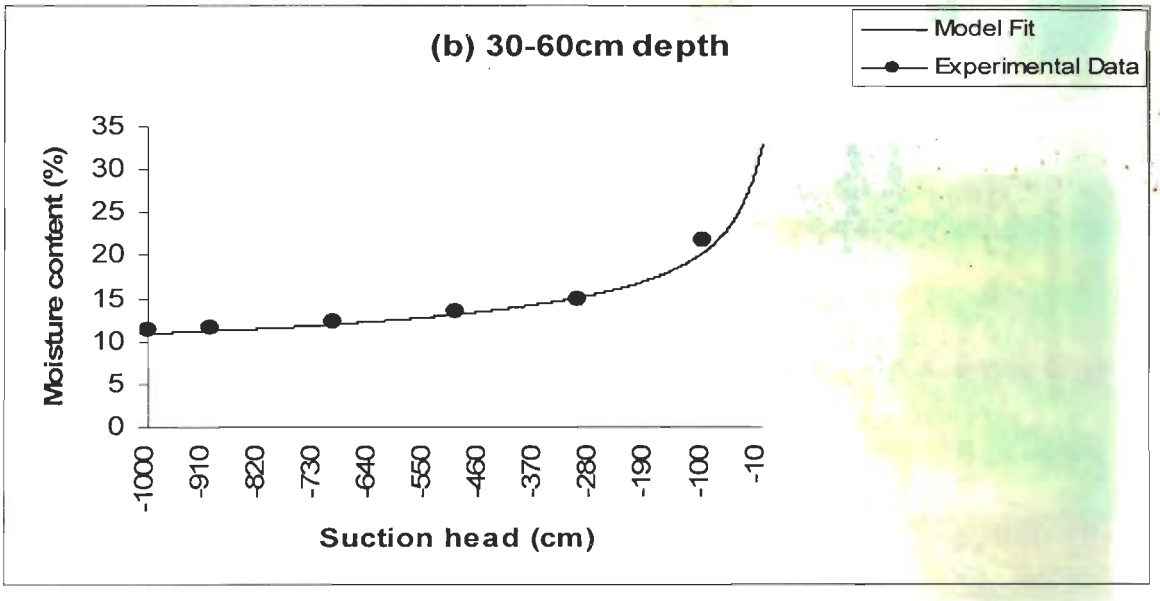

Figs. 4.6: Van Genuchten model fit for soil moisture data at location 4

4.4.7 Manning's Roughnes Coefficient

Manning's coefficient n is determined using Strickler's formula (Chow, 1959) as

$$n = 0.041 D_{50}^{1/6} \tag{4.6}$$

where, D_{50} is particle size for which 50% of the particles are smaller, in meters. The value of D_{50} for the four samples at the surface are obtained as 0.00033m, 0.00028m,

0.00023m, and 0.00027m respectively. The average D_{50} value for the field is obtained as 0.0002775m. Using eqn. 4.6 the value of n is obtained as 0.0105.

4.5 FIELD EXPERIMENT

4.5.1 Field Slope

The field slope S_0 is determined using a dumpy level. Plate 4.7 shows the dumpy level set up in the field during the experiment. The slopes of the two border strips in the experimental station obtained are 0.007 and 0.0106 respectively.

Plate 4.7: Set up of Dumpy level during experiment

4.5.2 Border strip irrigation experiments

Irrigation experiments are carried out on two border strips in the experimental station during January to May, 2009. Prior to the experiment, both the border strips are cleared off grass and leveled. Soil moisture measurement sensors are installed at 5 m intervals. At locations near to the inlet, the sensors are installed at a higher depth and the depth is gradually reduced as one moves towards the tail end. Table 4.8 shows the

depth at which sensors are installed along the length of each of the border strips. The geometric and flow details of the two border strips are given in Table 4.9. The relevant soil parameters of the border strips are given in Table 4.10. Several irrigation advance and recession runs were conducted on both the border strips. Few of these runs were not successful due to experimental limitations in measuring the different flow variables. In the analysis, the data from two experimental runs, one for each border is presented.

Table 4.8: Depth of Soil moisture measurement sensors along the border strips

Distance from the inlet (m)	0	5	10	15
Depth (m)	0.4	0.3	0.2	0.1

Table 4.9: Geometric and flow details of border strips

Description	Border Strip 1	Border Strip 2
Length (m)	15.0	17.0
Width (m)	4.0	5.0
Slope (S_0)	0.007	0.0106
Inlet Discharge ($m^3/s/m$)	0.000571428	0.000595238
Cut off time (min)	320	430

Table 4.10: Soil Parameters

Soil parameters	Value
Saturated hydraulic conductivity (K_{sat}) (cm/hr)	2.916057
Van Genuchten retention parameter α_v (cm^{-1})	0.056
Van Genuchten retention parameter and n_v	1.44
Saturated moisture content (θ_s)	0.33
Residual moisture content (θ_r)	0.01
Manning's Coefficient (n)	0.0105

4.5.2.1 Border strip 1

Before conducting irrigation experiment, stakes were driven into the soil at 1m interval to measure the advance and recession of an irrigation event. Prior to the experiment, tensiometer readings and moisture content measurements at different depths at 5 m intervals along the border strip are made. Table 4.11 shows the moisture content and pressure head measurements made at different depths along the border strip prior to irrigation for border strip 1. The experimental run was started by irrigating the border strip and measuring the advance, recession, moisture content and pressure heads. Plate 4.8 shows the irrigation event under progress for the border strip 1. A stop watch was started, when water started flowing into the border strip. Advance time and flow depths were recorded as the water reached the successive stakes. Water was allowed to drain freely at the tail end of the border strip. Water inflow into the border strip was continued till cutoff time so that water gets infiltrated sufficiently deep into subsurface to enable soil moisture measurements. Recession measurements were also noted after the cutoff time. Table 4.12 shows the advance, summation of flow depths and recession data for the border strip 1.

Plate 4.8: Measurement of Irrigation events under progress for border strip 1

Table 4.11: Moisture content and pressure head prior to irrigation-Border strip 1

Depth (cm)	Length along Border strip (m)							
	0		5		10		15	
	Moisture Content (%)	Pressure Head (cm)	Moisture Content (%)	Pressure Head (cm)	Moisture Content (%)	Pressure Head (cm)	Moisture Content (%)	Pressure Head (cm)
0	12.6		11.4		12.9		12.4	
10	14.5		14.3		14.6		14.2	115.0
20	13.2		14.5		14.2	120.0	13.4	
30	13.7		13.8	125.0	13.1		13.6	
40	12.9	143.0	13.5		13.6		12.7	
50	13.3		13.4		12.9		13.0	
60	14.0		12.8		12.8		13.5	

Table 4.12: Advance, Summation of flow depths and Recession data-Border Strip1

Border strip 1			
Distance (m)	Advance time (Min)	Summation of flow depths (cm)	* Recession time (Min)
1	0.42	4.8	
2	0.60	5.8	0.35
3	1.00	8.0	
4	1.33	10.2	
5	1.90	12.7	0.85
6	2.6	15.1	
7	3.28	17.3	
8	4.0	19.8	
9	5.0	22.0	1.35
10	6.0	25.0	
11	7.33	27.7	
12	8.42	30.0	
13	9.5	31.3	1.8
14	10.9	33.6	
15	13.0	36.5	

* Recession is measure with cutoff time as reference

Table 4.13 presents the soil moisture and pressure head taken immediately after cutoff at different depths along the border strip. The numerical model developed in chapter 3 is applied to predict advance, recession and subsurface moisture contents. Fig. 4.7 compares the model predicted advance and recession with the experimentally measured data. It can be clearly seen from Fig. 4.7, that model predictions are in close agreement with the experimental data. Fig. 4.8 presents the comparison between the model predicted and experimentally observed moisture contents at different depths along the border strip. For comparison, the tensiometer readings are converted to corresponding moisture contents using the Van-Genuchten constitutive relationship with $\alpha_v = 0.056$ cm^{-1} and $n_v = 1.44$. From Fig. 4.8, it can be seen that the model predicted moisture contents are slightly higher than the experimentally observed moisture contents all along the border strip. However, it can be seen that the difference is minimal indicating accuracy of the model predictions.

Table 4.13 Moisture content and pressure head after irrigation-Border strip 1

Depth (cm)	Length along Border strip (m)							
	0		5		10		15	
	Moisture Content (%)	Pressure Head (cm)	Moisture Content (%)	Pressure Head (cm)	Moisture Content (%)	Pressure Head (cm)	Moisture Content (%)	Pressure Head (cm)
0	33.0		33.0		33.0		33.0	
10	33.0		33.0		33.0		33.0	0.0
20	33.0		32.8		32.9	3.0	33.0	
30	32.5		32.4	5.0	33.0		32.8	
40	32.3	7.0	31.9		32.4		32.0	
50	31.8		32.0		31.8		31.6	
60	31.5		31.8		31.5		31.4	

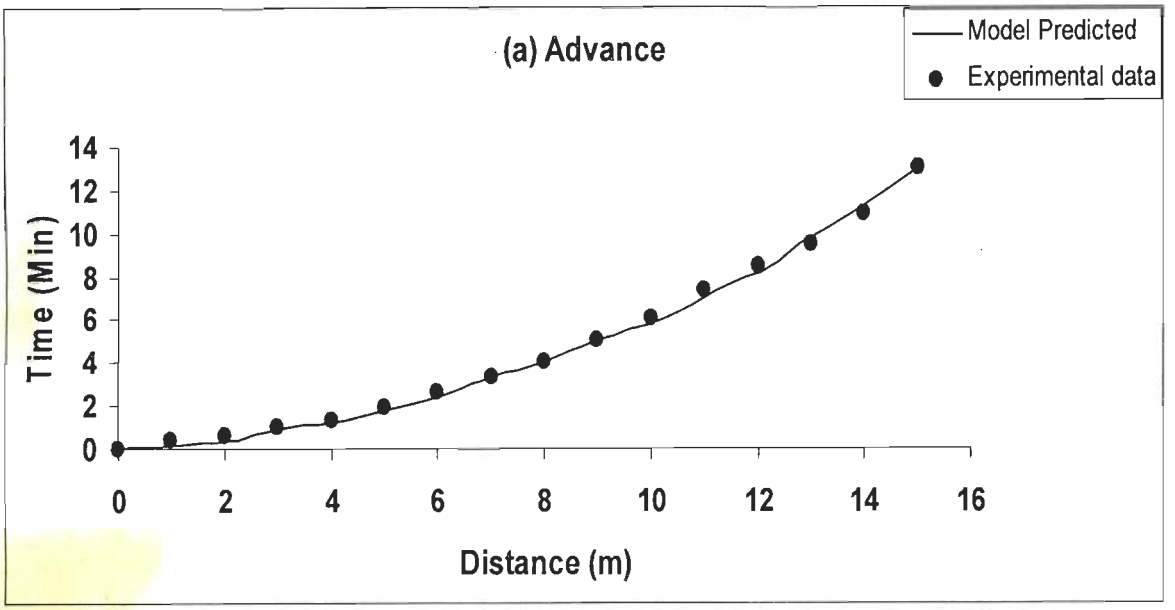

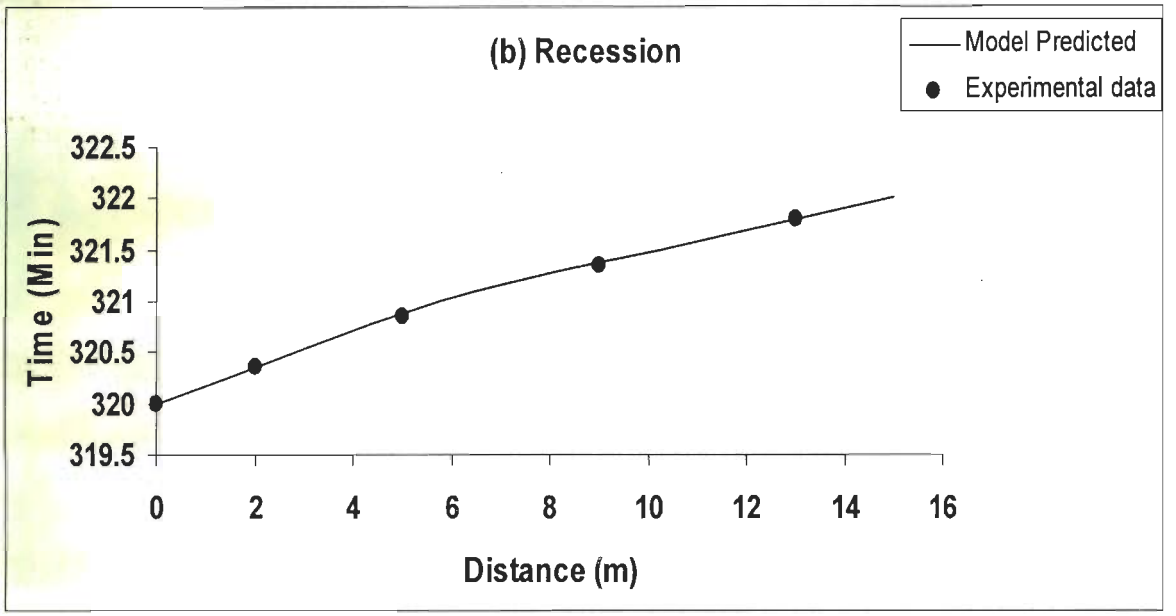

Fig. 4.7: Comparison of model predicted and experimentally observed advance and recession-border strip 1

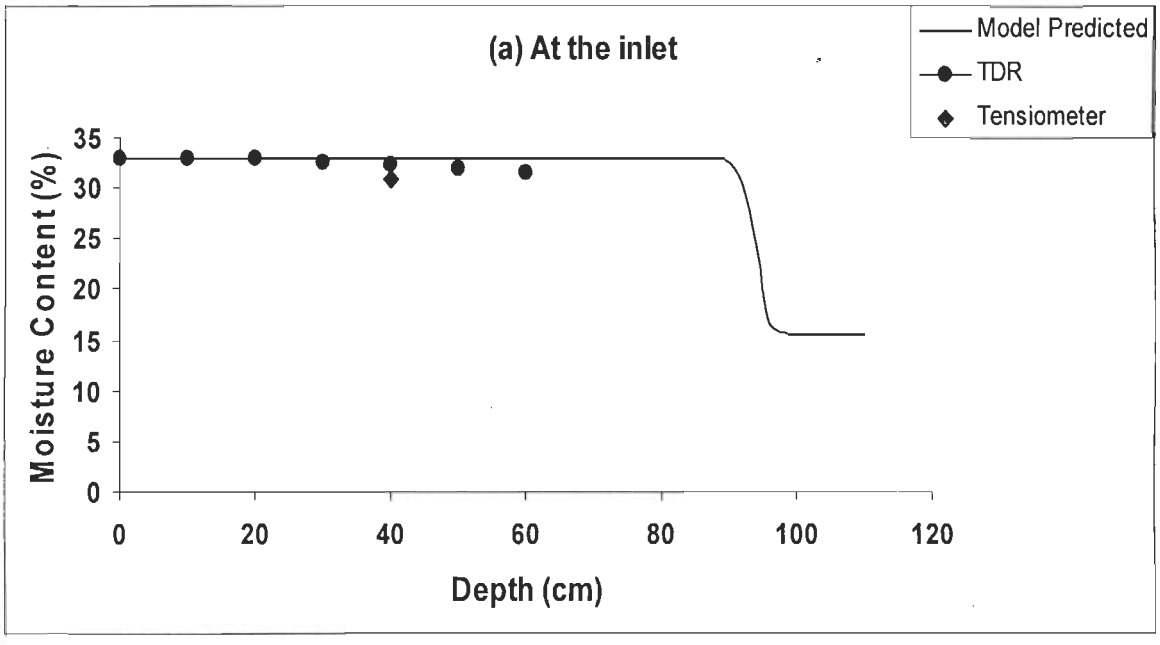
(a) At the inlet
Model Predicted
TDR
Tensiometer
Moisture Content (%)
35
30
25
20
15
10
5
0
0
20
40
60
80
100
120
Depth (cm)

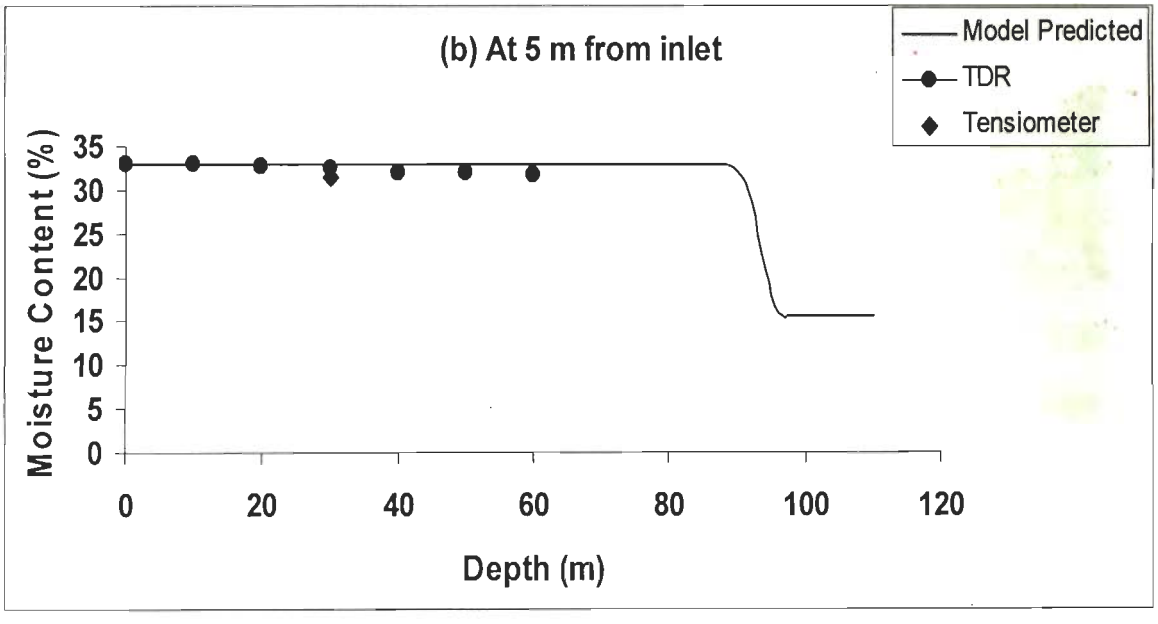
(b) At 5 m from inlet
Model Predicted
TDR
Tensiometer
Moisture Content (%)
35
30
25
20
15
10
5
0
0
20
40
60
80
100
120
Depth (m)

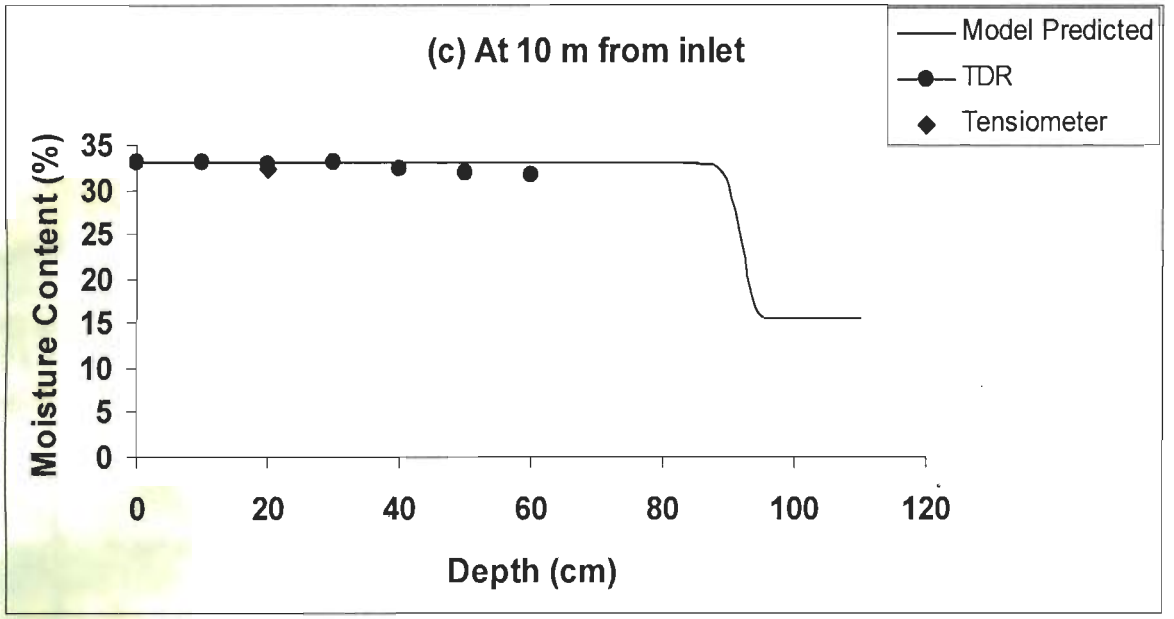

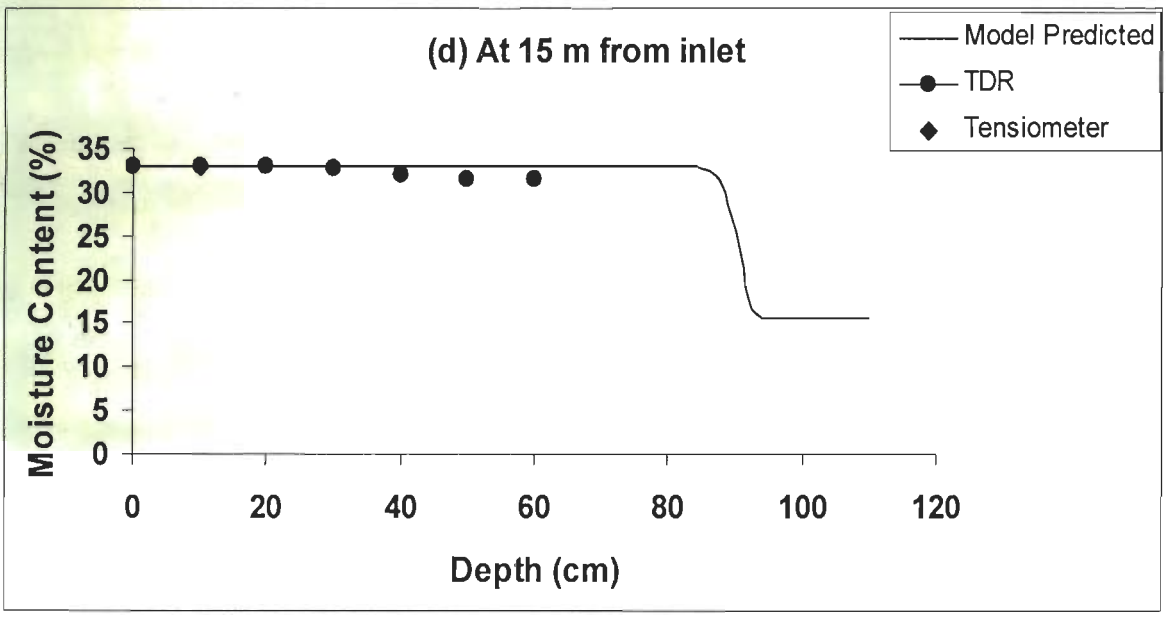

Fig. 4.8: Comparison of model predicted and experimentally observed moisture content-border strip 1

4.5.2.2 Border strip 2

Before conducting irrigation experiment, stakes were driven into the soil at 1m interval to measure the advance and recession of an irrigation event. Prior to the experiment, tensiometer readings and moisture content measurements at different depths at 5m intervals along the border strip are made. Table 4.14 shows the moisture

content and pressure head measurements made at different depths along the border strip, prior to irrigation for border strip 2. The experimental run was started by irrigating the border strip and measuring the advance, recession, moisture content and pressure heads. Plate 4.9 shows the irrigation event under progress for the border strip 2. A stop watch was started, when water started flowing into the border strip. Advance time and flow depths were recorded as the water reached the successive stakes. Water was allowed to drain freely at the tail end of the border strip. Water inflow into the border strip was continued till cutoff time so that water gets infiltrated sufficiently deep into subsurface to enable soil moisture measurements. Recession measurements were also noted after the cutoff time. Table 4.15 shows the advance, summation of flow depths and recession data for the border strip 2.

Table 4.14: Moisture content and pressure head prior to irrigation-Border strip 2

Depth (cm)	Length along Border strip (m)							
	0		5		10		15	
	Moisture Content (%)	Pressure Head (cm)	Moisture Content (%)	Pressure Head (cm)	Moisture Content (%)	Pressure Head (cm)	Moisture Content (%)	Pressure Head (cm)
0	8.5		7.9		9.2		11.5	
10	13.9		14.6		14.0		14.4	119.0
20	13.5		14.5		12.9	152.0	13.5	
30	14.3		13.6	141.0	13.8		13.0	
40	13.0	150.0	13.3		13.6		14.1	
50	13.8		12.8		12.7		13.8	
60	14.0		13.7		12.4		13.3	

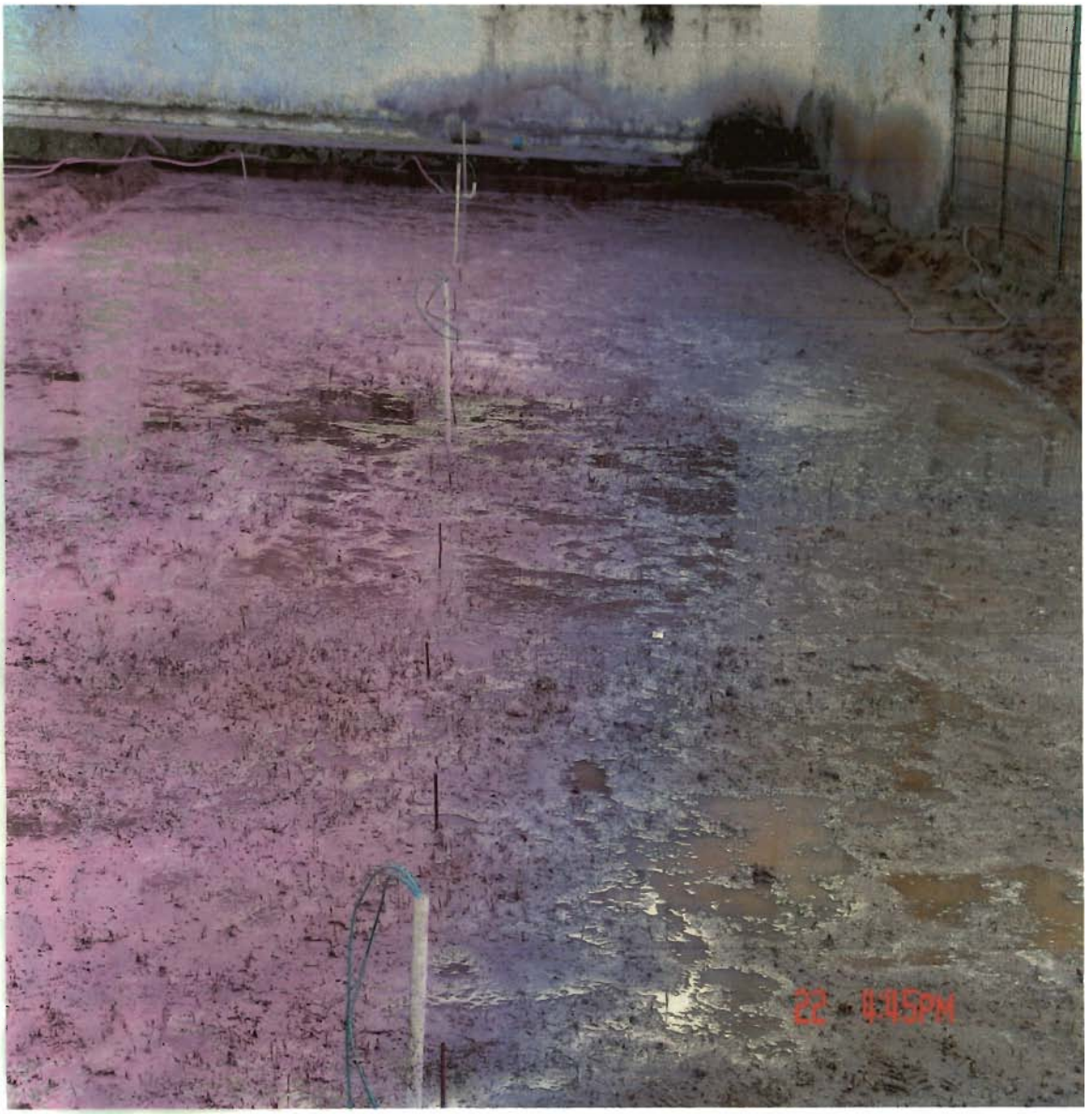

Plate 4.9: Measurement of Irrigation events under progress for border strip 2

Table 4.15: Advance, Summation of flow depths and Recession data-Border Strip2

Border 2			
Distance (m)	Advance time (Min)	Summation of flow depths (cm)	* Recession time(Min)
1	0.17	2.7	
2	0.5	4.5	0.25
3	0.83	7.0	
4	1.25	8.6	
5	1.83	11.0	0.6
6	2.5	12.3	
7	3.33	13.5	
8	4.33	16.6	1.0
9	5.25	20.8	
10	6.42	23.0	
11	7.83	26.0	
12	9.33	27.5	1.4
13	11.0	30.5	
14	13.25	32.0	
15	16.5	34.5	
16	20.0	36.8	
17	25.0	39.5	2.0

- Recession is measure with cutoff time as reference

Table 4.16 presents the soil moisture and pressure head taken immediately after cutoff at different depths along the border strip. The numerical model developed in chapter 3 is applied to predict advance, recession and subsurface moisture contents. Fig. 4.9 compares the model predicted advance and recession with the experimentally measured data. It can be clearly seen from Fig. 4.9, that model predictions are in close agreement with the experimental data. Fig. 4.10 presents the comparison between the model predicted and experimentally observed moisture contents at different depths along the border strip. For comparison, the tensiometer readings are converted to corresponding moisture contents using the Van-Genuchten constitutive relationship with α_v = 0.056 cm^{-1} and n_v = 1.44. From Fig. 4.10, it can be seen that the model predicted moisture contents are slightly higher than the experimentally observed

moisture contents all along the border strip. However, it can be seen that the difference is minimal indicating accuracy of the model predictions.

Table 4.16 Moisture content and pressure head after irrigation-Border strip 2

Depth (cm)	Length along Border strip (m)							
	0		5		10		15	
	Moisture Content (%)	Pressure Head (cm)	Moisture Content (%)	Pressure Head (cm)	Moisture Content (%)	Pressure Head (cm)	Moisture Content (%)	Pressure Head (cm)
0	33.0		33.0		33.0		33.0	
10	33.0		33.0		33.0		33.0	2.0
20	33.0		32.7		33.0	4.0	33.0	
30	32.4		32.5	6.0	32.6		32.7	
40	32.0	8.0	32.6		32.2		32.4	
50	32.1		32.0		31.9		32.0	
60	31.6		31.7		31.5		30.6	

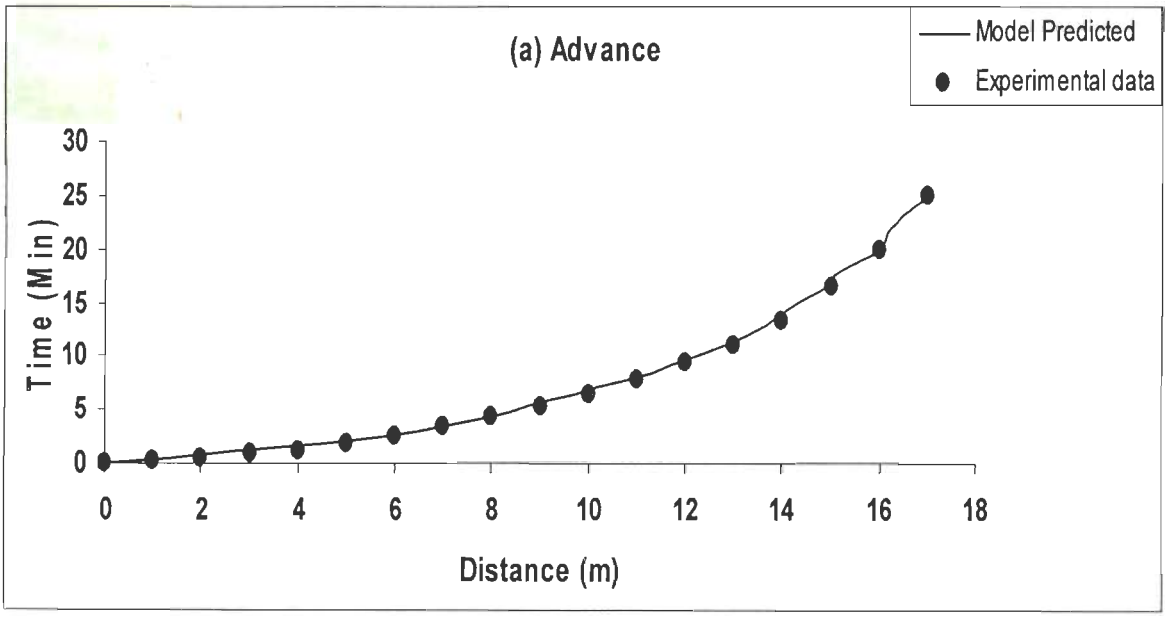

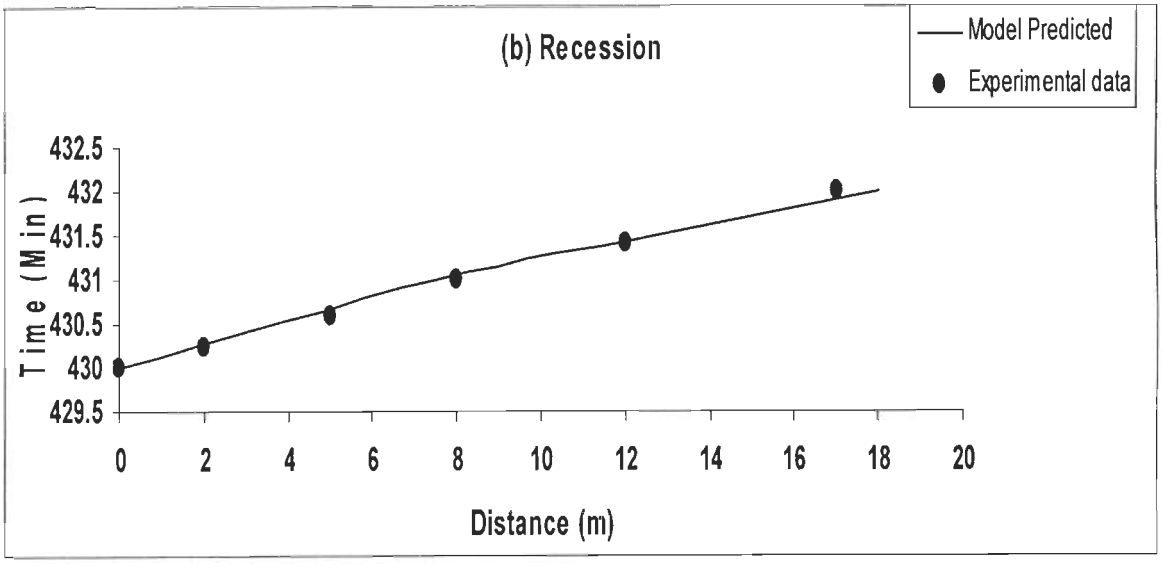

Fig. 4.9: Comparison of model predicted and experimentally observed advance and recession-border strip 2

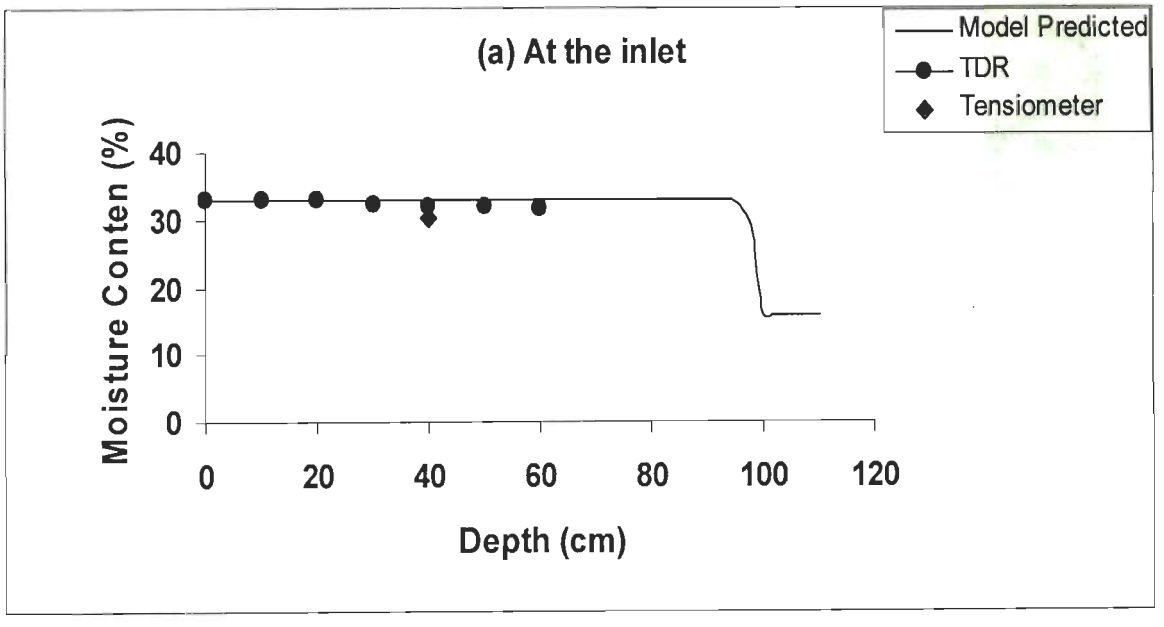

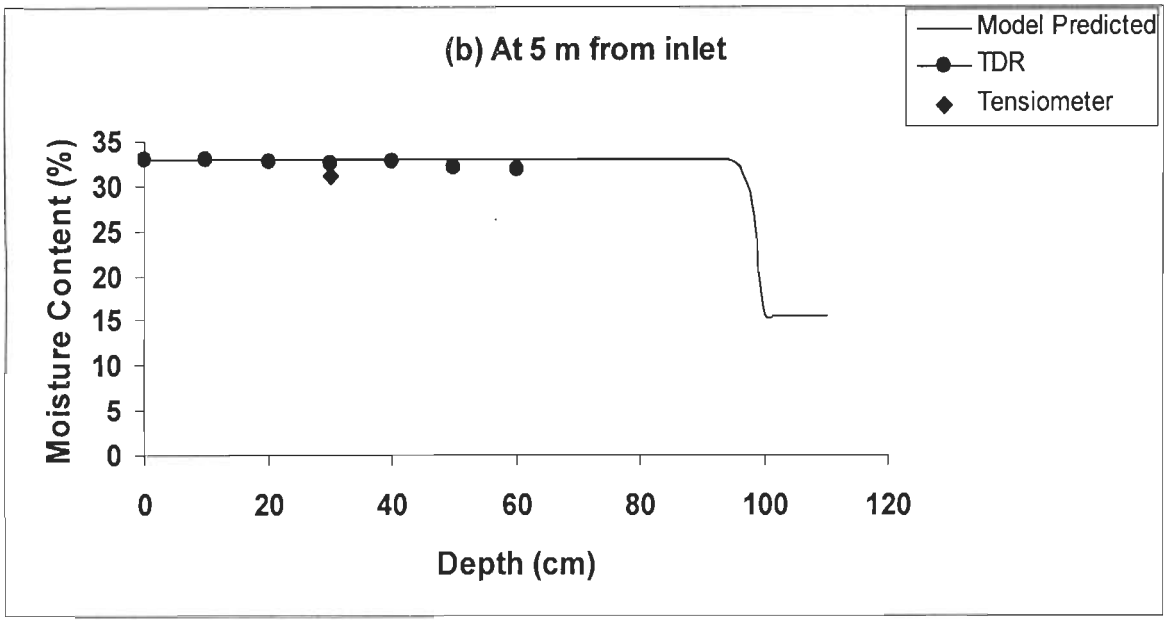
(b) At 5 m from inlet
Model Predicted
TDR
Tensiometer
Moisture Content (%)
35
30
25
20
15
10
5
0
0
20
40
60
80
100
120
Depth (cm)

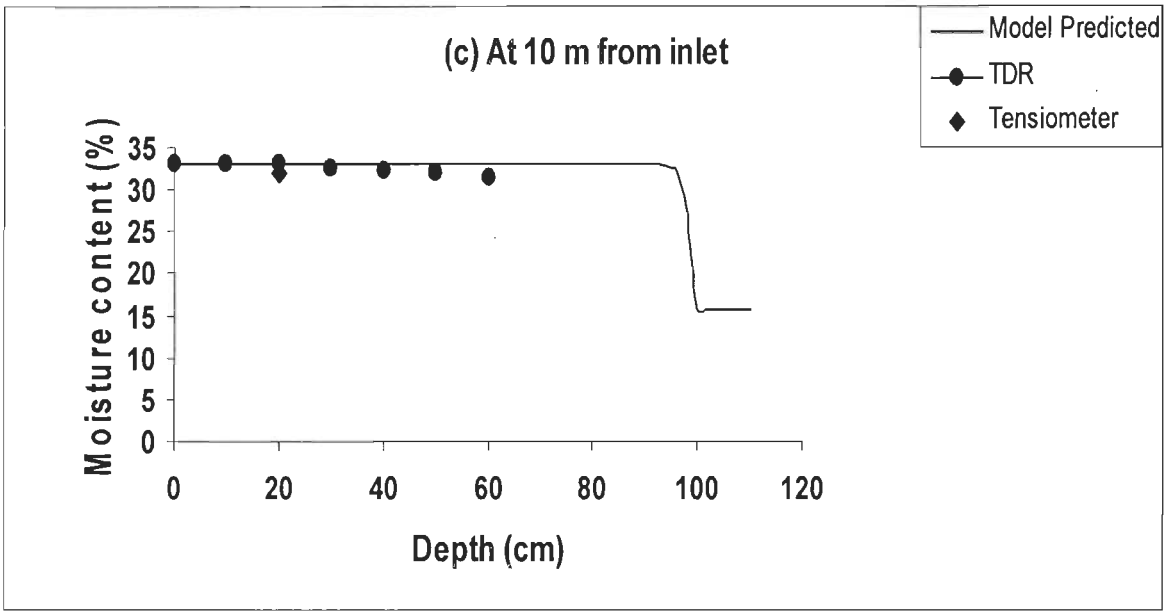
(c) At 10 m from inlet
Model Predicted
TDR
Tensiometer
Moisture content (%)
35
30
25
20
15
10
5
0
0
20
40
60
80
100
120
Depth (cm)

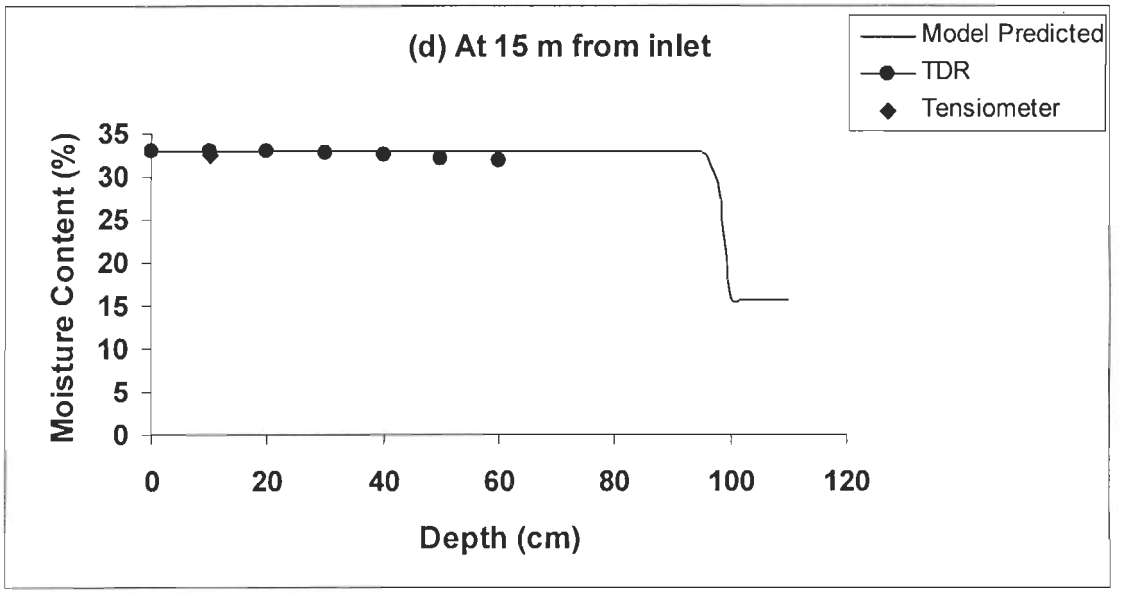

Fig. 4.10: Comparison of model predicted and experimentally observed moisture content-border strip 2

4.6 CLOSURE

In this Chapter, detailed laboratory and field irrigation experiments are described. The laboratory experiments involve the determination of physical properties of the soil such as textural properties, bulk density, particle density, porosity saturated hydraulic conductivity and soil moisture characteristic using Pressure Plate Extractor test. The detailed field irrigation experiments involve both overland and subsurface flow measurements. These surface and subsurface flow measurements are used to asses the performance of the numerical model developed in chapter 3 in predicting both overland and subsurface flow variables. It is indicated from the Figs. 4.7, 4.8 and 4.9, 4.10 for border strip 1 and 2 respectively, that the model predictions are in good agreement with the field observed surface as well as subsurface data for both the borders.

CHAPTER 5

ESTIMATION OF INFILTRATION PARAMETERS

5.1 INTRODUCTION

In chapter 3, a numerical model has been developed to predict irrigation advance, recession and subsurface wetting front movement in a border strip irrigation system. The accurate prediction of these events mainly depends on the system parameters such as Manning's roughness coefficient n and infiltration parameters: saturated hydraulic conductivity K_{sat}, water retention parameters α_v, n_v, θ_s and θ_r. Among these, the estimation of infiltration parameters at field level is one of the difficult tasks (Walker and Skogerboe, 1987). For a relatively big field, estimation of infiltration parameters using infiltrometers requires that the test be conducted at many places. Further, these parameters may not represent the infiltration phenomenon at field scale. An alternative to these direct measurement techniques is to employ inverse techniques for parameter estimation. In such an approach, the infiltration parameters are estimated by minimizing the deviations between the model predicted and field observed flow attributes such as irrigation advance, recession, flow depth and wetting front movement. In the present chapter, a parameter estimation model is developed by coupling the numerical model developed in chapter 3 with a Sequential unconstrained minimization technique (SUMT). The issues of identifiability and uniqueness are discussed by estimating the parameters from hypothetical data. The details of model development and application are discussed in the following sections.

5.2 INVERSE PROBLEM

The inverse problem involves the estimation of infiltration K_{sat}, α_v, n_v, θ_s and θ_r from irrigation event data of border strip irrigation. Among these parameters θ_s is usually taken as the porosity of the soil and θ_r is a fitting parameter to fit $\theta - \psi$ data at very low moisture content (i.e., very dry state of soil) and does not has much influence on soil moisture dynamics. Hence, the present study is limited to the estimation of parameters K_{sat}, α_v and n_v.

5.2.1 General Formulation of Estimation Problem

The inverse problem is formulated as a nonlinear optimization problem, i.e., the infiltration parameters are estimated by minimizing the deviation between field observed and model predicted response. The objective function is defined as

$$\min \phi(\mathbf{b}, L_i) = \sum_{i=1}^{x} v_i \sum_{j=1}^{m_{i,j}} \sum_{k=1}^{m_{i,k}} \sum_{p=1}^{m_{i,p}} W_{j,k,p} \left[L_i^*(t_j, x_k, z_p) - L_i(t_j, x_k, z_p, \mathbf{b}) \right]^2 \qquad (5.1)$$

where, L represents the different sets of measurements, $m_{i,j}$, $m_{i,k}$, and $m_{i,p}$ are number of specific times, specific distances from the inlet and specific depths in the subsurface at which measurements are made in a particular set, $\boldsymbol{b}$ is the parameter vector represented as $\boldsymbol{b} = \{K_{sat}, \alpha_v, n_v\}^T$, $L_i^*(t_j, x_k, z_p)$ represents the vector of experimentally observed irrigation advance, recession, flow depth and moisture contents measure at time t_j, distance x_k and depth z_p. $L_i(t_j, x_k, z_p, \boldsymbol{b})$ represents the vector of model predicted irrigation advance, recession, flow depth and moisture contents obtained by solving the direct problem (Eqs. 3.1, 3.2 and 3.8) for a given parameter vector $\boldsymbol{b}$, v_i and $W_{j,k,p}$ are the weights associated with a particular measurement set or observation respectively. $W_{j,k,p}$ is considered as 1 and v_i for each measurement set is taken as the inverse of the measurement variance σ_i^2. The minimization of objective function is accomplished by

using Sequential Unconstrained Minimization Technique (SUMT). The objective is to find the optimum parameter vector ***b*** that minimizes the objective function (Eq. 5.1). When the observation errors are assumed to be independent and normally distributed the weighting matrix ***W*** becomes an identity matrix and the Eq. (5.1) reduces to simple ordinary least squares (OLS) problem.

$$\min \phi(\mathbf{b}, L_i) = \sum_{i=1}^{x} v_i \sum_{j=1}^{m_{i,j}} \sum_{k=1}^{m_{i,k}} \sum_{p=1}^{m_{i,p}} \left[L_i^*(t_j, x_k, z_p) - L_i(t_j, x_k, z_p, \mathbf{b}) \right]^2 \tag{5.2}$$

The OLS formulation has probably been the most popular one for parameters estimation. Its attraction is due to its simplicity and because of requiring minimum amount of information. OLS yields optimal parameter estimates when observation errors are normally distributed, are uncorrelated and have a constant variance (Kool et al., 1987), when these conditions are not met, the OLS method will no longer yield optimum parameter estimates in terms of precision and minimum variance.

5.2.2 Solution Algorithm

The minimization of objective function (5.2) is carried out using Sequential Unconstrained Minimization Technique (SUMT) proposed by Fiacco and McCormick (1968). SUMT is usually a gradient based traditional optimizer, wherein the problem of constrained minimization is posed as a sequence of unconstrained minimizations by adding sequentially attenuating penalty functions to the objective function. Consider the following typical constrained minimization problem:

Minimze $\phi(X)$ with respect to vector X, subject to the constraints:

$$g_j(X) \leq 0, \quad j = 1, \ldots, m \tag{5.3}$$

This problem is converted to the following unconstrained minimization problem:

$$\text{Minimize } \phi(\mathbf{X}) = f(\mathbf{X}) + r \sum_{j=1}^{m} G\left[g_j(\mathbf{X})\right] \tag{5.4}$$

where, $G[g_j(X)]$ are the penalty functions associated with violation of the corresponding assigned constraints, and r is an optimization parameter. Typically interior penalty functions $[-1/g_j(X)]$ would be finite and positive in the feasible region, but blow up to plus infinity as the solution approaches the constraint. This is a very strong disincentive for the solution to cross the feasible region, and would thus ensure implementation of the constraints implicitly. However, the solution of the unconstrained minimization would represent the solution of the original constrained minimization problem, provided the penalty parameter r tends to zero. Assigning a very low value to r right in the beginning leads to the problem of poor convergence in the unconstrained minimization of the objective function ϕ. This problem is overcome by initially starting with a moderate value of r, and gradually reducing it through a parameter c in successive unconstrained minimizations say (k) and $(k+1)$ (i.e., $r_{k+1} = c.r_k$ where, $c < 1$) until the desired level of convergence among sequential unconstrained minima is obtained. The main advantage of this approach is that one may pick up an appropriate algorithm of unconstrained minimization from a wide array. Fig. 5.1 shows the flow chart for the interior penalty function method. The numerical model developed in Chapter 3 is coupled with SUMT routine (Rao, 1979) and is presented in Appendix II.

5.3 SYNTHETIC DATA

Synthetic irrigation advance, flow depth and moisture content data is generated by solving Eqs. 3.1, 3.2 and 3.8 using the numerical model developed in Chapter 3. The relevant flow, hydraulic and soil parameters used for generation of synthetic data is given in Table 5.1. Table 5.2 presents the synthetic irrigation advance data and summation of flow depths up to irrigation advance at different times. Synthetic

moisture content data at different locations along the border strip at cutoff time is presented in Table 5.3.

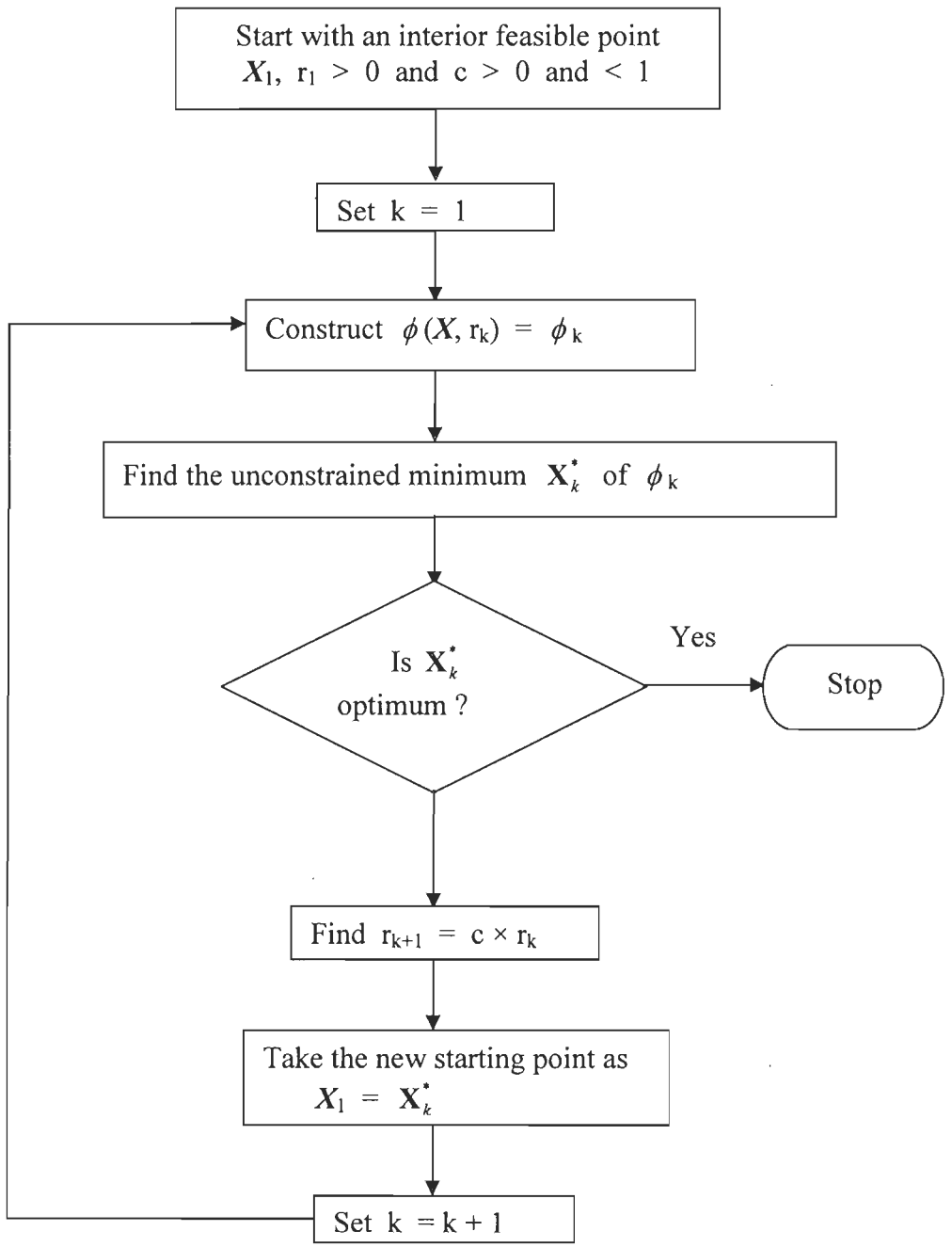

Fig. 5.1: Flow Chart of Interior Penalty Function Method

Table 5.1: Parameters used for generation of synthetic data

Parameter	Value
Initial flow depth, h_{ini} (m)	0.005
Discharge, q (m^3/sec/m)	0.0005238
Border Slope, S_0	0.007
Manning's roughness coefficient, n	0.0305
Saturated hydraulic conductivity, K_{sat} (m/sec)	1.38888×10^{-6}
Retention parameters, α_v (m^{-1})	2.0
Retention parameters, n_v.	2.3
Saturated moisture content, θ_s	0.33
Residual moisture content, θ_r	0.01
Initial pressure head in subsurface (m)	-1
Cutoff time (min)	180

Table 5.2: Synthetic irrigation advance and flow depth data

Time (Min)	Irrigation advance (m)	Summation of flow depths (m)
10	10.50	0.231
20	14.00	0.310
30	17.00	0.376
40	19.00	0.421
50	21.25	0.470
60	23.00	0.509
70	24.50	0.542
80	25.75	0.570
90	27.00	0.598
100	28.25	0.625
110	29.50	0.653
120	30.50	0.675
130	31.50	0.697
140	32.50	0.719
150	33.50	0.741
160	34.25	0.758
170	35.00	0.775
180	36.00	0.796

Table 5.3: Synthetic moisture content data

Depth (cm)	Length along Border strip (m)			
	0	5	10	15
	Moisture content			
5	0.329	0.329	0.329	0.329
10	0.327	0.327	0.326	0.326
15	0.314	0.313	0.312	0.307
20	0.288	0.286	0.280	0.264
25	0.158	0.154	0.142	0.131
30	0.127	0.127	0.127	0.127
35	0.127	0.127	0.127	0.127
40	0.127	0.127	0.127	0.127
45	0.127	0.127	0.127	0.127
50	0.127	0.127	0.127	0.127
55	0.127	0.127	0.127	0.127
60	0.127	0.127	0.127	0.127
65	0.127	0.127	0.127	0.127
70	0.127	0.127	0.127	0.127
75	0.127	0.127	0.127	0.127
80	0.127	0.127	0.127	0.127
85	0.127	0.127	0.127	0.127
90	0.127	0.127	0.127	0.127
95	0.127	0.127	0.127	0.127
100	0.127	0.127	0.127	0.127

5.4 PARAMETER ESTIMATION

The robustness of the optimization procedure is studied by varying the number of unknown parameters (K_{sat}, α_v, and n_v) to be estimated from 1 to 3. In addition, the efficacy of the optimization procedure is analyzed by starting the initial guesses of individual parameters considerably far away from their true values. The parameter estimates is carried out first by giving surface data (irrigation advance or flow depths) to study whether the optimization results in unique estimation of all the parameters. In

cases, where the surface data is found to be inadequate, subsurface data is also included in the optimization. The parameter estimation is discussed in detail in the following sections.

5.4.1 Case 1: Estimation of One Unknown Parameter (K_{sat}, α_v or n_v)

Case 1 considers the estimation of one unknown parameter while treating the other two parameters as constant to their respective values used for the generation of hypothetical data. Further two sub cases (Case A and Case B) are considered. In case A, the initial guess of the parameter is over estimated while in case B it is under estimated. The initial guess of parameters K_{sat} and α_v is over and under estimated by one order while the range of parameter n_v is considered from 1.2 to 5 as n_v can't take values less than 1 (Van Genuchten 1980). Table 5.4 presents the parameter estimates obtained by giving summation of the flow depths or irrigation advance data in the optimization. It can be seen from Table 5.4 for the case, in which the summation of flow depths is used in the optimization, the parameter estimates almost converged to the true values. However, parameter estimates obtained by using irrigation advance data do not converge to the true values. This is due to the fact that, the irrigation advance predicted by the numerical model depends on the grid size (Δx) at the ground surface. While predicting the irrigation advance, the numerical model checks whether the flow depth is more than the initial flow depth. For cases, where the irrigation advance falls between the surface nodal points, the numerical model assigns the distance to the preceding node as the irrigation advance. It is to be noted here that the accuracy of parameters using irrigation advance data can be improved by reducing the surface grid size (Δx). Further, Table 5.4 suggests that starting the initial guess as under estimated value results in less number of iterations for the optimization to converge to the optimal solution. It is also observed that, the provision of both irrigation advance

and summation of flow depth data also resulted in estimated parameters converging to the true values. Hence for further estimation, the summation of flow depths is used.

Table 5.4 Parameter Estimates for Hypothetical flow depth and irrigation advance data-Case 1

Case A (Over estimate)				Case B (Under estimate)			
Parameter Estimation with flow depth							
Parameter	True value	Initial guess	Final estimate	No. of Iterations	Initial guess	Final estimate	No. of Iterations
α_v (cm^{-1})	0.02	0.2	0.019985	5	0.002	0.019997	3
n_v	2.3	5.0	2.2955	3	1.2	2.2986	2
K_{sat} (cm/hr)	5.0	50.0	4.97646	12	0.5	4.98268	9
Parameter Estimation with advance distance							
α_v (cm^{-1})	0.02	0.2	0.019894	6	0.002	0.019687	5
n_v	2.3	5.0	2.269616	5	1.2	2.272636	4
K_{sat} (cm/hr)	5.0	50.0	5.005512	13	0.5	5.00842	8

5.4.2 Case 2: Estimation of Two Unknown Parameters {(α_v, n_v), (K_{sat}, α_v) (K_{sat}, n_v,)}

In this case, among the three parameters, two are considered as unknown and are estimated while keeping other parameter as constant to its respective value used for generation of hypothetical data. Such an estimation results in three combinations of two unknown parameters; (α_v, n_v), (K_{sat}, α_v) and (K_{sat}, n_v,). For each of these combinations, four sub sets are considered. In case A, the initial guess of the parameters are over estimated from their true values. In case B, the initial guess of the parameters are under estimated. In case C, the initial guess of the first parameter is over estimated while, the initial guess of the second parameter is under estimated. In contras, in case D, the initial

guess of the first parameter is under estimated while, the initial guess of the second parameter is over estimated. During the optimization runs, it was observed that in case of starting the optimization with overestimated values as given in Table 5.4, the algorithm had problems in converging to the true values. Hence, the overestimated initial guesses are reduced to 20 cm/hr, 0.1 cm^{-1} and 4 for K_{sat}, α_v and n_v respectively. Table 5.5 presents the details of parameter estimation for the sub cases A, B, C and D. It can be seen from Table 5.5 that, the parameter estimates converge nearly to the true values for all the sub cases. In addition, it is also seen from Table 5.5 that starting the initial guess as under estimated values results in least number of iterations for the optimization to converge to the true values.

Table 5.5 Parameter Estimates for the Hypothetical flow depth data-Case 2

Parameters	True values	Case A (Over estimate)			Case B (Under estimate)			Case C (Mixed) Type I			Case D (Mixed) Type II		
		Initial guess	Final estimated value	No. of iterations	Initial guess	Final estimated value	No. of iterations	Initial guess	Final estimated value	No. of iterations	Initial guess	Final estimated value	No. of iterations
α_v (cm^{-1})	0.02	0.1	0.020092		0.002	0.019899		0.1	0.02014		0.002	0.01954	
n_v	2.3	4.0	2.27861	16	1.2	2.28854	15	1.2	2.28576	21	4.0	2.28654	19
K_{sat} (cm/hr)	5.0	20.0	4.971376		0.5	4.960213		20.0	4.965846		0.5	4.89965	
α_v (cm^{-1})	0.02	0.1	0.01896	20	0.002	0.01956	14	0.002	0.01869	18	0.1	0.01905	22
K_{sat} (cm/hr)	5.0	20.0	4.89764		0.5	4.97902		20.0	4.94602		0.5	4.970238	
n_v	2.3	4.0	2.27985	18	1.2	2.27835	13	1.2	2.29483	15	4.0	2.28963	17

5.4.3 Case 3: Estimation of Three Unknown Parameters (K_{sat}, α_v and n_v)

Case 3 considers the simultaneous estimation of three parameters K_{sat}, α_v and n_v from flow depth as well as flow depth and moisture content data. Table 5.6 shows the details of parameter estimation when flow depth data alone is used in the objective function for optimization. From Table 5.6 it is can be seen that the optimization does not converge to the true values for both under and over estimated initial guesses. This is due to the unidentifiability of the infiltration parameters (Katopodes, 1990). Due to this, in addition to flow depth data, the moisture content data at different depths during irrigation advance is also included in the objective function for optimization. Table 5.7 shows the parameter estimation details when moisture content data in addition to flow depth data is used in the optimization. In this case also, it was observed that optimization does not converge to the true values for under, over and mixed estimated initial guesses. A similar observation was also made by Katopodes (1990) during simultaneous estimation of three parameters from surface and subsurface profile depth. It can be concluded that simultaneous identification of all the three infiltration parameters is not possible with flow depth and moisture content data alone.

Table 5.6 Parameter Estimates for the Hypothetical flow depth data-Case 3

Parameters	True values	Case A (Over estimate)			Case B (Under estimate)			Case C (Mixed) Type I		
		Initial guess	Final estimated value	No. of iterations	Initial guess	Final estimated value	No. of iterations	Initial guess	Final estimated value	No. of iterations
α_v (cm^{-1})	0.02	0.1	0.021707		0.002	0.017905		0.1	0.021812	
n_v	2.3	4.0	2.155833		1.2	2.17654		1.2	2.167542	
K_{sat} (cm/hr)	5.0	20.0	5.200005	17	0.5	4.725563	15	20.0	5.175846	19

Table 5.7 Parameter Estimates for the Hypothetical flow depth and Moisture content data-Case 3

Parameters	True values	Case A (Over estimate)			Case B (Under estimate)			Case C (Mixed) Type I		
		Initial guess	Final estimated value	No. of iterations	Initial guess	Final estimated value	No. of iterations	Initial guess	Final estimated value	No. of iterations
α_v (cm^{-1})	0.02	0.1	0.021603		0.002	0.01815		0.1	0.021926	
n_v	2.3	4.0	2.37056		1.2	2.20048		1.2	2.40245	
K_{sat} (cm/hr)	5.0	20.0	5.30081	16	0.5	4.82573	14	20.0	5.30748	18

5.5 ESTIMATION OF INFILTRATION PARAMETERS FROM FIELD EXPERIMENTS

Having applied the parameter estimation model to hypothetical data, the model is used to estimate the infiltration parameters from the two border strip irrigation experiments explained in section 4.5.2. Since the three infiltration parameters (K_{sat}, α_v and n_v) can't be identified uniquely from advance, flow depth and moisture content data, only the two parameters α_v and n_v are estimated by fixing the value of K_{sat} = 2.916057 cm/hr which was obtained using Guelph permeameter (section 4.4.5) The relevant data for parameters are given in Table 4.12 and 4.15 for border strips 1 and 2 respectively. Table 5.8 shows the optimal infiltration parameter estimates obtained from border strip experiments. Figs. 5.2, 5.3 and 5.4 show the experimentally observed and model predicted irrigation advance, recession and moisture content profiles respectively using the optimal parameter estimates given in Table 5.8 for border strip 1. Similarly Figs. 5.5, 5.6 and 5.7 show the experimentally observed and model predicted irrigation advance, recession and moisture content profiles respectively using the optimal parameter estimates given in Table 5.8 for border strip 2.

Table 5.8 Optimal Infiltration Parameter Estimates from Border Strip Experiments

Parameters	Border Strip 1	Border Strip 2
α_v (cm^{-1})	0.054	0.05
n_v	1.45	1.42

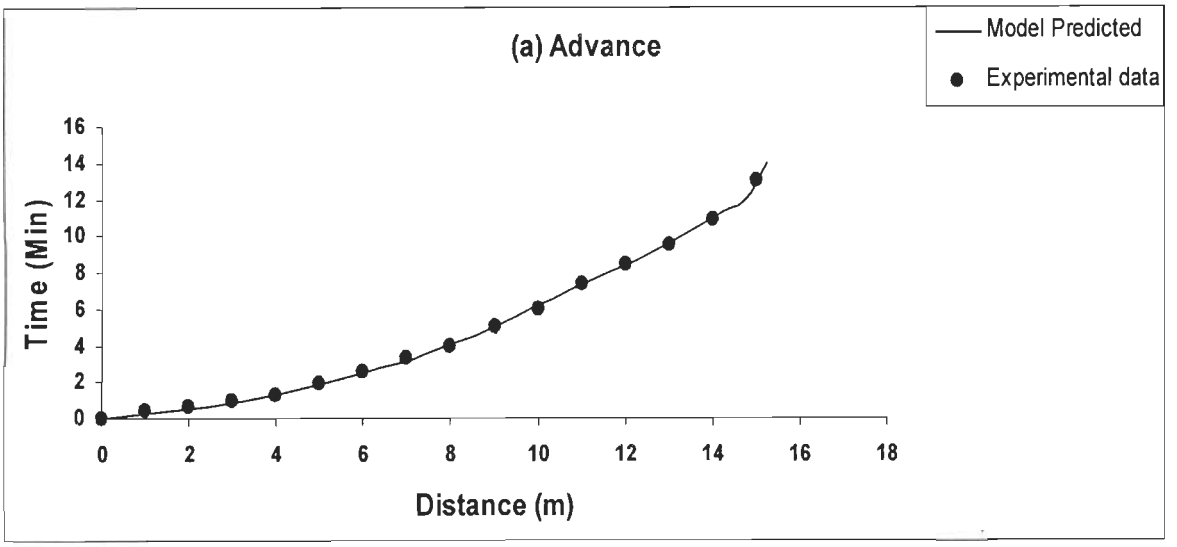

Fig. 5.2 Comparison of model predicted and experimentally observed advance for border strip 1

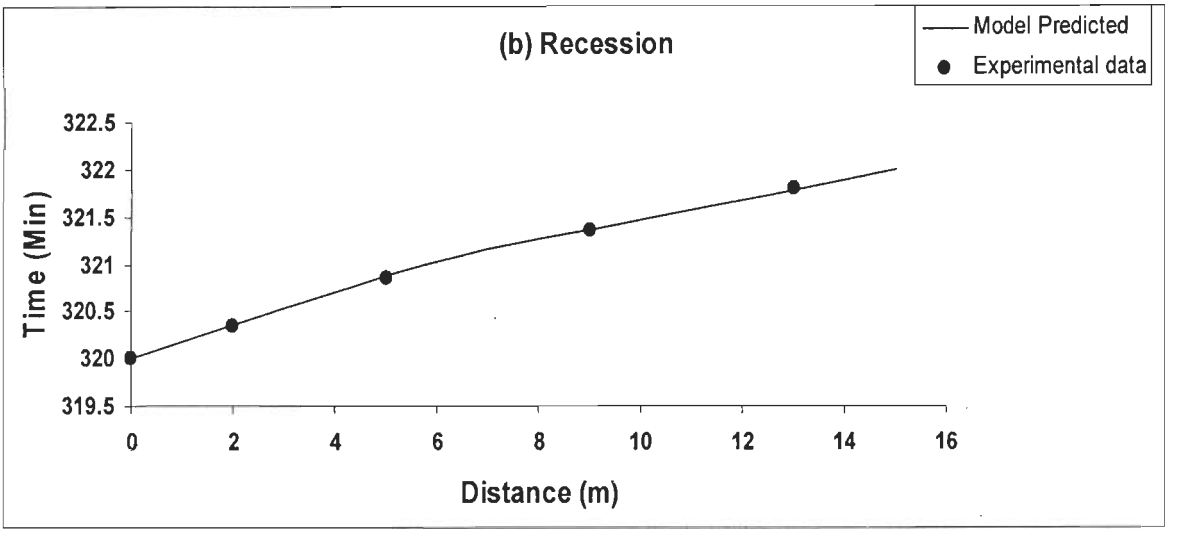

Fig. 5.3 Comparison of model predicted and experimentally observed recession for border strip 1

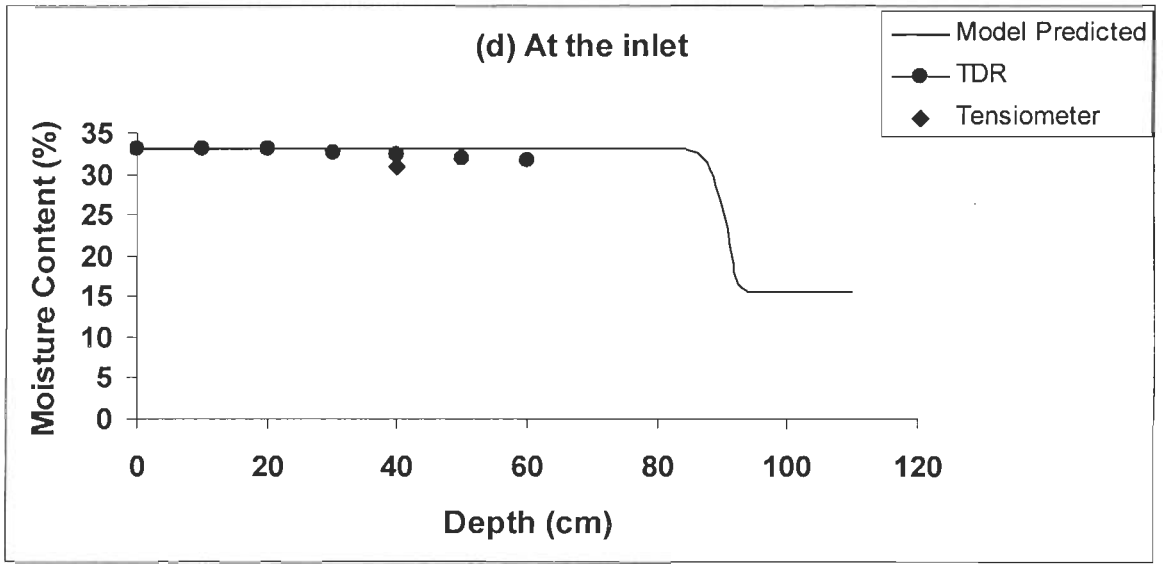
(d) At the inlet
Model Predicted
TDR
Tensiometer
Moisture Content (%)
35
30
25
20
15
10
5
0
0
20
40
60
80
100
120
Depth (cm)

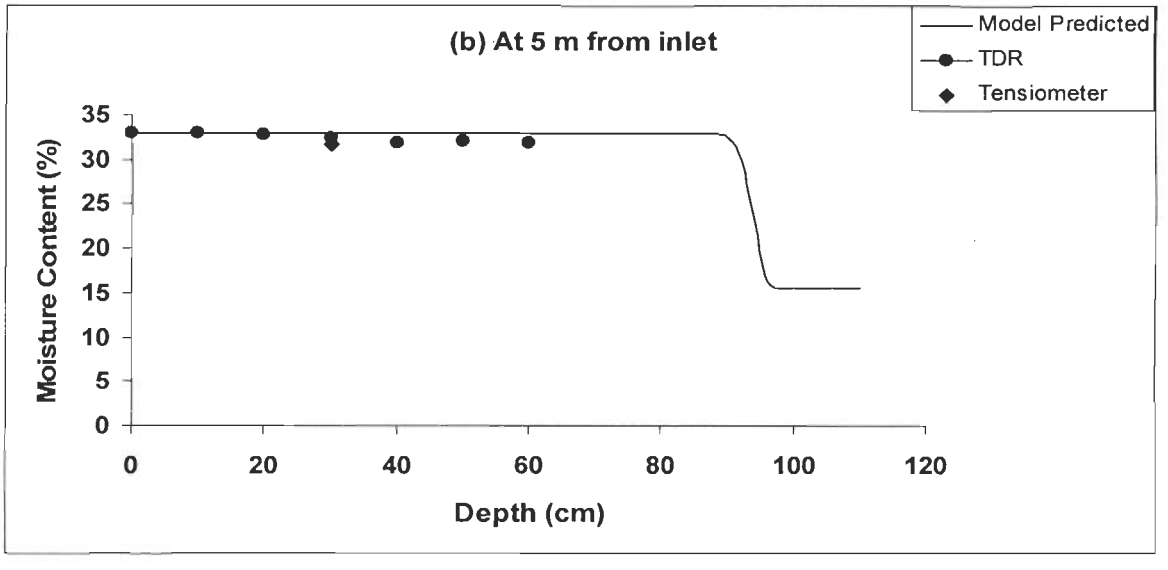
(b) At 5 m from inlet
Model Predicted
TDR
Tensiometer
Moisture Content (%)
35
30
25
20
15
10
5
0
0
20
40
60
80
100
120
Depth (cm)

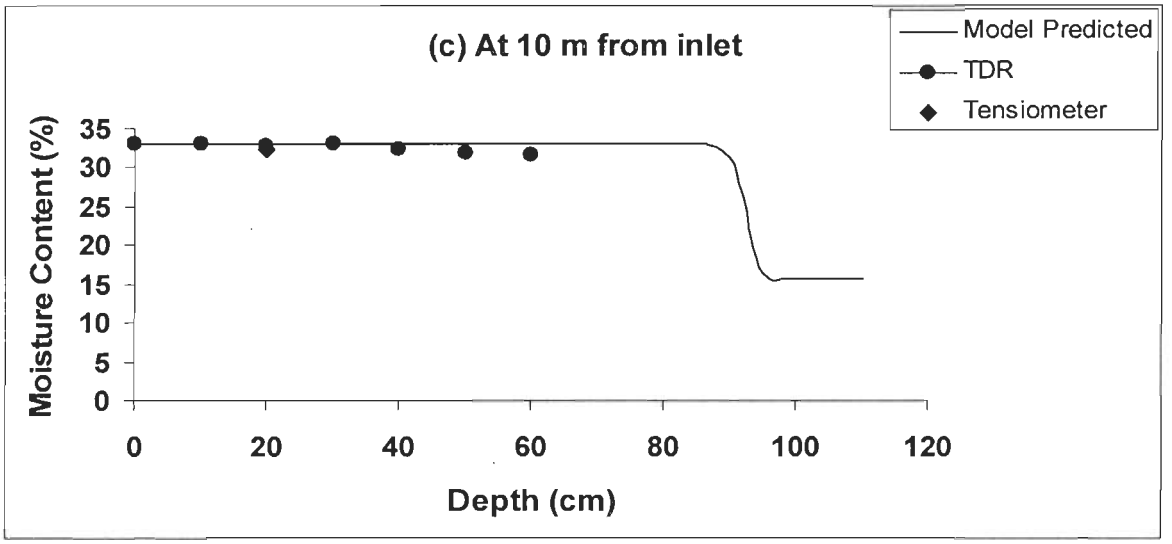

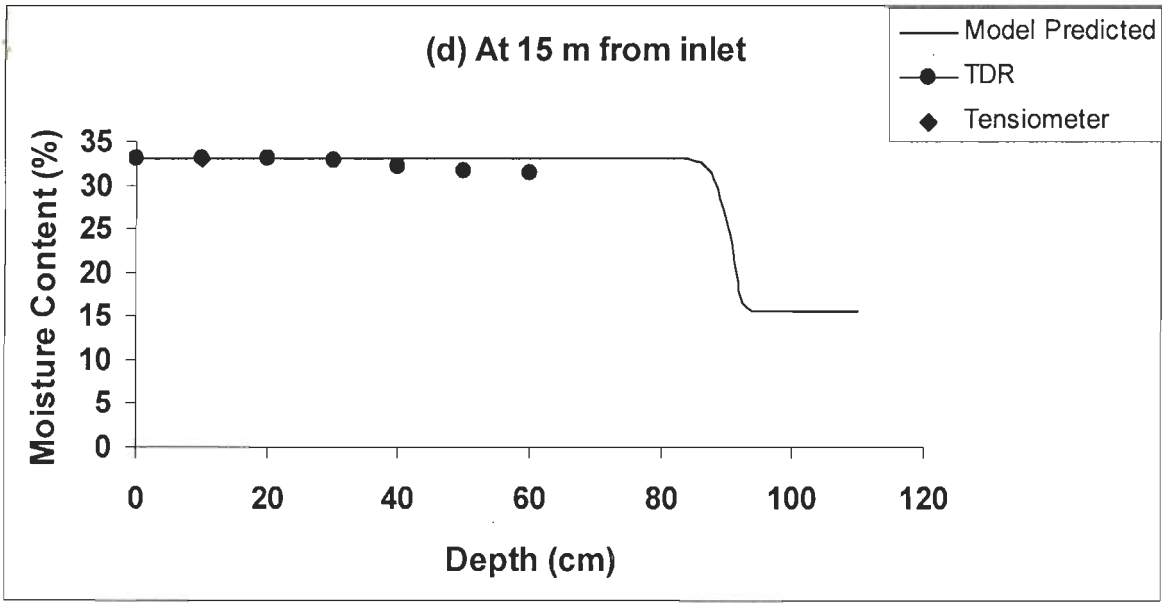

Fig. 5.4 Comparison of model predicted and experimentally observed moisture content profile for border strip 1

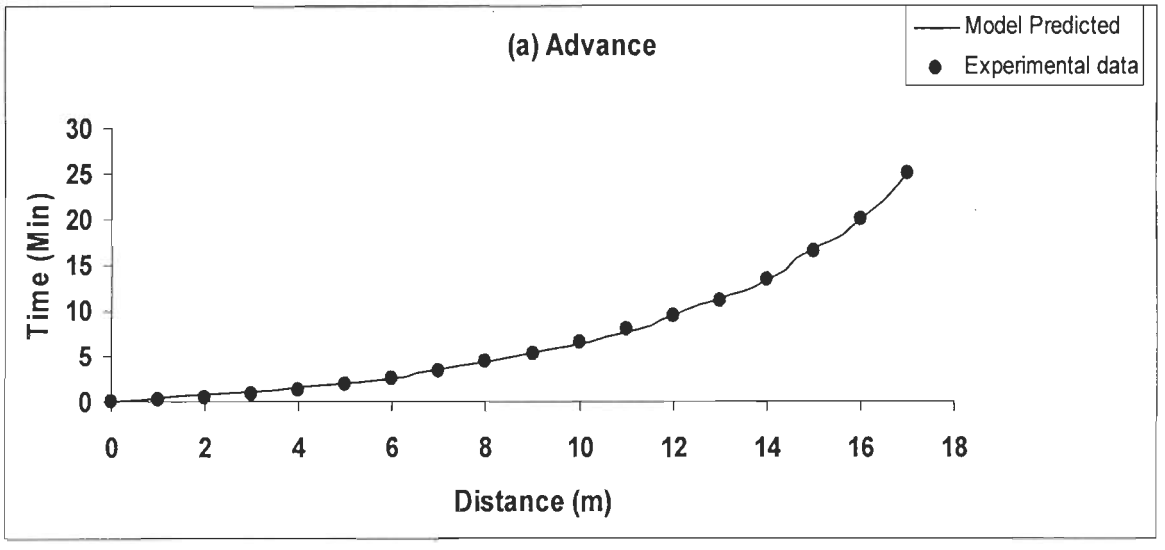

Fig. 5.5 Comparison of model predicted and experimentally observed advance for border strip 2

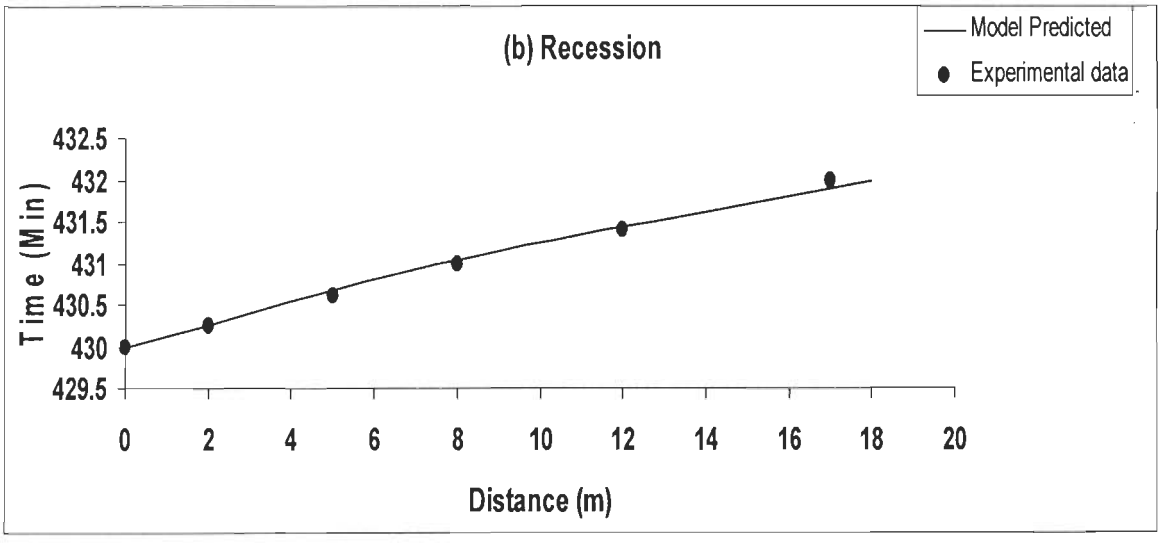

Fig. 5.6 Comparison of model predicted and experimentally observed recession for border strip 2

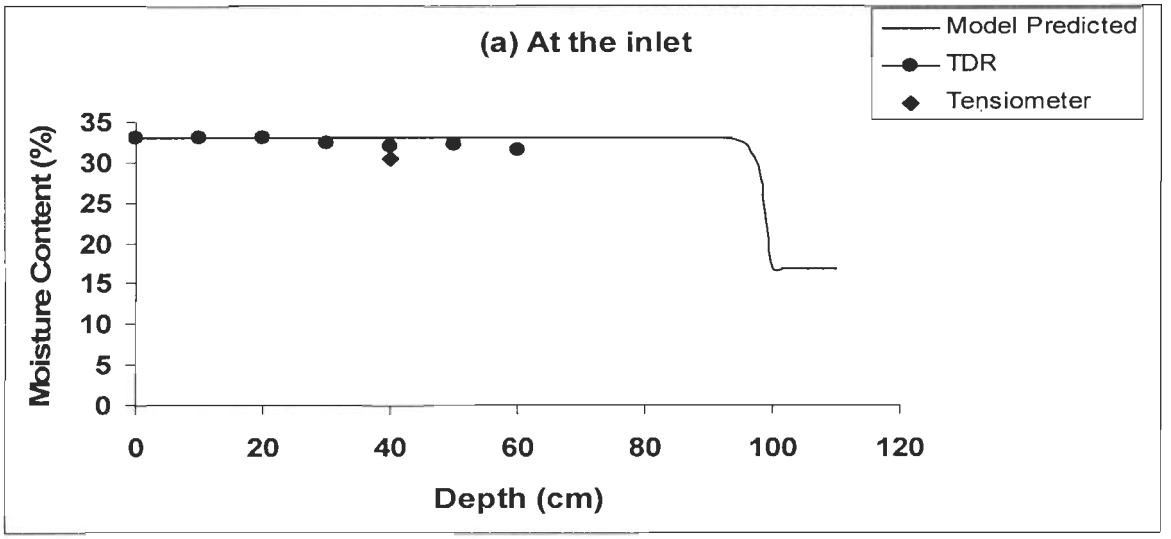
(a) At the inlet
Model Predicted
TDR
Tensiometer
Moisture Content (%)
0
5
10
15
20
25
30
35
0
20
40
60
80
100
120
Depth (cm)

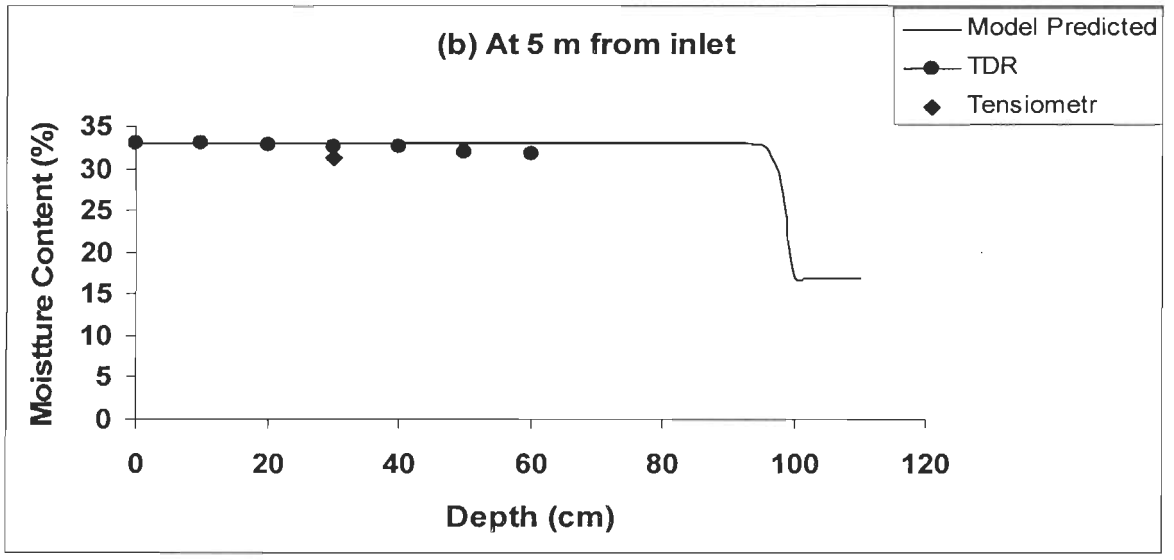
(b) At 5 m from inlet
Model Predicted
TDR
Tensiometr
Moistture Content (%)
0
5
10
15
20
25
30
35
0
20
40
60
80
100
120
Depth (cm)

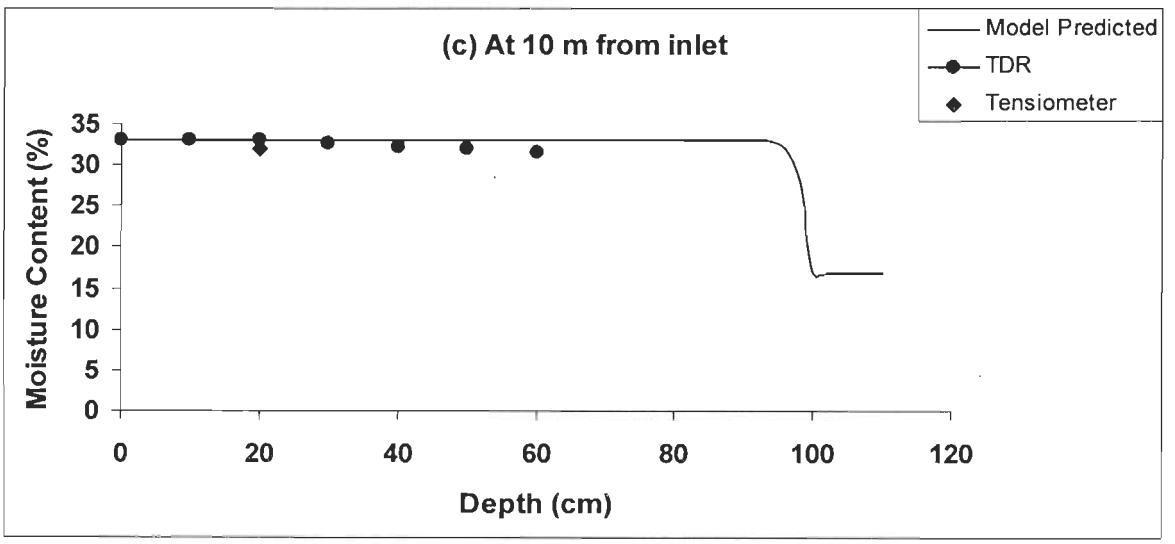
(c) At 10 m from inlet
Model Predicted
TDR
Tensiometer
Moisture Content (%)
0
5
10
15
20
25
30
35
0
20
40
60
80
100
120
Depth (cm)

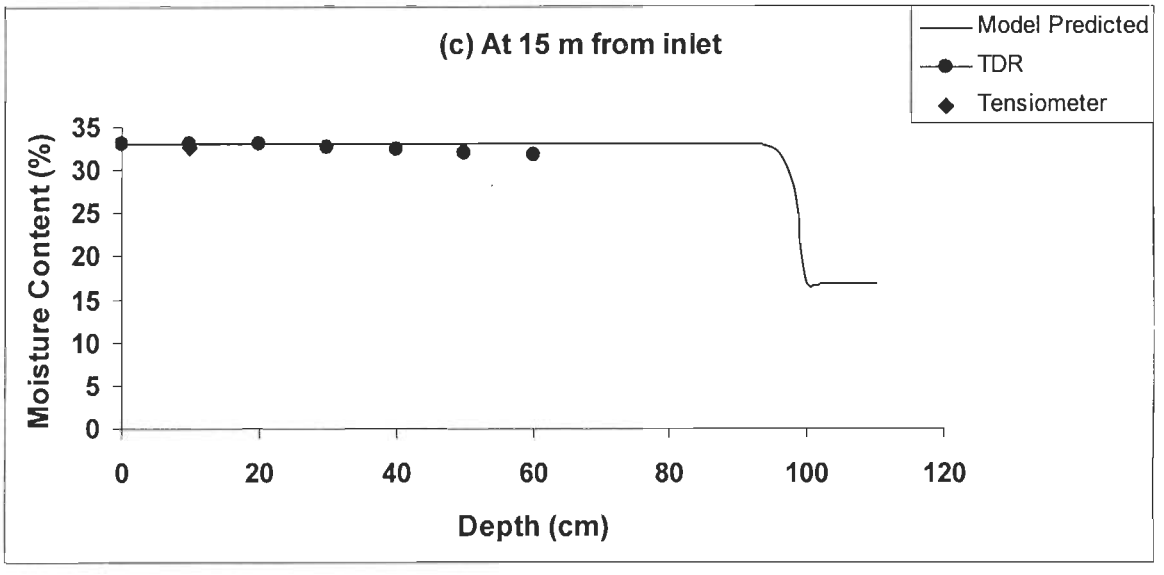

Fig. 5.7 Comparison of model predicted and experimentally observed moisture content profile for border strip 2

5.6 CLOSURE

In the present chapter, a parameter estimation model is developed by coupling the numerical model developed in Chapter 3 with a Sequential Unconstrained Minimization Technique (SUMT). The issues of identifiability and uniqueness are discussed by estimating the parameters from hypothetical data. The robustness of the optimization procedure is studied by varying the number of unknown parameters (K_{sat}, α_v, and n_v) to be estimated from 1 to 3. In addition, the efficacy of the optimization procedure is analyzed by starting the initial guesses of individual parameters considerably far away from their true values. It is observed that using summation of flow depths in the objective function results in the optimization converging to the true values as compared to irrigation advance data. It is also observed that identification of all the three parameters from flow depth and subsurface moisture content data is not possible. The model is also applied to estimate the two infiltration parameters from two border strip experiments explained in Chapter 4.

CHAPTER 6
CONCLUSIONS

6.1 GENERAL

The present study is concerned with the development of a numerical model for the analysis of border strip irrigation system and a parameter estimation model for the estimation of infiltration parameters. The overland flow is assumed to be governed by the Saint-Venant equations and the subsurface flow by the Richards equation. A coupled overland-subsurface hydrodynamic numerical model is developed by solving Saint-Venant equations for overland and 1-D Richards equation in mixed form for subsurface flow. MacCormack explicit finite difference scheme is used to solve the Saint-Venant equations while a mass conservative fully implicit finite difference scheme is employed to solve the Richards equation. The numerical model is validated by comparing model predicted irrigation advance and recession with reported data from literature. Comprehensive field experiments are conducted on two border strips to assess the performance of the numerical model in the prediction of subsurface moisture content profile.

The accurate prediction of irrigation events depends on system parameters such as Manning's roughness coefficient and infiltration parameters: Saturated hydraulic conductivity K_{sat}, unsaturated soil retention parameters, α_v, and n_v. The determination of these infiltration parameters at field level is one of the tedious tasks. Moreover, these parameters may not represent the infiltration phenomenon at field scale. An alternative to direct measurement techniques is to employ inverse techniques for parameter estimation. In such a procedure, the parameters are estimated by minimizing the deviations between the model predicted and field observed flow attributes such as

irrigation advance, flow depth and moisture contents in the subsurface. In this tudy, a parameter estimation model is developed by coupling the numerical model with a Sequential Unconstrained Minimization Technique (SUMT). The issues of identifiability and uniqueness are ascertained by estimating the parameters (K_{sat}, α_v, and n_v) from hypothetical data. The robustness of the optimization procedure is studied by varying the number of unknown parameters to be estimated from 1 to 3. In addition, the efficacy of the optimization procedure is analyzed by starting the initial guesses of individual parameters considerably far away from their true values. The parameter estimation is carried out first by giving surface data (irrigation advance or flow depths) to study whether the optimization results are in unique estimation of all the parameters. In cases, where the surface data is found to be inadequate, subsurface data is also included in the optimization.

6.2 CONCLUSIONS

1. The hydrodynamic model developed is capable of accurately predicting the irrigation advance and recession.
2. The model predicted moisture contents differ marginally from the experimental observations. This may be due to the assumption of vertical movement of moisture in the subsurface.
3. It is observed that with only irrigation advance and summation of flow depths data, only two among the three parameters K_{sat}, α_v and n_v can be uniquely estimated.
4. Defining the objective function in terms of flow depths results in the optimization converging to the true values as compared to irrigation advance.

5. Inclusion of moisture contents data in the objective function does not ensure simultaneous estimation of all the three parameters.

6. While estimating only one parameter, the optimization algorithm converges to the true values, even though the initial guess is far away from the true values.

7. In case of estimation of two parameters, the radius of search has to be reduced in order for the optimization algorithm to converge to the true values.

8. During simultaneous estimation of two parameters, starting the initial guess as under estimated results in the least number of iterations for the optimization algorithm to converge to the true values.

9. Parameter estimation using experimental data of two border strip experiments indicate that the parameter estimates are quite close to the values obtained using direct measurements. It indicates that parameter estimation technique can be applied with confidence for the estimation of infiltration parameters.

6.3 SCOPE FOR FUTURE WORK

Certain issues are worth mentioning for future investigation.

1. Inclusion of lateral subsurface flow in better prediction of subsurface moisture content profiles needs to be studied.

2. The effect of data errors and bias induced by the objective function or parameter estimates needs to be studied.

3. Correlation among the soil infiltration parameters on their identifiability needs to be studied in detail.

BIBLIOGRAPHY

1. Abbott, M. B. (1985). "Computational hydraulics: Elements of the theory of free surface flows". Pitman, London, England.
2. Akan, A. O. and Yen, B. C. (1981). "Mathematical model of shallow water flow over porous media." J. Hydraulic Division, 107(Hy4), 479-494.
3. Alazba, A. A. (1999). "Simulating furrow irrigation with different inflow pattern." J. Irrig. Drain.Eng., 125(1),12-18.
4. Ankeny, M. D. Mushtaque, A. Kaspar, T. and Horton, R. (1991). "Simple field method for determining unsaturated hydraulic conductivity." J. Soil Sci. Am. 55, 467-470.
5. Bali, Khaled and Wallender, W.W. (1987). "Water application under varying soil and intake opportunity time." Transactions of the American Society of Agricultural Engineers, 30(2), 442-448.
6. Barry, D. A., Parlange, J. Y. and Sivapalan (1993). "A class of exact solutions for Richards equation." J. Hydrology, 142; 29-46.
7. Bautista, E. and. Wallender, W. W. (1985). "Spatial variability of infiltration in furrows." Trans. ASAE, 28(6), 1846-1851.
8. Bautista, E. and. Wallender, W. W. (1992). "Hydrodynamic furrow irrigation model with specified space steps". J. Irrig. and Drain. Engg, ASCE, 118(3), 450-465.
9. Bautista, E. and. Wallender, W. W. (1993). "Identification of furrow intake – parameters from advance times and rates". J. Irrig. and Drain. Engg, ASCE, 119(2) 295-311.

10. Bassett, D. L. (1972). "Mathematical model of water advance in border irrigation". Trans., ASAE, 15(5), 992-995.

11. Bassett, D. L., and Fitzsimmons, D. W. (1976). "Simulating overland flow in border irrigation". Trans., ASAE, 19(4), 666-671.

12. Beck, J. V. and Arnold, K. J., (1977). "Parameter estimation in Engineering and Science". Willey, New York, N.Y., 501.

13. Brooks, R. H., and Corey, A. T. (1964). "Properties of porous media affecting fluid flow." J. Irrigation Drainage Division. ASCE, 92,61-88.

14. Boreli, M. and Vachaud, G. (1966). "Note sur la determination de la teneur en cau residuelle et sur la variation de la permeabilite relative sans les sols nonsatures." C. R. Acad. Sci., 263: 698-691.

15. Broad-Bridge, P. and White, I. (1988). "Constant rate–rainfall infiltration: A versatile nonlinear model 1, Analytical solution." Water Resour. Res., 24(1), 145-154.

16. Brutsaert, W. (1971). "A functional iteration technique for solving the Richards equation applied to two dimensional infiltration problems." J. Water Resou. Res., 7(6), 1583-1596.

17. Burdine, N. T. (1953). "Relative permeability calculation from size distribution data." Trans., ASME. 198, 71-78.

18. Campbell, G. S. (1974). "A simple method for determining unsaturated conductivity from moisture retention data." J. Soil Sci. 117, 311-314.

19. Celia, M. A., Bouloutas, T. E. and Zabra, R. (1990). "A general mass-conservative numerical solution for the unsaturated flow equation." Water Resour. Res. 26(7), 1483-1496.

20. Chaudhary, M. H., (1993). "Open channel flow". Prentice-Hall, Englewood Cliffs, N.J.

21. Chen, C. L. (1970). "Surface irrigation using kinematic-wave model". J. Irrigation and Drainage Division, ASCE, 96(IR1), Proc. Paper 7134, 39-46.

22. Chen, C. L. and Hansen, V. E. (1966). "Theory and characteristics of overland flow". Trans. ASAE, 9, 20-26.

23. Childs, J., Wallender, W. W. and Hopmans, J. W. (1993). "Spatial and seasonal variation of furrow infiltration". J. Irrig. and Drain. Engg., ASCE, 119(1), 74-90.

24. Childs, E. C. and Collis-George, N. (1950). "The permeability of porous materials." Proc., Roy. Soc. Ser. A., 201, 392-405.

25. Chow, V. T. and Ben-Zvi, A. (1973). "Hydrodynamic modeling of two-dimensional watershed flow". J. Hydraulic Division, 99(Hy11), 2023-2040.

26. Celia, M. A., Bouloutas, E. T., and Zabra, R. L. (1990). "A general mass-conservative numerical solution for the unsaturated flow equation". J. Water Resources Research, 26(7), 1483-1496.

27. Clemmens, A. J. (1979). "Verification of the zero-inertia model for border irrigation". Trans. ASAE, 22(6), 1306-1309.

28. Clement, T.P. Wise, W. R. and Molz, F. J. (1994). "A physically based, two-dimensional, finite- difference algorithm for modeling variably saturated flow". J. hydrology, 161, 71-90.

29. Clemente, R.S., De Jong, R., Hayhoe, H., Reynolds, W.D. and Hares, M. (1994). "Testing and comparison of three unsaturated soil water flow models". J. Agricultural Water Management, 25, 135-152.

30. Cooley, R. L. (1983). "Some new procedures for numerical solution of variable saturated flow problems". Water Resources Research, 19(5), 1271-1285.

31 Cunge, J. A., and Woolhiser, D. A. (1975). "Irrigation systems, in unsteady flow in open channels". edited by K. Mahmood and V. Yevjevich, chap. 13, pp. 522-537, Water Resources Publications, Fort Collins, Colo.

32. Dane, J. H. (1980). "Comparison of field and laboratory determined hydraulic conductivity values." J. Soil Sci. Soc. Am., 44, 228-231.

33. Dane, J. H. and Hruska, S. (1983). "In situ determination of soil hydraulic properties during Drainage." Soil. Sci. Soc. Am. J. , 47, 619-624.

34. David, A. H., Abrahams, A. D. and Pitman, E. B. (2006). "One and two-dimensional modelling of overland flow in semiarid shrubland, Jornada basin, New Mexico". Hydrological Processes, 20, 1027-1046.

35. Davis, J. R. (1961). "Estimating rate of advance for irrigation furrows". Trans. ASAE, 57(4), 52-54

36. Diskin, M. H. and Simon, E. (1977). "A procedure for the selection of objective functions for hydraulic simulation models". Journal of Hydrology, 34, 129-149.

37 Dogan, A. and Motz, L. H. (2005, a). "Saturated-Unsaturated 3D groundwater model. I: Development". Journal of Hydrologic Engineering, 10(6), 492-504.

38. Dogan, A. and Motz, L. H. (2005, b). "Saturated-Unsaturated 3D groundwater model. II: Verification and Application". Journal of Hydrologic Engineering, 10(6), 505-515.

39. Elliot, R. L. and Walker, W. R. (1982). "Field evaluation of furrow infiltration and advance functions". Trans. ASAE, 25, 396-400.

40. Elliott, R. L., Walker, W. R. and Skogerboe, G. V. (1982). "Zero-inertia modeling of furrow irrigation advance". J. Irrigation and Drainage Division, ASCE, 108(IR3), Proc. Paper 17340, 179-195.

41. El-Kadi, A. I. and Ge Ling, (1993). "The courant and peclet number criteria for the numerical solution of the Richards equation." Water Resour. Res., 29(10), 3485-3494.

42. Fangmeier, D. D. and Ramsey, M. K. (1978). "Intake characteristics of irrigation furrow." Transactions, American Society of Agricultural Engineers, 219(4), 696-700.

43. Feddes, R. A., Kotwalik, P. J. and Zaradny, H. (1978). "Simulation of field water use and crop yield". Central for Agricultural Publishing and Doumentation, Wageningen, The Netherlands.

44. Feddes, R. A., Kabat, P., Bakel, P. J. T., Bronswijk, J. J. B. and Halbertsma, J. (1988). "Modeling soil water dynamics in the unsaturated zone-state of the art". Journal of Hydrology, 100, 69-111.

45. Fiacco, A. V. and McCormick, G. P. (1968). "Nonlinear programming: Sequential Unconstrained Minimization Technique. Willey, New York.

46. Fok, Y. S. and Bishop, A. A. (1965). "Analysis of water advance surface irrigation". J. Irrig. Drain. Div., ASCE, 91(1), 99-116.

47. Fonken, D. W., Carmody, T., Laursen, E. M. and Fangmeier, D. D. (1980). "Mathematical model of border irrigation". J. Irrig. Drain. Div. Am. Soc. Civ. Eng., 106(IR3), 203-220.

48. Fonteh, M. F. and Podmore, T. (1993). "A physically based infiltration model for furrow irrigation". Agric. Water Manage. 23, 271-284.

49. Friedman, A. (1964). "Partial Differential Equations of parabolic type". Prentice-hall, Englewood Cliffs, N. J.

50 Garabedian, P. (1964). "Partial Differential Equations". John Wiley, New York.

51. Ghidaoui, M.S. and Prasad, K. S. H. (2000). "A priori identification of unsaturated soil parameters." ASCE, Proc., J. Irrig. and Drain. Div., 126(3), 163-171.

52. Ghosh, R. K. (1980). "Estimation of soil-moisture characteristics from mechanical properties of soils." J. Soil Sci.., 130, 60-63.

53. Govindaraju, R. S. Kavvas, M. L. and Tayfur, G. (1992). "A simplified model for two-dimensional overland flows". Water Resources Research, 27(8), 1885-1898.

54. Gottardi, G. and Venutelli, M. (1992). "Moving finite element model for one-dimensional infiltration in unsaturated soil." Water Resour. Res., 28, 3259-3267.

55. Gribb, M. M. (1996). "Parameter estimation for determining hydraulic properties of a fine sand from transient flow measurements". Water Resources Research, 32(7), 1965-1974.

56. Guardo, M., Oad, R.. and Podmore, T. H. (2000). "Comparison of zero-inertia and volume balance advance-infiltration models". J. Hydraul. Eng., 126(6), 457-465.

57. Gupta, S. C. and Larsen, W. E. (1979). " Estimating soil water retention characteristics from particle size distribution, organic matter percent and bulk density." Water Resour. Res., 15(6), 1633-1635.

58. Hall, W. A. (1956). "Estimating irrigation border flow". Agricultural Engineering, 37, 263-265.

59. Hari Prasad et al. (2003). "Estimation of unsaturated soil parameters: Effect of data errors and choice of objective function". The Indian Society for Hydraulics. ISH, J. 9, 46-60.

60. Hari Prasad, K.S., Mohan Kumar, M.S. and Shekhar, M. (2001). "Modeling flow through unsaturated zone: Sensitivity to unsaturated soil properties". Sadhana, Indian Academy of Sciences, 26(6), 517-528.

61. Hari, Prasad, K.S., Mohan Kumar, M.S., Shekhar, M. and Chandrashekar, B. (2005). "A simple numerical model for assessment of groundwater recharge." J. IWRS, 25(1), 49-60.

62. Hart, W. E., Bassett, D. L. and Strelkoff, T. (1968). "Surface irrigation hydraulic-kinematics". J. Irrig. Drain. Div. Am. Soc. Civ. Eng., 94(IR4), 419-440.

63. Hartley, D. M. (1992). "Interpretation of Kostiakov infiltration parameters for borders". J. Irrig. and Drain. Engg., ASCE, 118(1), 156-165.

64. Haverkamp, R., Parlange, J. Y., Starr, J. L., Schmitz,G., and Fuentes, C. (1990). "Infiltration under ponded conditions, 3; A predictive equation based on physical parameters." Soil Sci., 149(4), 292-300.

65. Haverkamp, R. and Vauclin, M. (1979). "A note on estimating finite difference interblock hydraulic conductivity values for transient unsaturated flow problems". Water Resources Research, 15(1), 181-187.

66. Haverkamp, R., Vauclin M., Touma, J. Wierenga, P. and Vachaud, .G. (1977). "Comparison of numerical simulation models for one-dimensional infiltration". Soil Sci. Soc. Am. J., 41 285-294.

67. Hills, R. G., Porro, I., Hudson, D. B. and Wierenga, P. J. (1989). "Modeling one-dimensional infiltration into very dry soils, 1. Model development and evaluation". Water Resources Research, 25(6), 1259-1269.

68. Hiscock, K.M., and Grischeck, T. (2002). "Attenuation of groundwater pollution by bank infiltration". J. Hydrology, 266, 139-144.

69. Hong, L. D., Akiyama, J. and Ura, M. (1994). "Efficient mass conservative numerical solution for the two-dimensional unsaturated flow equations". J. Hydroscience Hydraulic Engineering, 11(2), 1-18.

70. Hornung, U. and Messing, W. (1980). "A predictor-corrector alternating-direction implicit method for two-dimensional unsteady saturated-unsaturated flow in porous media". J. Hydrol., 47, 317-323.

71. Hoover and Grant, W. J. (1983). "Numerical fitting of the Gardner equation to hydraulic conductivity and water retention data." Trans. ASAE, 26(5), 1401-1408.

72. Hornung, U. and Messing, W. (1983). "Truncation errors in the numerical solution of horizontal diffusion in saturated/unsaturated media". Adv. Water Resour., 6, 165-168.

73. Huang, K. Zhang, R. and Van Genuchten, M. T. (1994). "An Eulerian-Langrangian approach with an adaptively corrected method of characteristics to simulate vatiably saturated water flow." Water Resour. Res., 30(2), 499-507

74. Huyakorn, P. S. Springer, E. P., Guvansen, V. and Woodsworth, T. D. (1986)."A three dimensional finite element model for simulating water flow in variably saturated porous media." Water Resour. Res. 22(13), 1790-1808.

75. Izzard, C. E. (1944). "The surface profile of overland flow. Trans". Am. Geophys. Union, 25, 959.

76. Janz, T. C. and Stonier, R. J. (1995). "Modeling water flow in cropped soils: water uptake by plant roots". Environment international, 21, 705-709.

77. Jayens, D. B. (1986)."Simple model of border irrigation." J. Irrig. and Drain. Engg., ASCE, 112(2), 172-184.

78. Jobling, G. A. and Turner, A. K. (1973). "Physical model study of border strip irrigation". J. Irrig. Drain. Div., Am. Soc. Civ. Eng., 99(IR4), 493-510.

79. Kaluarachchi, J. J. and Parker, J. C. (1987). "Finite element analysis of water flow in variably saturated soils." J. Hydrology, 90, 269-291.

80. Katopodes, N. D. and Strelkoff, T. (1977). "Dimensionless solution of border irrigation advance". J. Irrig. and Drain. Div., ASCE, 103(4), 401-407.

81. Katopodes, N. D. and Strelkoff, T. (1977a). "Hydrodynamics of border irrigation-complete model". J. Irrig. and Drain. Div., ASCE, 103(3), 309-323.

82. Katopodes, N. D., Tang, J. H., and Clemmens, A. J. (1990). "Estimation of surface irrigation parameters". J. Irrig. Drain. Engg., 116(5), 676-696.

83. Kincaid, D. C., Heermann, D. F., and Kruse, E. G. (1972). "Hydrodynamics of border irrigation advance." Trans., ASCE, 15(4), 674-680.

84. Kirkland, M. R., Hills, R. G. and Wierenga, P. G. (1992). "Algorithm for solving Richards' equation for variably saturated soils". Water Resour. Res. 28, 2049-2058.

85. Kool, J.B., Parker, J.C., and Van Genuchten, M.T. (1985). "Determining soil hydraulic properties from one step-outflow experiments by parameter estimation, I: Theory and numerical studies". Soil. Sci. Soc. Am. J., 49, 1348-1354.

86. Kool, J. B. Parker, J. C. and Van Genuchten, M. Th. (1987). "Parameter estimation for unsaturated flow and transport models–A review." J. of Hydrology. 91, 255-293.

87. Kool, J. B. and Parker, J. C. (1988). "Analysis of the inverse problem for transient unsaturated flow." Water Resour. Res., 24, 817-830.

88. Kubruly, C. S. (1977). "Distributed parameter system identification, a survey." Intr. J. Contr., 26(4), 509-535.

89. Langford, K. J. and Turner A. K. (1973). "An experimental study of the application of kinematic-wave theory to overland flow". J. of Hydrology. 18, 125-145.

90. Letha, J. and Elango (1994). "Simulation of mildly saturated flow." J. Hydroloy, 154, 1-17.

91. Lewis, M. R. and Milne, W. E. (1938). "Analysis of border irrigation". Agricultural Engineering, 19,267-272.

92. Ligget, J. A. and Cunge, J. A. (1975). "Numerical methods of solution of the unsteady flow equations: Unsteady flow in open channels". K. Mahmood and V. Yevjevich, eds. Vol. 1, Water Resources Publications, FortCollins, Colo., 89-182.

93. Mailhol, J. C. Priol, M. and Benali, M. (1999). "A furrow irrigation model to improve furrow irrigation practices in the Gharb valley of Morocco". Agric. Water Manage., 42(1), 65-80.

94. Messing, I. and Jarvis, N. J. (1990). "Seasonal variation in field-saturated hydraulic conductivity in two swelling clay soils in Sweden." European Journal of Soil Sci., 41(2), 229-237.

95. Milly, P. C. D. (1985). "A mass-conservative procedure for time-stepping in models of unsaturated flow". Adv. Water Resour., 8, 32-36.

96. Morris, E. M. and Woolhiser, D. A. (1980). "Unsteady one-dimensional flow over a plane: Parttial equilibrium and recession hydrographs". Water Resources Research, 16, 355-360.

97. Mualem, Y. (1974). "A conceptual model of hysteresis." J. Water Resour. Res. 10(3), 514-520.

98. Mualem, Y. (1976). "A new model for predicting the hydraulic conductivity of unsaturated porous media". Water Resour. Res., 12(3), 513-522.

99. Nandagiri, L., and Prasad, R., (1996). "Relative performance of textural models in estimating soil moisture characteristic". J. Irrigation and Drainage, 131(3), 238-248.

100. Narasimhan, T. N. and Witherspoon, P. N. (1977). "Numerical model for saturated-unsaturated flow in deformable porous media, 1. Theory". Water Resources Research, 13, 657-664.

101. Narasimhan, T. N. and Witherspoon, P. N. (1978). "Numerical model for saturated-unsaturated flow in deformable porous media, 3. Applications". Water Resources Research, 14(6), 1017-1034.

102. Neuman, S. P. (1973). "Saturated-unsaturated seepage by finite elements." J. Hydraulic Div., ASCE, 99(HY12): 2233-2250.

103. Neuumann, S. P. Feddes, R. A. and Bresler, E. (1975). "Finite element analysis of two dimensional flow in soil considering water uptake by roots. I: Theory, J. Soil Sci. Soc. Am., 35, 224-230.

104. Ojha, C.S.P., Singh, V.P. and Adrian, D. (2003). "Determination of critical head in soil piping". J. Hydraulic Engineering, ASCE, 1299(7), 511-518.

105. Panoconi, C., Aldama, A. A. and Wood, E. F. (1991). "Numerical evaluation of iterative and noniterative methods for the solution of nonlinear Richards equation". Water Resour. Res. 27(6), 1147-1163.

106. Parker, J.C., Kool, J.B., and Van Genuchten, M.T. (1985). "Determining soil hydraulic properties from one step-outflow experiments by parameter estimation, II: Experimental studies". Soil. Sci. Soc. Am. J., 49, 1354-1359.

107. Parlange, J. Y. (1971). "Theory of water movement in soils, II. One-dimensional infiltration". Soil Sci., 111, 170-174.

108 Parlange, J. Y. (1972). "Theory of water movement in soils. 6, effect of water depth over soil". Soil Sci. 113, 308-312.

109. Parlange, J. Y., Havercamp, R., and Touma, J. (1985). "Infiltration under ponded condition. 1: Optical analytical solution and comparison with experimental observation". Soil Sci., 139(4), 305-311.

110. Persson, M. and Berndtsson, R. (1998). "Estimating transport parameters in an undisturbed soil column using time domain reflectometry and transfer function theory". J. Hydrology, 205, 232-247.

111. Philip, J. R. (1969). "Theory of infiltration." Adv. Hydro. Sci., 5, 215-206.

112. Philuip, J. R. and Farrell, D. A. (1964). "General solution of the infiltration advance problem in irrigation hydraulics". J. Geophys. Res., 69, 621-631.

113. Playan, E., Walker, W. R., Merkley, G. P. (1994). "Two-dimensional simulation of basin irrigation, I: Theory". J. Irrig. and Drain. Engg., ASCE, 120(5), 837-856.

114. Playan, E., Walker, W. R., Merkley, G. P. (1994). "Two-dimensional simulation of basin irrigation, II: Applications". J. Irrig. and Drain. Engg., ASCE, 120(5), 857-870.

115. Poulovassilis, A. (1962). "Hysteresis of pore water an application of the concept of independent domain." J. Soil Sci., 93, 405-412.

116. Pullan, A. J. (1990). "The quasilinear approximation for unsasturated porous media flow." Water Resour. Res. 26(6), 1219-1234.

117. Ram, R. S. and Lal, R. (1971). "Recession flow in border irrigation". J. Agric. Eng. India, 8(3), 62-70.

118. Ram, R. S. and Singh, V. P. (1982). "Evaluation of models of border irrigation recession". J. Agric. Eng. Res., 27, 235-252.

119. Ram, R. S., Singh, V. P. and Prasad, S. N. (1983). "Mathematical modeling of border irrigation". Water Resour. Rep. 5, Dep. of Civ. Eng., La. State Univ., Baton Rouge.

120. Rathfelder, K. and Abriola, L. M. (1994). "Mass conservative numerical solutions of the head based Richards equation". Water Resources Research, 30(9), 2579-2586.

121. Rawls, W. J., Ahuja, L. R., Brakensiek, D. L. and Adel, Shirmohammadi (1992). "Infiltration and soil water movement."Handbook if Hydrology, McDraw Hill Inc., New York, Chapter 5, 5.1-5.51.

122. Rayej, M. and Wallender, W. W. (1988). "Time solution of kinematic-wave model with stochastic infiltration". J. Irrig. and Drain. Engg., ASCE, 114(4), 605-621.

123. Reddy, J. M. and Singh, V. P. (1994). "Modelling and error analysis of kinematic wave equations of furrow irrigation". Irrig. Sci., 15, 113-122.

124. Remson, I., Honberger, G. M. and Molz, F. J. (1971). "Numerical methods in subsurface hydrology". Wiley-Interscience, New York, N. Y., 389.

125. Renolds, W. D. and Elrick, D. E. (1985). "In-situ measurements of field saturated hydraulic conductivity, sorptivity and alpha parameter using the Guelph Permeameter." J. Soil Sci., 140(4), 292-302.

126. Renolds, W. D. and Elrick, D. E. (1986). "A method for simultaneous in-situ measurement in the vadose zone of field-saturated hydraulic conductivity, sorptivity and the conductivity-pressure head relationship." Ground Water Monitoring Review, winter, 84-95

127. Richards, L. A. (1931). "Capillary conduction of liquids through porous medium". Physics, 1, 318-333.

128. Rao, S. S. (1979) "Optimization: Theory and Applications". Wiley Eastern limited, New Delhi.

129. Ross, P. J. (1990). "Efficient numerical methods for infiltration using Richards equation". Water Resour. Res., 26(2), 279-290.

130. Ross, P. J. (1986). "Zero-inertia and kinematic wave models for furrow and border irrigation". CSIRO division of soil, Townsville, Australia.

131. Roth, R. L., Fonken, D. W., Fangmeier, D. D. and Atchison, K. T. (1974). "Data for border irrigation models." Trans., ASAE, 17(1), 157-161.

132. Russo, D., Bresler, E., Shani, U. and Parker, J.C. (1991). "Analyses of infiltration events in relation to determining soil hydraulic properties by inverse problem methodology". Water Resources Research, 27(6), 1361-1373.

133. Rubin, J. (1968). "Theoretical analysis of two dimensional transient flow of water in unsaturated and partly unsaturated soils." J. Soil Sci. Soc. Of Am., 32, 607-615.

134. Sakkas, J. G., and Strelkoff, T. (1974). "Hydrodynamics of surface irrigation-advance phase". J. Irrig. and Drain. Div., ASCE, 100(IR1), 31-48.

136. Salter, P. J. and Williams, J. B., (1965). "The influence of texture on the moisture characteristics of soil, I. A, critical comparison of techniques for determining the available water capacity and moisture characteristic curve of a soil." J. Soil Sci., 16, 1-15.

137. Sato, T., Tanahashi, H. and Loaiciga, H. A. (2003). "Solute dispersion in a variably saturated sand". Water Resources Research, 39(6),1155.

138. Schmitz, G., Havercamp, R., and Palacios, O. (1985). "A coupled surface-subsurface model for shallow water flow over initially dry soil". Proc., 21st Congr. IAHR, Int. Assoc. for Hydr. Res., 1, 23-30.

139. Schmitz, G. H. and Seus, G. J. (1990). "Mathematical zero-inertia modeling of surface irrigation: advances in borders". J. Irrig. Drain. Engg., 116(5), 603-615.

140. Schmitz, G. H. and Seus, G. J. (1992). "Mathematical zero-inertia modeling of surface irrigation: advances in furrow". J. Irrig. Drain. Engg., 118(1), 1-18.

141. Schmitz, G. H., Lennartz, F., Singh, R. and Raghuwanshi, N. (2005). "Modeling flow and sediment transport phenomena for improved furrow irrigation management". *Project Rep.*, Volkswagen Foundation, Institute of Hydrology and Meteorology, TU Dresden, Germany and the Agricultural and Food Engineering Dept., Indian Institute of Technology, Kharagpur, India.

142. Schwankl, L. J., Raghuwanshi, N. S. and Wallender, W. W. (2000). "Furrow irrigation performance under spatially varying conditions". J. Irrig. and Drain. Engg. 126(6), 355-361.

143. Scott, P. S., Farquhar, G. J. and Kouwen, N. (1983). "Hysteresis effects of net infiltration." American Soc. Of Agri. Eng., St., Joseph, Mich, Publ. 11-83, 163-170.

144. Sherman, B. and Singh V. P. (1978). "A Kinematic model for surface irrigation". Water Resources Research, 14(2), 357-364.

145. Sherman, B. and Singh V. P. (1982). "A Kinematic model for surface irrigation: An extension". Water Resources Research, 18(3), 659-667.

146. Singh, V. and Bhallamudi, S. M. (1996). "Complete hydrodynamic border irrigation model". J. Irrig. and Drain. Engg., ASCE, 122(4), 189-197.

147. Singh, V. and Bhallamudi, S. M. (1998). "Conjunctive surface-subsurface modeling of overland flow". Advances in water resources, 21(7), 567-579.

148. Singh, P. and Chauhan, H. S. (1972). "Shape factors in irrigation water advance equation". J. Irrig. Drain. Div., ASCE, 98(IR3), Proc. Paper 9212, 443-458.

149. Singh, V. P. and Ram, R. S. (1983). "A kinematic model for surface irrigation: verification by experimental data". Water Resources Research, 19(6), 1599-1612.

150. Singh, V. P. (1994). "Accuracy of kinematic wave and diffusion wave approximations for space independent flows". Hydrological Processes, 8, 45-62.

151. Smith, R. E. (1972). "Border irrigation advance and ephemeral flood waves". J. Irrig. Drain. Div. Am. Soc. Civ. Eng., 98(IR2), 289-307.

152. Strelkoff, T., and Katopodes, N. D. (1977). "Border irrigation hydraulics with zero inertia". J. Irrig. Drain. Div., ASCE, 103(3), 325-342.

153. Strelkoff, T. (1969). "One-Dimensional Equations of Open-Channel Flow". J. Hydraulics Division, ASCE, 95(HY3), Proc. Paper No. 6557, 861-876.

154. Strelkoff, T. (1970). "Numerical solution of the Saint-Venant equations". J. Hydraulic Division, ASCE, 96(HY1), Proc. Paper No.7043, 223-252.

155. Tayfur, G. Kavvas, M. L., Govindaraju, R. S. and Storm, D. E. (1993). "Applicability of St. Venant equations for 2-D overland flow over rough infiltrating surfaces". J. Hydraulic Eng. ASCE, 119(1), 51-63.

156. Taylor, H. M. and Luthin, J. N. (1969)."Computer methods for transient analysis of water table aquifer." Water Resour. Res., 5(1), 144-152.

157. Thomas, H. R. and Rees, S. W. (1991). "A comparison of field-monitored and numerically predicted moisture movement in unsaturated soil". Int. J. for numerical and analytical methods in Geomech., 15, 417-431.

158. Thomas, H. R. and Rees, S. W. (1990). "Modeling field infiltration into unsaturated clay". J. Geotechnical Engg., ASCE, 116(10), 1483-1501.

159. Todsen, M. (1971). "On the solution of transient free-surface flow problems in porous media by finite-difference methods". J. Hydrol., 12, 177-210.

160. Trout, T.J., Garcia-Castillas, I.G. and Hart, W.E. (1982). "Soil water engineering: field and laboratory manual". Academic publishers, Jaipur, India.

161. Van Genuchten, M. Th. (1980). "A closed form equation for predicting the hydraulic conductivity of unsaturated soils". Soil. Sci. Soc. Am. J., 44, 892-898.

162. Vieira, J. H. D. (1983). "Conditions governing the use of approximations for the Saint-Venant equations for shallow surface water flow". J. Hydrol., 60, 43-58.

163. Vogel, T. and Hopmans, J. W. (1992). "Two-dimensional analysis of furrow infiltration". J. Irrig. and Drain. Engg. 118(5), 791-806.

164. Wallender, W. W., and Rayej, M. (1990). "Shooting method for Saint-Venant equations for furrow irrigation". J. Irrig. and Drain. Engg., ASCE, 116(1), 114-122.

165. Wallender, W. W. (1986). "Furrow model with spatially varying infiltration". Trans. ASAE, 29(4), 1012-1016.

166. Wallender, W. W., and Rayej, M. (1987). "Economic optimization of furrow irrigation with uniform and nonuniform soil". Trans. ASAE, 30(5), 1425-1429.

167. Walker, W. R. and Humpherys, A. S. (1983). " Kinematic-wave furrow irrigation model". J. Irrig. and Drain. Engg., ASCE, 109(4), 377-391.

168. Walker, W. R. and Skogerboe, G. V. (1987). "Surface Irrigation: Theory and Practice". Prentice Hall, Inc., Eglewood cliffs, New Jersey 07632.

169. Warrick, A. W., Islas, A. and Lomen, D. O. (1991). "An analytical solution to Richrds equation for time-varying infiltration." Water Resour. Res. 27, 463-766.

170. Wasseling, J. and Wit, K. E. (1969). "An infiltration method for the determination of capillary conductivity of unsaturated soil cores: Water in the unsaturated zone. IASH/AISH-UNESCO, Proceedings of Wageningen Symposium, 1, 223-234.

171. Weir, G. J. (1983). "A mathematical model for border strip irrigation". Water Resour. Res., 19(4), 1011-1018.

172. Wike, O. and Smerdon, E. T. (1965). "A solution of the irrigation advance problem". J. Irrig. Drain. Div. Am. Soc. Civ. Eng., 91(IR3), 23-34.

173. Wohling, th., Schmitz, G. H. and Mailhol, J. C. (2004a). "Modelling 2D-infiltration in irrigation furrows". J. Irrig. Drain. Eng., 130(4), 1-8.

174. Wohling, th., Singh, R. and Schmitz, G. H. (2004b). "Physically based modelling of interacting surface-subsurface flow during furrow irrigation advance". J. Irrig. Drain. Eng., 130(5), 349-356.

175. Wohling, Th. Frohner, A., Schmitz, G. H. and Liedl, R. (2006). "Efficient solution of the coupled one-dimensional surface-two-dimensional subsurface flow during furrow irrigation advance". J. Irrig. and Drain. Eng., 132(4), 380-388.

176. Wohling, Th. and Schmitz, G. H. (2007). "Physically based coupled model for simulating 1D surface-2D subsurface flow and plant water uptake in irrigation furrows. I: Model development". J. Irrig. and Drain. Eng., 133(6), 538-547.

177. Wohling, Th. and Mailhol, J. C. (2007). "Physically based coupled model for simulating 1D surface-2D subsurface flow and plant water uptake in irrigation furrows. II: Model test and evaluation". J. Irrig. and Drain. Eng., 133(6),

178. Woolhiser, D. A. and Liggett, J. A. (1967). "Unsteady one-dimensional flow over a plane-the rising hydrograph". Water Resources Research, 3(3), 753-771.

179. Yeh, W. W. G. (1986). "Review of parameter identification procedures in groundwater hydrology: The inverse problem". Water Resour. Res., 22(2), 95-108.

180. Yu, F. X. and Singh V. P. (1990). "Analytical model for furrow irrigation". J. Irrig. Drain. Eng., 116(2), 154-171.

181. Zerihun, D., Feyen, J. and Reddy, J. M. (1996). "Sensitivity analysis of furrow-irrigation performance parameters". J. Irrig. and Drain. Engg., 122(1), 49-57.

182. Zhang, W. and Cundy, T. W. (1989). "Modeling of two-dimensional overland flow". Water Resources Research, 25(9), 2019-2035.

183. Zhu, J.L. and Satish, M.G. (1999). "Stochastic analysis of macrodispersion in a semi confined aquifer". Transport in porous media, Netherlands, 35, 273-297.

184. Zijlstra and Dane, J. H. (1996). "Identification of hydraulic parameters in layered soils based on Quasi-Newton Method". J. of Hydrology., 181, 233-250.

APPENDIX-I

NUMERICAL MODEL FOR ANALYSIS OF SURFACE AND SUBSURFACE FLOWS

```
C     ------------------------------------------------
C     PROGRAMME FOR SOLUTION OF SAINT VENANTS EQUATIONS

      USING MACCORMACK SCHEME AND RICHRDS EQUATION USING

      IMPLICIT SCHEME
C     ------------------------------------------------------
C     h      : Surface water depth(m)
C     q      : Discharge(m3/s per meter width)
C     f      : Cummulative Infiltration(m)
C     hn     : New value of h
C     qn     : New value of q
C     fn     : New value of f
C     tou    : Time of infiltration, i.e., time thewater
C              has been in contact with the siol
C     tarr   : Time of wave arrival (seconds)
C     dist   : Distance along flow direction
C     quns   : Unsteady Discharge rate at u/s end
C     trec   : Time of recession start
C     qini   : Initial discharge
C     hini   : Initial depth
C     fini   : Initial cummulative infiltration
C     t      : Time of advance
C     dt     : Time increament
C     dx     : Nodal spacing(Grid distance) in surface
C    delz    : Nodal spacing (grid distance)in subsurface
C     s0     : Longitudinal slope)
C     rn     : manning's roughness coefficient
C     n      : number of section  (surface)
C     np     : number of nodes in surface
C     crn    : Courrant Number
C     g      : Acceleration due to gravity
C     tmax   : Total time
C     lmax   : Total length
C     slength : Depth of unsatursated zone
C     nnodes  :No. of nodes along depth of subsurface soil
C    siini    : Pressure head in subsurface soil
C   alpha,en,em: VanGenuchten's parametes
C   satk       : Saturated conductivity
C thetas&thetar : saturated and residual moisture content of subsurface soil
C   maxiter  : No. of maximum iteration
```

```
C   epsilon    : Covergence limit
C   nprint     : No. of times, the output required to be printed
C   tprint     : the of time at which the result is printed
C   lprint     : index of time (numbers)
C       ------------------------------------------------
        parameter(nn=1000)
        parameter(nnn=300)

        dimension h(nn),q(nn),f(nn),hp(nn),qp(nn),
        dimension fp(nn),fcp(nn)
        dimension hc(nn),qc(nn),fz(nn),hold(nn),hpre(nn),
        dimension tprint(nn)
        dimension siold(nn,nnn),sinew(nn,nnn),thetapre(nnn)
        dimension dpre(50)

        open(unit=21,file='bordko.dat')
        open(unit=22,file='tar.out')
        open(unit=23,file='dep.out')
        open(unit=24,file='in.out')
        open(unit=25,file='trial.out')
        open(unit=26,file='sinew.out')

        read(21,*)hini,s0,rn,crn,lmax
        read(21,*)quns,g,dx,tmax,trec
        read(21,*)slength,nnodes,siini,alpha,en,satk,
     *              thetas,thetar,ss
        read(21,*)maxiter,epsilon
        read(21,*)nprint
        read(21,*)(tprint(i),i=1,nprint)

c-------------------------------------------------------
c       STARTING
c-------------------------------------------------------

        qini = hini**(1.66667)*sqrt(s0)/rn

        fini = 0.0

        write(22,*)" INPUT DATA"
        write(22,*)"qini,hini,fini,s0,rn,crn,lmax,slength,nnodes,siini"
        write(22,*)qini,hini,fini,s0,rn,crn,lmax,slength,nnodes,siini
        write(22,*)"quns, g, dx, tmax,alpha,en,satk,thetas,thetar"
        write(22,*)quns,g,dx,tmax,alpha,en,satk,thetas,thetar
        write(22,*)"maxiter,epsilon,ss,nprint,tprint"
        write(22,*)maxiter,epsilon,ss,nprint,tprint



        n = lmax/dx
        np = n+1
```

```
      delz=slength/(nnodes-1)
      em=1-1/en

      t = 0.0
      c3=(rn/sqrt(s0))**0.6

       do i = 1,np
        q(i) = qini
        h(i) = hini
        f(i) = fini
        fcp(i)=fini
       enddo

       do i=2,np-1
       do j=1,nnodes
        if(j .eq. nnodes)then
        siold(i,j)=h(i)
        else
        siold(i,j)=siini
        endif
       enddo
       enddo

c      do j=1,nnodes
c      write(22,13)siold(2,j)

13     format(8(1x,f14.7))
c      enddo

      lprint=1

       do while(t .le. tmax)

c-------------------------------------------------------
c      UNSTEADY COMPUTATIONS
c-------------------------------------------------------
C      STABILITY CHECK
c-------------------------------------------------------

       do i=1,np
        hold(i)=h(i)
       enddo

       do i = 1 , np
        dt = dx/(abs(q(i)/h(i))+sqrt(g*h(i)))
        if(i .eq. 1)dtmin = dt
        if(dt .le. dtmin) dtmin = dt
       enddo

        dt = crn*dtmin
```

```
          t = t + dt

          write(22,*) 'time=', t

          dtdx=dt/dx

c-----------------------------------------------------
c         CALCULATION FOR NEXT TIME STEP
c-----------------------------------------------------
c         UPSTREAM BOUNDARY CALCULATION
c-----------------------------------------------

          cr = q(2)/h(2)+sqrt(g*h(2))
          sf=q(2)*q(2)*rn*rn/(h(2)**3.33333)
          cn=q(2)-cr*h(2)+g*dt*h(2)*(s0-sf)

          if(t .lt. trec)then
           qups=quns
          else
           qups=qini
          endif
           hups = (qups-cn)/cr
          if(hups .lt. hini)then
           hups=hini
          endif

          fups = 0.0

c-----------------------------------------------------
c         DOWNSTREAM BOUNDARY/UNIFORM FLOW CONDITION
c-----------------------------------------------

          if(h(np).gt.hini) then
                cl=q(n)/h(n)-sqrt(g*h(n))
                sf=q(n)*q(n)*rn*rn/(h(n)**3.33333)
                cp=q(n)-cl*h(n)+g*dt*h(n)*(s0-sf)

                iter = 0
                qdown = q(n)

                diff = 1.0

            do while((iter.le.15).and.(abs(diff).gt.1.0e-04))
                 iter = iter+1
                 fq=qdown-cp-cl*c3*(qdown**0.6)
                 dfq=qdown-cl*c3*0.6/(qdown**0.4)
                 diff=-fq/dfq
                 qdown=qdown+diff
                 enddo
```

```
            if(iter.gt.15)write(*,*)"iter fails at d/s"
              hdown=(qdown-cp)/cl
            endif

c-------------------------------------------------
c       INTERIOR NODES / PREDICTOR
c-------------------------------------------------

          do i = 2,n
c          write(*,*)'node number',i
c          write(25,*)'node number',i
c          pause

          term1=q(i+1)**2/h(i+1)+0.5*g*h(i+1)*h(i+1)
          term2 = q(i)**2/h(i)+0.5*g*h(i)*h(i)
          sf =q(i)*q(i)*rn*rn/(h(i)**3.33333)
          qp(i) = q(i)-dtdx*(term1-term2)+ g*dt*h(i)*(s0-sf)
          cons1 = h(i)+f(i)-dtdx*(q(i+1)-q(i))

c          write(*,*)'entering infiltration'
c          write(25,*)'entering infiltration'


          if(h(i) .le. hini)then
             fp(i)=fini
            do j=1,nnodes
             if(j .lt. nnodes)then
               sinew(i,j)=siini
             else
               sinew(i,j)=hini
             endif
            enddo
          else

          call infiltration (siold,alpha,en,satk,thetas,thetar,em,ss,i,
     *          delz,dt,nnodes,sinew,maxiter,epsilon,nn,nnn,fp)

c          write(*,*)'node number',i
c          write(*,*)'infiltration subroutine completed'
c          write(25,*)'node number',i
c          write(25,*)'infiltration subroutine completed'

c          pause

          endif
          fcp(i)=fcp(i)+fp(i)*dt
          hp(i) = cons1 - fcp(i)

          enddo
```

```
      write(22,*)'sinew values after infiltration'
      write(22,13)(sinew(2,j),j=1,nnodes)

c     u/s and d/s boundary condition

      fcp(1) =0.0
      hp(1) = hups
      qp(1) = qups

      if(h(np).gt.hini) then
            fcp(np) = fcp(n)
            hp(np) = hdown
            qp(np) = qdown

      else

            fcp(np) = fcp(n)
            hp(np) = hp(n)
            qp(np) = qp(n)
      endif

c-------------------------------------------------------
c     END OF PREDICTOR/ START OF CORRECTOR
c-------------------------------------------------------

      do i = 2,n
       term1=qp(i)*qp(i)/hp(i)+0.5*g*hp(i)*hp(i)
       term2=qp(i-1)*qp(i-1)/hp(i-1)+0.5*g*hp(i-1)*hp(i-1)
       sf=qp(i)*qp(i)*rn*rn/(hp(i)**3.33333)
       qc(i)=q(i)-dtdx*(term1-term2)+g*dt*hp(i)*(s0-sf)
       cons1=h(i)+f(i)-dtdx*(qp(i)-qp(i-1))

       fz(i)=fcp(i)

       hc(i)=cons1-fz(i)
       enddo


C     Boundary Conditions

       fz(1) =0.0
       hc(1) = hups
       qc(1) = qups

       if(h(np).gt.hini) then
            fz(np) = fz(n)
            hc(np) = hdown
            qc(np) = qdown
       else
```

```
                fz(np) = fz(n)
                hc(np) = hc(n)
                qc(np) = qc(n)
            endif


c-------------------------------------------------------
c     END OF CORRECTOR PART
c-------------------------------------------------------
C       FINAL VALUES AT (n+1) TIME LEVEL
c-------------------------------------------------------

           do i =1,np
            h(i) = 0.5*(hp(i)+hc(i))
            q(i) = 0.5*(qp(i)+qc(i))
            f(i) = 0.5*(fcp(i)+fz(i))
           enddo

      if((t-dt) .lt. tprint(lprint).and. t .gt. tprint(lprint))then
            write(26,*)'time'
            write(26,*)t
            write(26,*)'tprint(lprint)'
            write(26,*)tprint(lprint)

           do i= 1,np
             hpre(i)=hold(i)+((tprint(lprint)-(t-dt))/dt)*(h(i)-hold(i))
           enddo

            write(26,*)'hpre values'
            write(26,13)(hpre(i),i=1,np)

           iconv = 0
           inode = 2

c          dpre(lprint) = 0.0

           do while (iconv .eq. 0)
           if (hpre(inode) .gt. hini)then
           dpre(lprint) = (inode-1)*dx
c          dpre(lprint) = dpre(lprint)+h(inode)
           else

           iconv = 1
           endif
           inode = inode+1
           enddo

           write (26,*) 'distance of hpre'
           write(26,13) dpre(lprint)
```

```
      do i=2,62,4

       write(26,*)'node number',i
       write(26,*)'thetapre'

       do j=1,nnodes
     sitemp=siold(i,j)+((tprint(lprint)-(t-dt))/dt)*
*    (sinew(i,j)-siold(i,j))
        if(sitemp .ge. 0.0)then
         thetapre(j)=thetas
              else
         thetapre(j)=thetar+(thetas-thetar)*f7(sitemp,alpha,em,en)
        endif
       enddo
       write(26,13)(thetapre(j),j=1,nnodes)
       write(26,*)'sinew values after infiltration'
       write(26,13)(sinew(i,j),j=1,nnodes)
      enddo
       lprint=lprint+1
      endif

      do i=2,(np-1)
       do j=1,nnodes
        if(j.eq.nnodes) then
          siold(i,j)=h(i)
        else
          siold(i,j)=sinew(i,j)
        endif
       enddo
      enddo
      enddo
      stop
      end

       subroutine infiltration(siold,alpha,en,satk,thetas,thetar,
*     em,ss,i,delz,dt,nnodes,sinew,maxiter,epsilon,nn,nnn,fp)
       dimension siold(nn,nnn),sinew(nn,nnn),fp(nn),siassum(nnn),
*                    alhs(nnn,nnn),rhs(nnn)

       iconv=0
       iter=1

c      write(25,*) 'siold values'
c      write(25,*) (siold(i,j),j=1,nnodes)

       do while (iconv .eq. 0)
c             write(*,*) 'i=',i
c         write(*,*) 'iter=',iter
c         write(25,*) 'i=',i
c         write(25,*) 'iter=',iter
```

```
      if (iter .eq. 1)then
        do j=1,nnodes
        siassum(j)=siold(i,j)
        enddo
      else
        do j=1,nnodes
        siassum(j)=sinew(i,j)
        enddo
      endif

c     write(25,*) 'siassum values'
c     write(25,*) (siassum(j),j=1,nnodes)


c           pause

      call coeff(siold,siassum,alpha,en,em,satk,thetas,
     *          thetar,ss,nnodes,dt,delz,i,nn,nnn,alhs,rhs)
      call solve(alhs,rhs,nnodes,i,nn,nnn,sinew)
      call convergence(siassum,sinew,i,nnodes,iter,
     *                          maxiter,epsilon,nn,nnn,iconv)

      iter=iter+1

      enddo

      call fpcomputation(siold,sinew,alpha,en,em,satk,i,
     *           delz,nnodes,nn,nnn,fp)

      return
      end

      subroutine coeff(siold,siassum,alpha,en,em,satk,thetas,thetar,
     *        ss,nnodes,dt,delz,i,nn,nnn,alhs,rhs)
      dimension siold(nn,nnn),siassum(nnn),alhs(nnn,nnn),rhs(nnn)

      do j=1,nnodes
        do k=1,nnodes
          alhs(j,k)=0.0
          enddo
      enddo

      do j=1,nnodes
       rhs(j)=0.0
      enddo

c     write(25,*) 'alhs and rhs '

      do j=1,nnodes
```

```
      if (j .eq. 1)then
        if (siassum(j) .ge. 0.0)then
          temptheta1=1
        else
          temptheta1=f7(siassum(j),alpha,em,en)
        endif
        thetanew1=thetar+temptheta1*(thetas-thetar)

        if (siassum(j+1).ge.0.0)then
          temptheta2=1.0
        else
          temptheta2=f7(siassum(j+1),alpha,em,en)
        endif
          thetanew2=thetar+temptheta2*(thetas-thetar)

          tempk1=satk*f2(temptheta1,em)
          tempk2=satk*f2(temptheta2,em)

          tempc1=f3(temptheta1,alpha,em,thetas,thetar)
          tempc2=f3(temptheta2,alpha,em,thetas,thetar)
          if(siold(i,j).ge.0.0)then
            tempthetao=1.0
          else
            tempthetao=f7(siold(i,j),alpha,em,en)
          endif

          thetaold = thetar+tempthetao*(thetas-thetar)
c                   qbot=0.0

          qbot=-tempk1

                    a=tempk1/(delz*delz)

                    c=(tempk1+tempk2)/(2.0*delz*delz)

                    s=(ss*thetanew1)/(thetas*dt)

                    b=-(a+c+(tempc1/dt)+s)

                    d=-(tempk2-tempk1)/(2.0*delz)

                    e=(thetanew1-thetaold)/dt

                    f=(tempc1/dt)

                    g=a*2.0*delz*((qbot/tempk1)+1.0)

                    alhs(j,j)=alhs(j,j)+b

                    alhs(j,j+1)=alhs(j,j+1)+c+a
```

```
                rhs(j)=rhs(j)+(d+e-f*siassum(j)-s*siold(i,j)-g)

                alhs(j,j)=1.0

                alhs(j,j+1) =0.0

                rhs(j)=siold(i,j)

c               write(25,110) alhs(j,j),alhs(j,j+1),rhs(j)
c110            format(4(1x,e14.7))

              else if(j.eq.nnodes)then

                alhs(j,j-1)=0.0
                alhs(j,j)=1.0
                rhs(j)=siold(i,j)
c               write(25,110) alhs(j,j-1),alhs(j,j),rhs(j)

              else
              if(siassum(j).ge.0.0)then
               temptheta1=1.0
              else
               temptheta1= f7(siassum(j),alpha,em,en)
              endif
               thetanew1=thetar+temptheta1*(thetas-thetar)
              if(siassum(j+1).ge. 0.0)then
               temptheta2=1.0
              else
               temptheta2= f7(siassum(j+1),alpha,em,en)
                   endif
                   thetanew2=thetar+temptheta2*(thetas-thetar)

             if(siassum(j-1).ge. 0.0)then
               temptheta3=1.0
             else
               temptheta3= f7(siassum(j-1),alpha,em,en)
                  endif

                    thetanew3=thetar+temptheta3*(thetas-thetar)

                         tempk1=satk*f2(temptheta1,em)

                         tempk2=satk*f2(temptheta2,em)

                         tempk3=satk*f2(temptheta3,em)

                         tempc1=f3(temptheta1,alpha,em,thetas,thetar)

               tempc2=f3(temptheta2,alpha,em,thetas,thetar)
```

```
        tempc3=f3(temptheta3,alpha,em,thetas,thetar)

      if(siold(i,j).ge. 0.0)then
        tempthetao=1.0
      else
        tempthetao=f7(siold(i,j),alpha,em,en)
      endif

        thetaold=thetar+tempthetao*(thetas-thetar)

      a= (tempk1+tempk3)/(2.0*delz*delz)

      c=   (tempk1+tempk2)/(2.0*delz*delz)

      s= (ss*thetanew1)/(thetas*dt)

      b=-(a+c+(tempc1/dt)+s)

      d=-(tempk2-tempk3)/(2.0*delz)

      e= (thetanew1-thetaold)/dt

      f= tempc1/dt

      alhs(j,j-1)=alhs(j,j-1)+a

      alhs(j,j)=alhs(j,j)+b

      alhs(j,j+1)=alhs(j,j+1)+c

      rhs(j)=rhs(j)+(d+e-f*siassum(j)-s*siold(i,j))

c     if(j.eq.(nnodes-1)) then
c       write(25,*) 'a=', a
c                   write(25,*) 'c=', c
c                   write(25,*) 's=', s
c                   write(25,*) 'b=', b
c                   write(25,*) 'd=', d
c                   write(25,*) 'e=', e
c                   write(25,*) 'f=', f
c           endif

c     write(25,110) alhs(j,j-1),alhs(j,j),alhs(j,j+1),rhs(j)

      endif
     enddo

      return
      end
```

```
      subroutine solve(alhs,rhs,nnodes,i,nn,nnn,sinew)
      dimension alhs(nnn,nnn),rhs(nnn),sinew(nn,nnn),beta(nnn),
     *          gama(nnn),z(nnn)

c     write(25,*) 'Entering solve subroutine'
c     write(25,*) 'node number=',i
c     do j=2,nnodes
c       if(j.eq.1) then
c         write(25,110) alhs(j,j),alhs(j,j+1),rhs(j)
c       elseif(j.eq.nnodes) then
c         write(25,110) alhs(j,j-1),alhs(j,j),rhs(j)
c       else
c         write(25,110) alhs(j,j-1),alhs(j,j),alhs(j,j+1),rhs(j)
c       endif
c     end do
c110  format(4(1x,e14.7))

      beta(1)=alhs(1,1)

      do j=1,(nnodes-1)
       gama(j)=alhs(j,j+1)/beta(j)
       beta(j+1)=alhs(j+1,j+1)-alhs(j+1,j)*gama(j)
      enddo

c     write(25,*)'beta values'
c     write(25,*)(beta(j),j=1,nnodes)
c     write(25,*)'gama values'
c     write(25,*)(gama(j),j=1,nnodes)

      z(1)=rhs(1)/beta(1)

      do j=2,nnodes
       z(j)=(rhs(j)-alhs(j,j-1)*z(j-1))/beta(j)
      enddo
      sinew(i,nnodes)=z(nnodes)
      do k=1,(nnodes-1)
      sinew(i,nnodes-k)=z(nnodes-k)-gama(nnodes-k)*
     *          sinew(i,nnodes-k+1)

c     print*,sinew(i,nnodes-k)
      enddo

c     write(25,*) 'sinew values'
c     write(25,*)(sinew(i,j),j=1,nnodes)

      return
      end
```

```
      real function f2(theta,em)
c     calculates unsaturated hydraulic conductivity using Mualem's
c
c     equation Vangenutchen's model is used for moisture content
c
c           pressure head relationship

            a=(1.0-theta**(1.0/em))**em
            f2=(theta**0.5)*((1.0-a)**2.0)

            return
            end

            real function f3(theta,alpha,em,thetas,thetar)

c           calculates soil moisture capacity('c')Vangenuchten's model
c           is used for moisture content pressure head relationship

            a=(1.0-theta**(1.0/em))**em
c           wrtite *,a
           b=(alpha*em*(thetas-thetar))/(1.0-em)
c          write *,b
            f3=b*(theta**(1.0/em))*a

            return
            end

            real function f7(si,alpha,em,en)

c           determines moisture content, given pressure head using
c
c           Vangenuchten's model

            a=1.0+((alpha*(abs(si)))**en)
            f7=(1.0/a)**em
            return
            end

            real function f1 (theta,alpha,em,en)

c           determines pressure head, given moisture content
c
c           using Vangenuchten's model

            a=(1.0/(theta**(1.0/em)))-1.0
            f1=-(a**(1.0/en))/alpha
            return
            end
```

```
      subroutine convergence(siassum,sinew,i,nnodes,iter,
*                    maxiter,epsilon,nn,nnn,iconv)

      dimension siassum(nnn),sinew(nn,nnn)

      if(iter .eq. 1)then
        iconv=0
       do j=1,nnodes
       siassum(j)=sinew(i,j)
       enddo

       else if(iter .eq. maxiter)then
           iconv=1
       else
        great=abs(sinew(i,1)-siassum(1))

         do j=2,nnodes
          great1=abs(sinew(i,j)-siassum(j))
          if(great1 .ge. great)then
            great=great1
          endif
         enddo

        if(great .le. epsilon)then
          iconv=1
        else
          iconv=0
        endif

      endif

      write(*,*) 'great=',great
      write(*,*) 'iconv=',iconv

      return
      end

      subroutine fpcomputation(siold,sinew,alpha,en,em,
*                    satk,i,delz,nnodes,nn,nnn,fp)

  dimension siold(nn,nnn),sinew(nn,nnn),fp(nn)

      sitemp1=(sinew(i,nnodes-1)+siold(i,nnodes-1))/2

      if(sitemp1.ge.0.0)then
       temptheta1=1.0
       tempk1=satk
      else

        temptheta1=f7(sitemp1,alpha,em,en)
```

```
        tempk1=satk*f2(temptheta1,em)
      endif

      sitemp2=(sinew(i,nnodes)+siold(i,nnodes))/2

      if(sitemp2.ge.0.0)then

        temptheta2=1.0
            tempk2=satk
      else
        temptheta2=f7(sitemp2,alpha,em,en)
        tempk2=satk*f2(temptheta2,em)
      endif
        averagek=(tempk1+tempk2)/2

        fp(i)=abs(-averagek*(((sinew(i,nnodes)-sinew(i,nnodes-1))
     *              /delz)+1))
      return
      end
```

APPENDIX-II

PARAMETER ESTIMATION MODEL FOR ESTIMATING INFILTRATION PARAMETERS USING INVERSE PROCEDURES

```
C       PARAMETER ESTIMATION MODEL FOR ESTIMATING

        INFILTRATION PARAMETERS USING SEQUENTIAL

        UNCONSTRAINED MINIMIZATION TECHNIQUE (SUMT)
C       ------------------------------------------------------------------

        dimension x(4), xn(4),xopt(4),grad(4),s(4),gradn(4),y(4),
     *          hy(4), gk(8),gg(8),h(4,4),xmm(4,4),xnn(4,4)

        common/count/nfun,ngrad
        common/miter/itlim
        common/conv/maxin,maxgr
        common/param/ti(100),dd(100),ux(4),vx(4)

c       common/para1/q,dr
        common/para2/nt

        common/para3/hini,s0,rn,crn,lmax,quns,g,dx,tmax,trec,slength,
     *  nnodes,siini,thetas,thetar,ss,maxiter,epsilon,nprint,
     *  tprint(50)

c       open(unit=10,file='unconfined.dat')
        open(unit=21,file='optn1.dat')
        open(unit=22,file='tar.out')
        open(unit=23,file='dep.out')
        open(unit=24,file='in.out')
        open(unit=25,file='trial.out')
        open(unit=26,file='sinew.out')
        open(unit=27,file='opt.out')
        open(unit=28,file='opt1.out')
        read(21,*)hini,s0,rn,crn,lmax
        read(21,*)quns,g,dx,tmax,trec
        read(21,*)slength,nnodes,siini,thetas,thetar,ss
        read(21,*)maxiter,epsilon
        read(21,*)nprint
        read(21,*)(tprint(i),i=1,nprint)
        read(21,*)n,nt
        read(21,*)(x(i),i=1,n)
        read(21,*)(ux(i),i=1,n)
        read(21,*)(vx(i),i=1,n)
        read(21,*)(ti(i),i=1,nt)
```

```
      read(21,*)(dd(i),i=1,nt)

C     data m,maxpi,c,r,eps,epss,stepo/2,5,0.1,0.06,0.05,0.01,1.0/
      data m,maxpi,c,r,eps,epss,stepo/6,5,0.1,0.06,0.05,0.01,0.25/

      write(27,*)" INPUT DATA"
      write(27,*)"hini,s0,rn,crn,lmax,slength,nnodes,siini"
      write(27,*)hini,s0,rn,crn,lmax,slength,nnodes,siini
      write(27,*)"quns,g,dx,tmax,trec,thetas,thetar"
      write(27,*)quns,g,dx,tmax,trec,thetas,thetar
      write(27,*)"maxiter,epsilon,ss,nprint,tprint"
      write(27,*)maxiter,epsilon,ss,nprint
      write(27,*)(tprint(i),i=1,nprint)
      write(27,*)"n,nt,x,ux,vx,ti,dd"
      write(27,*)n,nt,x,ux,vx
      write(27,*)(ti(i),i=1,nt)
      write(27,*)(dd(i),i=1,nt)

c     stop

c      do i= 1,nt
c        read(10,*) ti(i),dd(i)
c      end do

       nfun =0
       itlim = 4
       maxin = 5
       maxgr = 3

       k=1

30     call uncon(n,m,r,eps,epss,stepo,x,xn,xopt,h,grad,s,
     *       gradn,y,hy,xmm,xnn,gk,gg,f,obj,ii)

       if(k.eq.maxpi) go to 20
         r= c*r
         do   10 i=1,n
10         x(i)=xopt(i)
       k=k+1
         go to 30
20     stop
      end

       subroutine uncon(n,m,r,eps,epss,stepo,x,xn,xopt,h,grad,s,
     *          gradn,y,hy,xmm,xnn,gk,gg,f,obj,ii)

       common/count/nfun,ngrad
       common/miter/itlim
       common/conv/maxin,maxgr
```

```
      dimension x(n),xopt(n),h(n,n),grad(n),s(n),gradn(n),
     *   y(n),hy(n),xn(n),gk(m),gg(m),xmm(n,n),xnn(n,n)


      do 10 i=1,n
       do 10 j=1,n
10       h(i,j) = 0.


      do 20 i=1,n
20          h(i,i) = 1.


      ii=1


      call ftn(gk,x,f,obj,n,m,r)

      call gradt(x,gg,n,m,r,grad,f)


      write(*,111) r,f,obj
111   format(//,1x,'starting values for unconstrained
     *   minimization',/,2x,'r=',e12.5,'pf=',e15.8,
     *   2x,'obj=',e15.8)
      write(*,112)(x(i),i=1,n)

112   format(2x,'x(i) are', /,2x,4e15.8,/,2x,4e15.8)
      write(*,113)(gk(i),i=1,m)
113   format(2x,'gk(i) are', /,2x,4e15.8,/,2x,4e15.8)

c     pause

100   do 30 i=1,n
     s(i) = 0.
      do 30 j=1,n
30       s(i)= s(i)+h(i,j)*grad(j)


      do 40 i=1,n
40       s(i)=-s(i)
      sum = 0.
      do 1 i = 1,n
1        sum = sum + s(i)**2
      sum = sqrt(sum)


      do 2, i=1,n
2        s(i)= s(i)/abs(sum)
```

```
      call onedim(n,m,r,epss,stepo,slamda,x,xn,s,f,fn,obj,grad,
     *          gradn,gk,gg)


      do 50 i=1,n
50    x(i) = x(i) + slamda*s(i)


      write(*,114) ii,stepo,fn,obj,nfun,ngrad
114   format(/,2x,'iter=',i3,2x,'stepo=',e12.5,/,2x,'pf=',e12.5,
     *    2x,'obj=',e12.5,2x,'nfun=',i5,2x,'ngrad=',i5)

      write(*,112)(xn(i),i=1,n)
      write(*,113)(gk(i),i=1,m)

c     pause

      sum = 0.
      do 60 i=1,n
60    sum = sum + gradn(i)**2
      sum = sqrt(sum)

      if(sum.lt.eps) go to 110
      if(ii.eq.itlim) go to 110

      do 70 i= 1, n
70    y(i) = gradn(i)-grad(i)

      den = 0.
      do 3 i=1,n
3     den = den + s(i)*y(i)

      fac = slamda/den

      do 5 i=1,n
        do 5 j=1,n
5     xmm(i,j) = s(i)*s(j)*fac

      do 4 i=1,n
            hy(i) = 0.
       do 4 j=1,n
4             hy(i) = hy(i) + h(i,j)*y(j)

      do 6 i=1,n
        do 6 k=1,n
6     xnn(i,k) = hy(i)*hy(k)

      den = 0.

      do 7 j=1,n
```

```
7      den = den + y(j)*hy(j)

          do 8 i=1,n
            do 8 j=1,n
8         xnn(i,j)= -xnn(i,j)/den

          do 80 i=1,n
            do 80 j = 1,n
80         h(i,j) = h(i,j)+xmm(i,j)+xnn(i,j)

       if(ii/n*n.ne.ii) go to 39

          do 37 i=1,n
            do 37 j=1,n
37          h(i,j) = 0.0

       do 38 i=1,n
38        h(i,i) = 1.

39      continue

        ii = ii+1
           f = fn

           do 90 i=1,n
90      grad(i)=gradn(i)

           go to 100

110        do 120 i=1,n
120       xopt(i) = x(i)

           return
           end

           subroutine onedim(n,m,r,epss,stepo,slamda,x,xn,s,f,fn,
     *                obj,grad,gradn,gk,gg)


           common/count/nfun,ngrad
           common/conv/maxin,maxgr
           dimension x(n),xn(n),s(n),grad(n),gradn(n),gk(n),gg(n)

           nnfun=0
           nngrad=0

           write(*,191)(s(i),i=1,n)
191        format(/,2x,'cubic interpolation starts',/,'s(i)=',
     *       4e12.4,/,(3x,4e12.4))
```

```
      sum = 0.
          do 10 i=1,n
10        sum = sum+grad(i)*s(i)

          a=0.
          fa = f
          fap = sum
40      do 20 i=1,n
20        xn(i)=x(i)+stepo*s(i)

          call ftn(gk,xn,fn,obj,n,m,r)

          nnfun = nnfun + 1
          do 21 j=1,m
            if(gk(j).ge.0.0) go to 22
21      continue

          go to 41
22        stepo = stepo*0.5
          go to 40
41        continue

          call gradt(xn,gg,n,m,r,gradn,fn)

          nngrad = nngrad + 1

          sum = 0.
          do 30 i=1,n
30      sum = sum + gradn(i)*s(i)

        fb = fn
          fbp = sum
          if(fbp.gt.0.0) go to 110
          fa = fb
          fap = fbp
          a = stepo
          stepo = stepo*1.2
          go to 40

110     ii = 0
        b = stepo

160     z = 3.*(fa-fb)/(b-a)+fap+fbp
        q = sqrt(z*z-fap*fbp)
          slamda = a + (fap+z+q)*(b-a)/(fap+fbp+2.*z)
          ii=ii + 1

          do 120 i=1,n
120       xn(i) = x(i) + slamda*s(i)
```

```
      call ftn(gk,xn,fn,obj,n,m,r)

      nnfun = nnfun + 1

      call gradt(xn,gg,n,m,r,gradn,fn)

      nngrad = nngrad + 1

      sum = 0.
      sum1 = 0.
      sum2 = 0.

      do 130 i=1,n
       sum = sum + gradn(i)*s(i)
            sum1 = sum1 + gradn(i)**2
130         sum2 = sum2 + s(i)**2

      sum1 = sqrt(sum1)
      sum2 = sqrt(sum2)
      conv = abs(sum/(sum1*sum2))

      if(conv.le.epss) go to 140
      if(ii.ge.maxin) go to 140
      if(sum.gt.0.0) go to 150

      a = slamda
      fa = fn
      fap = sum
      go to 160

150   b = slamda
     fb = fn
      fbp = sum
      go to 160

140   stepo = slamda

      return
      end

      subroutine gradt(x,gg,n,m,r,grad,ff)

      dimension x(n),grad(n),gg(m)
      common/count/nfun,ngrad

      ngrad = ngrad + 1

      do 12 i=1,n
       xip = x(i)
       x(i) = 1.05*xip
```

```
            call ftn(gg,x,fbp,obj,n,m,r)
                x(i) = xip
                grad(i) = (fbp - ff)/(0.05*x(i))
12      continue

          return
          end

          subroutine ftn(gk,x,f,obj,n,m,r)

          dimension x(n),gk(m),dpre(50)
          common/count/nfun,ngrad
          common/param/ti(100),dd(100),ux(4),vx(4)
c         common/para1/q,dr
          common/para2/nt
          common/para3/hini,s0,rn,crn,lmax,quns,g,dx,tmax,trec,slength,
     *  nnodes,siini,thetas,thetar,ss,maxiter,epsilon,nprint,
     *  tprint(50)

          nfun = nfun + 1
          obj = 0.
          call hrd(x,dpre)

          write(28,*)'dpre'
          write(28,*)(dpre(i),i=1,nt)

          do i=1, nt
           obj=obj+(dd(i)-dpre(i))**2
          enddo

          write(28,*)'objetive function=',obj
          write(*,*) 'ux(i)=',ux(1)
          write(*,*) 'vx(i)=',vx(1)
c         pause

160     continue

        gk(1) = -x(1)+vx(1)
            gk(2) = -x(2)+vx(2)
        gk(3) = -x(3)+vx(3)
c           gk(4) = -x(4)+vx(4)
            gk(4) =  x(1)-ux(1)
        gk(5) =  x(2)-ux(2)
            gk(6) =  x(3)-ux(3)
c           gk(8) =  x(4)-ux(4)

            f = obj

            do 10 i=1,m
10          f = f - r/gk(i)
```

```
      return
      end

      subroutine hrd(yxz,dpre)

      common/para2/nt
      common/para3/hini,s0,rn,crn,lmax,quns,g,dx,tmax,trec,slength,
     *  nnodes,siini,thetas,thetar,ss,maxiter,epsilon,nprint,
     *  tprint(50)

      common/param/ti(100),dd(100),ux(4),vx(4)
      parameter(nn=1000)
      parameter(nnn=300)
      dimension h(nn),q(nn),f(nn),hp(nn),qp(nn),fp(nn),fcp(nn)
      dimension hc(nn),qc(nn),fz(nn),hold(nn),hpre(nn)
      dimension siold(nn,nnn),sinew(nn,nnn),thetapre(nnn)
      dimension dpre(50),yxz(4)

c     common/param/ti(100),dd(100),ux(4),vx(4)
c     common/para1/ux(4),vx(4)

      satk=yxz(1)
      alpha=yxz(2)
      en=yxz(3)
c      satk=5.0
c      en=  2.3
c     alpha=0.02

      write(*,*)'satk=',satk
      write(*,*)'alpha=',alpha
      write(*,*)'en=',en

c     pause


      if(
     *  (satk .le. vx(1)) .or. (satk .ge. ux(1))
     *  .or.
     *  (alpha .le. vx(2)) .or. (alpha .ge. ux(2))
     *  .or.
     *  (en .le. vx(3)) .or. (en .ge. ux(3))
     *  )then
      do i = 1,nprint
         dpre(i)=1.0e+10
      enddo
      else

      qini = hini**(1.66667)*sqrt(s0)/rn
```

```
      fini = 0.0

      write(22,*)" INPUT DATA"
      write(22,*)"qini,hini,fini,s0,rn,crn,lmax,slength,nnodes,siini"
      write(22,*)qini,hini,fini,s0,rn,crn,lmax,slength,nnodes,siini
      write(22,*)"quns, g, dx, tmax,alpha,en,satk,thetas,thetar"
      write(22,*)quns,g,dx,tmax,thetas,thetar
      write(22,*)"maxiter,epsilon,ss,nprint,tprint"
      write(22,*)maxiter,epsilon,ss,nprint,tprint


      ns = lmax/dx
      np = ns+1
      delz=slength/(nnodes-1)
      em=1-1/en

      t = 0.0
      c3=(rn/sqrt(s0))**0.6

       do i = 1,np
        q(i) = qini
        h(i) = hini
        f(i) = fini
        fcp(i)=fini
       enddo
       do i=2,np-1
       do j=1,nnodes
        if(j .eq. nnodes)then
        siold(i,j)=h(i)
        else
        siold(i,j)=siini
        endif
       enddo
       enddo
c      do j=1,nnodes
c      write(22,13)siold(2,j)
13     format(8(1x,f14.7))
c      enddo

      lprint=1

       do while(t .le. tmax)

c-------------------------------------------------------
c      UNSTEADY COMPUTATIONS
c-------------------------------------------------
C      STABILITY CHECK
c-------------------------------------------------

       do i=1,np
```

```
          hold(i)=h(i)
         enddo

         do i = 1, np
          dt = dx/(abs(q(i)/h(i))+sqrt(g*h(i)))
          if(i .eq. 1)dtmin = dt
          if(dt .le. dtmin) dtmin = dt
         enddo

          dt = crn*dtmin

          t = t + dt
          write(22,*) 'time=', t

          dtdx=dt/dx

c-------------------------------------------------------
c        CALCULATION FOR NEXT TIME STEP
c-------------------------------------------------------
c        UPSTREAM BOUNDARY CALCULATION
c-------------------------------------------------

          cr = q(2)/h(2)+sqrt(g*h(2))
          sf=q(2)*q(2)*rn*rn/(h(2)**3.33333)
          cn=q(2)-cr*h(2)+g*dt*h(2)*(s0-sf)

          if(t .lt. trec)then
            qups=quns
          else
            qups=qini
          endif
            hups = (qups-cn)/cr
          if(hups .lt. hini)then
            hups=hini
          endif
          fups = 0.0

c-------------------------------------------------
c        DOWNSTREAM BOUNDARY/UNIFORM FLOW CONDITION
c-------------------------------------------------

                if(h(np).gt.hini)then
                cl=q(ns)/h(ns)-sqrt(g*h(ns))
                sf=q(ns)*q(ns)*rn*rn/(h(ns)**3.33333)
                cp=q(ns)-cl*h(ns)+g*dt*h(ns)*(s0-sf)

                iter = 0
                qdown = q(ns)

                diff = 1.0
```

```
            do while((iter.le.15).and.(abs(diff).gt.1.0e-04))
                  iter = iter+1
                  fq=qdown-cp-cl*c3*(qdown**0.6)
                  dfq=qdown-cl*c3*0.6/(qdown**0.4)
                  diff=-fq/dfq
                  qdown=qdown+diff
            enddo
            if(iter.gt.15)write(*,*)"iter fails at d/s"
              hdown=(qdown-cp)/cl
            endif

c-----------------------------------------------
c           INTERIOR NODES / PREDICTOR
c-----------------------------------------------

            do i = 2,ns
c           write(*,*)'node number',i
c           write(25,*)'node number',i
c           pause
            term1=q(i+1)**2/h(i+1)+0.5*g*h(i+1)*h(i+1)
            term2 = q(i)**2/h(i)+0.5*g*h(i)*h(i)
            sf =q(i)*q(i)*rn*rn/(h(i)**3.33333)
            qp(i) = q(i)-dtdx*(term1-term2)+ g*dt*h(i)*(s0-sf)
            cons1 = h(i)+f(i)-dtdx*(q(i+1)-q(i))
c           write(*,*)'entering infiltration'
c           write(25,*)'entering infiltration'



            if(h(i) .le. hini)then
               fp(i)=fini
              do j=1,nnodes
               if(j .lt. nnodes)then
                 sinew(i,j)=siini
               else
                 sinew(i,j)=hini
               endif
              enddo
            else
            call infiltration (siold,alpha,en,satk,thetas,thetar,em,ss,i,
     *           delz,dt,nnodes,sinew,maxiter,epsilon,nn,nnn,fp)

c           write(*,*)'node number',i
c           write(*,*)'infiltration subroutine completed'
c           write(25,*)'node number',i
c           write(25,*)'infiltration subroutine completed'

c           pause

            endif
```

```
            fcp(i)=fcp(i)+fp(i)*dt
            hp(i) = cons1 - fcp(i)

            enddo

            write(22,*)'sinew values after infiltration'
            write(22,13)(sinew(2,j),j=1,nnodes)

c           u/s and d/s boundary condition

            fcp(1) =0.0
            hp(1) = hups
            qp(1) = qups
            if(h(np).gt.hini) then
                  fcp(np) = fcp(ns)
                  hp(np) = hdown
                  qp(np) = qdown
            else
                  fcp(np) = fcp(ns)
                  hp(np) = hp(ns)
                  qp(np) = qp(ns)
            endif

c-----------------------------------------------------------
c           END OF PREDICTOR/ start of CORRECTOR
c-----------------------------------------------------

            do i = 2,ns
            term1=qp(i)*qp(i)/hp(i)+0.5*g*hp(i)*hp(i)
            term2=qp(i-1)*qp(i-1)/hp(i-1)+0.5*g*hp(i-1)*hp(i-1)
            sf=qp(i)*qp(i)*rn*rn/(hp(i)**3.33333)
            qc(i)=q(i)-dtdx*(term1-term2)+g*dt*hp(i)*(s0-sf)
            cons1=h(i)+f(i)-dtdx*(qp(i)-qp(i-1))

             fz(i)=fcp(i)
             hc(i)=cons1-fz(i)
             enddo

C           Boundary Conditions

            fz(1) =0.0
            hc(1) = hups
            qc(1) = qups

             if(h(np).gt.hini) then
                  fz(np) = fz(ns)
                  hc(np) = hdown
                  qc(np) = qdown
            else
                  fz(np) = fz(ns)
```

```
            hc(np) = hc(ns)
            qc(np) = qc(ns)
          endif


c-------------------------------------------------------
c     END OF CORRECTOR PART
c-------------------------------------------------------
C          FINAL VALUES AT (ns+1) TIME LEVEL
c-------------------------------------------------

          do i =1,np
           h(i) = 0.5*(hp(i)+hc(i))
           q(i) = 0.5*(qp(i)+qc(i))
           f(i) = 0.5*(fcp(i)+fz(i))
          enddo

      if((t-dt) .lt. tprint(lprint).and. t .gt. tprint(lprint))then
           write(26,*)'time'
           write(26,*)t
           write(26,*)'tprint(lprint)'
           write(26,*)tprint(lprint)

           do i= 1,np
            hpre(i)=hold(i)+((tprint(lprint)-(t-dt))/dt)*(h(i)-hold(i))
           enddo
            write(26,*)'hpre values'
            write(26,13)(hpre(i),i=1,np)
            iconv=0
            inode=2
           dpre(lprint)=0.0
                  do while (iconv .eq. 0)
           if(hpre(inode) .gt. hini)then
            dpre(lprint)=dpre(lprint)+h(inode)
           else
            iconv=1
           endif
            inode=inode+1
          enddo

c          write(26,*)'distance of hpre'
c          write(26,13)dpre(lprint)

           do i=2,64,4

            write(26,*)'node number',i
            write(26,*)'thetapre'

            ttt=0.0
```

```
          do j =1,nnodes
        sitemp =siold(i,j)+((tprint(lprint)-(t-dt))/dt)*
     *  (sinew(i,j)-siold(i,j))
           if(sitemp .ge. 0.0)then
            thetapre(j) =thetas
                  else
            thetapre(j) =thetar+(thetas-thetar)*f7(sitemp,alpha,em,en)
           endif
          ttt = ttt+thetapre(j)
          enddo

          write(26,13)(thetapre(j),j=1,nnodes)
          write(26,*)'sinew values after infiltration'
          write(26,13)(sinew(i,j),j=1,nnodes)

         enddo

c        write(*,*)'sum of mc=',ttt

         dpre(lprint)=dpre(lprint)+ttt

         write(26,*)'distance of hpre'
         write(26,*)'dpre(lprint)'
         write(26,13)dpre(lprint)

          lprint=lprint+1
        endif

        do i=2,(np-1)
         do j=1,nnodes
          if(j.eq.nnodes) then
            siold(i,j)=h(i)
          else
            siold(i,j)=sinew(i,j)
          endif
         enddo
        enddo
        enddo
        endif
c       stop

        return
        end

          subroutine infiltration(siold,alpha,en,satk,thetas,thetar,
     *    em,ss,i,delz,dt,nnodes,sinew,maxiter,epsilon,nn,nnn,fp)
          dimension siold(nn,nnn),sinew(nn,nnn),fp(nn),siassum(nnn),
     *                    alhs(nnn,nnn),rhs(nnn)
         iconv=0
         iter=1
```

```
c      write(25,*) 'siold values'
c          write(25,*) (siold(i,j),j=1,nnodes)

           do while (iconv .eq. 0)
c                write(*,*) 'i=',i
c             write(*,*) 'iter=',iter
c             write(25,*) 'i=',i
c             write(25,*) 'iter=',iter

           if (iter .eq. 1)then
            do j=1,nnodes
            siassum(j)=siold(i,j)
            enddo
           else
            do j=1,nnodes
            siassum(j)=sinew(i,j)
            enddo
           endif

c          write(25,*) 'siassum values'
c          write(25,*) (siassum(j),j=1,nnodes)


c                pause

           call coeff(siold,siassum,alpha,en,em,satk,thetas,
     *             thetar,ss,nnodes,dt,delz,i,nn,nnn,alhs,rhs)
           call solve(alhs,rhs,nnodes,i,nn,nnn,sinew)
           call convergence(siassum,sinew,i,nnodes,iter,
     *                                maxiter,epsilon,nn,nnn,iconv)
           iter=iter+1
           enddo

           call fpcomputation(siold,sinew,alpha,en,em,satk,i,
          *                delz,nnodes,nn,nnn,fp)

           return
           end

           subroutine coeff(siold,siassum,alpha,en,em,satk,thetas,thetar,
     *             ss,nnodes,dt,delz,i,nn,nnn,alhs,rhs)
           dimension siold(nn,nnn),siassum(nnn),alhs(nnn,nnn),rhs(nnn)

            do j=1,nnodes
              do k=1,nnodes
                 alhs(j,k)=0.0
                 enddo
            enddo
            do j=1,nnodes
```

```
          rhs(j)=0.0
        enddo

c       write(25,*) 'alhs and rhs '
        do j=1,nnodes
        if (j .eq. 1)then
          if (siassum(j) .ge. 0.0)then
            temptheta1=1
          else
            temptheta1=f7(siassum(j),alpha,em,en)
          endif
          thetanew1=thetar+temptheta1*(thetas-thetar)

          if (siassum(j+1).ge.0.0)then
             temptheta2=1.0
          else
             temptheta2=f7(siassum(j+1),alpha,em,en)
          endif
             thetanew2=thetar+temptheta2*(thetas-thetar)

             tempk1=satk*f2(temptheta1,em)
             tempk2=satk*f2(temptheta2,em)

             tempc1=f3(temptheta1,alpha,em,thetas,thetar)
             tempc2=f3(temptheta2,alpha,em,thetas,thetar)
             if(siold(i,j).ge.0.0)then
               tempthetao=1.0
             else
               tempthetao=f7(siold(i,j),alpha,em,en)
             endif
             thetaold = thetar+tempthetao*(thetas-thetar)
c                      qbot=0.0
             qbot=-tempk1

                      a=tempk1/(delz*delz)
                      c=(tempk1+tempk2)/(2.0*delz*delz)
                      s=(ss*thetanew1)/(thetas*dt)
                      b=-(a+c+(tempc1/dt)+s)
                      d=-(tempk2-tempk1)/(2.0*delz)
                      e=(thetanew1-thetaold)/dt
                      f=(tempc1/dt)
                      g=a*2.0*delz*((qbot/tempk1)+1.0)
                      alhs(j,j)=alhs(j,j)+b
                      alhs(j,j+1)=alhs(j,j+1)+c+a
           rhs(j)=rhs(j)+(d+e-f*siassum(j)-s*siold(i,j)-g)
           alhs(j,j)=1.0
           alhs(j,j+1) =0.0
           rhs(j)=siold(i,j)

c          write(25,110) alhs(j,j),alhs(j,j+1),rhs(j)
```

```
c110        format(4(1x,e14.7))
          else if(j.eq.nnodes)then

            alhs(j,j-1)=0.0
            alhs(j,j)=1.0
            rhs(j)=siold(i,j)
c           write(25,110) alhs(j,j-1),alhs(j,j),rhs(j)
          else
          if(siassum(j).ge.0.0)then
           temptheta1=1.0
          else
           temptheta1= f7(siassum(j),alpha,em,en)
          endif
           thetanew1=thetar+temptheta1*(thetas-thetar)
          if(siassum(j+1).ge. 0.0)then
           temptheta2=1.0
          else
           temptheta2= f7(siassum(j+1),alpha,em,en)
               endif
               thetanew2=thetar+temptheta2*(thetas-thetar)

          if(siassum(j-1).ge. 0.0)then
           temptheta3=1.0
          else
           temptheta3= f7(siassum(j-1),alpha,em,en)
              endif
                thetanew3=thetar+temptheta3*(thetas-thetar)
                     tempk1=satk*f2(temptheta1,em)
                     tempk2=satk*f2(temptheta2,em)
                     tempk3=satk*f2(temptheta3,em)
                     tempc1=f3(temptheta1,alpha,em,thetas,thetar)
           tempc2=f3(temptheta2,alpha,em,thetas,thetar)
           tempc3=f3(temptheta3,alpha,em,thetas,thetar)
          if(siold(i,j).ge. 0.0)then
           tempthetao=1.0
          else
           tempthetao=f7(siold(i,j),alpha,em,en)
          endif
           thetaold=thetar+tempthetao*(thetas-thetar)
          a= (tempk1+tempk3)/(2.0*delz*delz)
          c=  (tempk1+tempk2)/(2.0*delz*delz)
          s= (ss*thetanew1)/(thetas*dt)
          b=-(a+c+(tempc1/dt)+s)
          d=-(tempk2-tempk3)/(2.0*delz)
          e= (thetanew1-thetaold)/dt
          f= tempc1/dt
          alhs(j,j-1)=alhs(j,j-1)+a
          alhs(j,j)=alhs(j,j)+b
          alhs(j,j+1)=alhs(j,j+1)+c
          rhs(j)=rhs(j)+(d+e-f*siassum(j)-s*siold(i,j))
```

```
c           if(j.eq.(nnodes-1)) then
c             write(25,*) 'a=', a
c                       write(25,*) 'c=', c
c                       write(25,*) 's=', s
c                       write(25,*) 'b=', b
c                       write(25,*) 'd=', d
c                       write(25,*) 'e=', e
c                       write(25,*) 'f=', f
c                 endif

c           write(25,110) alhs(j,j-1),alhs(j,j),alhs(j,j+1),rhs(j)

            endif
           enddo

            return
            end


          subroutine solve(alhs,rhs,nnodes,i,nn,nnn,sinew)

          dimension alhs(nnn,nnn),rhs(nnn),sinew(nn,nnn),beta(nnn),
     *          gama(nnn),z(nnn)

c         write(25,*) 'Entering solve subroutine'
c         write(25,*) 'node number=',i
c         do j=2,nnodes
c           if(j.eq.1) then
c             write(25,110) alhs(j,j),alhs(j,j+1),rhs(j)
c           elseif(j.eq.nnodes) then
c             write(25,110) alhs(j,j-1),alhs(j,j),rhs(j)
c           else
c             write(25,110) alhs(j,j-1),alhs(j,j),alhs(j,j+1),rhs(j)
c           endif
c         end do
c110      format(4(1x,e14.7))
          beta(1)=alhs(1,1)

          do j=1,(nnodes-1)
           gama(j)=alhs(j,j+1)/beta(j)
           beta(j+1)=alhs(j+1,j+1)-alhs(j+1,j)*gama(j)
          enddo

c         write(25,*)'beta values'
c         write(25,*)(beta(j),j=1,nnodes)
c         write(25,*)'gama values'
c         write(25,*)(gama(j),j=1,nnodes)

          z(1)=rhs(1)/beta(1)
```

```
      do j=2,nnodes
       z(j)=(rhs(j)-alhs(j,j-1)*z(j-1))/beta(j)
      enddo

      sinew(i,nnodes)=z(nnodes)
      do k=1,(nnodes-1)
      sinew(i,nnodes-k)=z(nnodes-k)-gama(nnodes-k)*
     *          sinew(i,nnodes-k+1)
c     print*,sinew(i,nnodes-k)

      enddo
c     write(25,*) 'sinew values'
c     write(25,*)(sinew(i,j),j=1,nnodes)

      return
      end
       real function f2(theta,em)

c       calculates unsaturated hydraulic conductivity using Mualem's
c     equation Vangenutchen's model is used for moisture content
c             pressure head relationship

              a=(1.0-theta**(1.0/em))**em
              f2=(theta**0.5)*((1.0-a)**2.0)

              return
              end

              real function f3(theta,alpha,em,thetas,thetar)

c             calculates soil moisture capacity('c')Vangenuchten's model
c             is used for moisture content pressure head relationship

      a=(1.0-theta**(1.0/em))**em
c             wrtite *,a
      b=(alpha*em*(thetas-thetar))/(1.0-em)
c     write *,b
              f3=b*(theta**(1.0/em))*a
              return
              end

              real function f7(si,alpha,em,en)

c             determines moisture content, given pressure head using
c     Vangenuchten's model

              a=1.0+((alpha*(abs(si)))**en)
              f7=(1.0/a)**em
              return
              end
```

```
      real function f1 (theta,alpha,em,en)

c     determines pressure head, given moisture content
c     using Vangenuchten's model

      a=(1.0/(theta**(1.0/em)))-1.0
      f1=-(a**(1.0/en))/alpha
      return
      end

      subroutine convergence(siassum,sinew,i,nnodes,iter,
     *                maxiter,epsilon,nn,nnn,iconv)
      dimension siassum(nnn),sinew(nn,nnn)

      if(iter .eq. 1)then
       iconv=0
       do j=1,nnodes
       siassum(j)=sinew(i,j)
       enddo
       else if(iter .eq. maxiter)then
           iconv=1
       else
        great=abs(sinew(i,1)-siassum(1))
         do j=2,nnodes
          great1=abs(sinew(i,j)-siassum(j))
          if(great1 .ge. great)then
            great=great1
          endif
         enddo
        if(great .le. epsilon)then
          iconv=1
        else
          iconv=0
        endif
      endif

c     write(*,*) 'great=',great
c     write(*,*) 'iconv=',iconv
      return
      end

      subroutine fpcomputation(siold,sinew,alpha,en,em,
     *                satk,i,delz,nnodes,nn,nnn,fp)
      dimension siold(nn,nnn),sinew(nn,nnn),fp(nn)

      sitemp1=(sinew(i,nnodes-1)+siold(i,nnodes-1))/2

      if(sitemp1.ge.0.0)then
       temptheta1=1.0
```

```
        tempk1=satk
      else
        temptheta1=f7(sitemp1,alpha,em,en)
        tempk1=satk*f2(temptheta1,em)
      endif
      sitemp2=(sinew(i,nnodes)+siold(i,nnodes))/2

      if(sitemp2.ge.0.0)then
        temptheta2=1.0
            tempk2=satk
      else
        temptheta2=f7(sitemp2,alpha,em,en)
        tempk2=satk*f2(temptheta2,em)
      endif
        averagek=(tempk1+tempk2)/2
        fp(i)=abs(-averagek*(((sinew(i,nnodes)-sinew(i,nnodes-1))
     *          /delz)+1))
      return
      end
```

LIST OF PUBLICATIONS

In Conference

Shobha Ram, K. S. Hariprasad and A. Gairola. "A Coupled Overland-Variably Saturated Flow Model for Border irrigation" 3rd International Perspective on Current & Future State of Water Resources & the Environment (EWRI OF ASCE), January 5-7, 2010, IIT Madras, Chennay, India.